The Impact of El Niño Southern Oscillation Events on Water Resource Availability in Central Sulawesi, Indonesia

A hydrological modelling approach

The Impact of El Niño Southern Oscillation Events on Water Resource Availability in Central Sulawesi, Indonesia

A hydrological modelling approach

Dissertation
zur Erlangung des Doktorgrades
der Mathematisch-Naturwissenschaftlichen Fakultäten
der Georg-August-Universität zu Göttingen

vorgelegt von

Constanze Leemhuis

aus Düsseldorf

Göttingen 2005

Referentin/Referent: Prof. Dr. Gerhard Gerold

Korreferentin/Korreferent: Prof. Dr. Bernd Diekkrüger

Tag der mündlichen Prüfung: 28.10.2005

CONTENTS

LIST OF FIGURES

LIST OF TABLES

LIST OF ABBREVIATIONS

CO_2	Carbon dioxide
d	Index of agreement
DEKLIM	German Climate Research Program
DTM	Digital terrain model
EI ($mm \cdot time^{-1}$)	Interception
ENSO	El Niño Southern Oscillation
ET ($mm \cdot time\ step^{-1}$)	Evapotranspiration
ETP ($mm \cdot time\ step^{-1}$)	Potential Evapotranspiration
ETR ($mm \cdot time\ step^{-1}$)	Real Evapotranspiration
FAO	Food and agricultural organization of the United Nations
IBK	Institute of Bioclimatology
IDW	Inverse distance weighting
IMPENSO	The Impact of ENSO) on water resource management and the Local Communities in Central Sulawesi / Indonesia
IWRM	Integrated water resource management
MAE	Mean absolute error
MHQ_{month}	average monthly high water discharge
MM5	Pennsylvania State University/National Center for Atmospheric Research mesoscale model
MNQ_{month}	average monthly low water discharge
MQ	average discharge
LAI ($m^2 \cdot m^{-2}$)	Leaf area index
LLNP	Lore Lindu National Park
PEST	Parameter estimation program
PHA	Potential homogeneous area
PTF	Pedotransfer functions
R^2	Coefficient of efficiency after Nash & Sutcliffe.
RMSE	Mean square error.
SAGA	System for automatic Geoecological analysis

SEWAB	Surface Energy and Water Balance model
SFB-552	Collaborative Research Centre (Stability of rainforest margins, Central-Sulawesi, Indonesia).
SOI	Southern Oscillation index
SST (°C)	Sea surface temperature
SST3 (°C)	Sea surface temperature, ENSO region 3
TANALYS	Topography analysis program
WASIM-ETH	Water balance Simulation Model

VORWORT

Die vorliegende Dissertation entstand in Rahmen des vom Bundesministerium für Bildung und Forschung geförderten Deutschen Klimaforschungsprogramms DEKLIM und war im Bereich Klimawirkungsforschung in das interdisziplinäre Projekt IMPENSO „Der Einfluß von ENSO (El Niño - Southern Oscillation) auf die Wasserressourcen und die lokale Bevölkerung in einem Regenwaldrandgebiet Indonesiens“ eingebettet.

An erster Stelle gilt mein Dank Herrn Prof. Dr. Gerhard Gerold, der diese Arbeit von Anfang an begleitet und in jeglicher Hinsicht unterstützt hat. Außerdem möchte ich Herrn Prof. Dr. Bernd Diekkrüger für die Übernahme des Koreferates meiner Arbeit meinen Dank aussprechen. Den Mitgliedern der IMPENSO - Mannschaft Frau Dr. Regina Birner, Prof. Dr. Gode Gravenhorst, Prof. Dr. Manfred Zeller, Dodo Gunawan und Alwin Keil gilt mein besonderer Dank für die interessante und fruchtbare interdisziplinäre Projektzusammenarbeit. Besonders möchte ich auch Frau Sabine Hippe für Ihre tatkräftige Hilfe in allen administrativen Belangen danken.
Ohne die Hilfe von Frau Oki Hadiyati für die Feldarbeit in Palu, Indonesien wäre diese Arbeit nicht möglich gewesen. Mein tiefster Dank gilt auch Dudi, Kemyl, Kiki, Dudin, Rina, Hendra, Dr. Heiner Kreilein und Robert Karsten. Die außerordentlich herzliche Aufnahme bei der Familie von Pak Sudarmi in Tomado hat meinen Aufenthalt in Zentral-Sulawesi zusätzlich bereichert. Für das Korrekturlesen dieser Arbeit, zahlreiche hilfreichen Kommentare und die moralische Unterstützung während der gesamten Promotionszeit möchte ich mich herzlich bei Ulrike Falk, Alexander Kleinhans, Georg Dechert und Kerstin de Vries bedanken. Mein Dank gilt ebenso allen anderen Mitarbeiterinnen und Mitarbeitern des Geographischen Institutes. Insbesondere danke ich auch meinen Eltern für ihre uneingeschränkte Unterstützung, die ich auf meinem bisherigen Lebensweg erfahren habe.

Constanze Leemhuis

SUMMARY

The El Niño/ Southern Oscillation (ENSO) phenomenon is the strongest known natural interannual climate fluctuation. The most recent two extreme ENSO events of 1982/83 and 1997/98 severley hit the socio-economy of main parts of Indonesia. As the climate variability is not homogeneous over the whole Archipelago of Indonesia, ENSO events cause negative precipitation anomalies of diverse magnitude and duration in different regions. Understanding the hydrology of humid tropical catchments is an essential prerequisite to investigate the impact of climate variability on the catchment hydrology. Together with the quantitative assessment of future water resource changes they are essential tools to develop mitigation strategies on a catchment scale. These results can be integrated into long term Integrated Water Resource Management (IWRM) strategies.

The general objective of this study is to investigate and quantify the impact of ENSO caused climate variability on the water balance and the implications for water resources of a mesoscale tropical catchment.

The mesoscale Palu River catchment (1°20`S, 21°01'E) is located in Central Sulawesi, Indonesia and covers an area of 2694 km². The topography of the catchment varies from 0-2500 m.a.s.l. Due to the monsoonal setting of Central Sulawesi ENSO years are described by decreased precipitation from July till October, which corresponds with the dry period. Up to 40 % of the basin is covered by mountainous rainforest (Lore Lindu Nationalpark). Illegal logging activities within the Lore Lindu Nationalpark constantly endanger the mountainous tropical rainforest ecosystems.

The Water Flow and Balance Simulation Model (WaSiM-ETH) is a process-based fully distributed catchment model. The spatial resolution is determinated by a grid and the time resolution can vary from minutes to days. The main processes of water flux, -storage and phase transition are simulated by physically-based simplified

process descriptions. WASIM-ETH has been sucessfully applied to the Gumbasa subcatchment (1275 km²) of the Palu River catchment. The calculated model efficiency of the calibration and validation period achieved satisfactory results, which verified the hydrological model as a suitable prediction tool. In addition a predictive sensitivity analysis was carried out. The simulation of the water balance with WASIM-ETH has applied to the period Sept. 2002- Sept. 2004. To obtain a feasible data source for the hydrological model an monitoring program of hydrological and meteorological data has been launched in September 2002 and is operating untill present. The simulation results of WASIM-ETH are characterized by uncertainties due to the model structure, uncertainties of input data and parametetrs and to the overall low data availability. Of major importance are:

(1) The uncertainty of areal precipitation regarding their spatial and temporal pattern has a strong effect on the overall modelling performance.
(2) A two year time series is not sufficient to obtain stable and reliable modelling results.
(3) The hydrological model is particular sensitive to the spatial pattern of soil physical properties.

The implications of possible future climate and land use conditions on the water balance of the Gumbasa River sample catchment were assessed by a scenario analysis, which simulates a sequence of possible future events. The scenarios quantify the changes of the water balance if the climate or the land use change for the base year 2003. For the generation of spatial and temporal variable caused rainfall anomalie scenarios as input data for a hydrological model of the Gumbasa River watershed a statistical scenario approach was applied. For the generation of land use scenarios an elevation dependent total change scenario was chosen. The conclusions of the scenario analysis with the hydrological model WASIM-ETH are:

(1) The scenario analysis with the hydrological model WASIM-ETH proves and quantifies that ENSO caused precipitation anomalies lead to an increase of the discharge variability.

(2) The modelling results demonstrate that beside local climate variability the catchment characteristics have an influence on the impact magnitude of ENSO related rainfall anomalies on the water balance of a catchment.

(3) Due to the soil data availability of the sample catchment the degree of surface disturbance is not considered by the land-use scenario. Therefore the most important factor of land use scenario uncertainty is the “low-flow problem”, because the infiltration rate is not correctly simulated by the applied scenarios.

A case study, calculation of the potential irrigation area of the Gumbasa River Irrigation Scheme, shows how the results of the scenario analysis of the hydrological model could be implemented for further agricultural evaluation and management. The outline, methodology, results and implications of the presented research study on the impact of ENSO events on the water resource availibility of a mesoscale tropical catchment in Central Sulawesi Indonesia represent a useful foundation for the implimentation of an Integrated Water Resource Management.

RINGKASAN

Kejadian ENSO (*El Nino Southern Oscillation*) adalah fenomena alami fluktuasi iklim antar tahunan terkuat yang diketahui. Dua peristiwa ENSO terakhir yaitu tahun 1982/1983 dan 1997/1998 sangat mempengaruhi kondisi sosial-ekonomi sebagian besar wilayah Indonesia. Mengingat variabilitas iklim tidak seragam diseluruh kepulauan Indonesia, peristiwa ENSO yang menyebabkan anomali negativ dari curah hujan berbeda besar dan lamanya dari satu tempat dengan tempat lainnya. Memahami hidrologi daerah tangkapan hujan di wilayah tropik basah adalah prasyarat yang mendasar dalam meneliti dampak variabilitas iklim di daerah aliran sungai. Bersama-sama dengan pendugaan kuantitatif perubahan sumber daya air dimasa mendatang, mereka adalah piranti utama dalam mengembangkan strategi penanganan dalam skala daerah tangkapan. Hasil-hasil ini untuk jangka panjang dapat di integrasikan kedalam strategi manajemen sumber daya air terpadu (Integrated Water Resource Management, IWRM).

Tujuan umum dari studi ini adalah meneliti dan mengkuantifikasikan dampak ENSO yang menyebabkan variabilitas iklim terhadap neraca air dan implikasinya terhadap sumber daya air dari daerah tangkapan berskala menengah di daerah tropis.

Daerah tangkapan berskala menengah Sungai Palu (1°20` LS, 121°01´ BT) berlokasi di Sulawesi Tengah, Indonesia dan mencakup areal seluas 2694 km2. Topografi daerah tangkapan bervariasi dari 0-2500 m d.p.l. Dengan adanya seting monsoon di Sulawesi Tengah, tahun-tahun ENSO dijelaskan dengan menurunnya jumlah curah hujan dari Juli sampai Oktober,yang berhubungan dengan periode musim kemarau. Kurang lebih 40% dari lembah sungai ditutupi oleh hutan hujan tropis (Taman Nasional Lore Lindu). Namunkegiatan penebangan hutan illegal di dalam taman nasional secara konstan mengancam ekosistem hutan hujan tropis.

Model simulasi neraca dan aliran air (WaSiM-ETH) adalah model hidrologi berbasis proses yang terdistribusi penuh untuk suatu wilayah tangkapan. Resolusi ruang ditentukan oleh sebuah grid dan resolusi waktu dapat bervariasi dari menit sampai hari. Proses utama dari limpahan air, penyimpanan dan fase transisi disimulasi oleh uraian proses berbasis fisik yang disederhanakan. WASIM-ETH telah berhasil diterapkan di daerah tangkapan Gumbasa (1275 km2) dari daerah aliran Sungai Palu. Perhitungan efisiensi model dari periode kalibarasi dan validasi memperoleh hasil yang memuaskan, yang telah memperlihatkan model hidrologi sebagai alat prediksi yang sesuai. Simulasi neraca air dengan model WASIM-ETH telah diterapkan untuk periode September 2002 – September 2004. Untuk mendapatkan sumber data yang layak bagi model hidrologi, program monitoring data hidrologi dan meteorologi telah di lakukan sejak September 2002 dan beroperasi sampai sekarang. Hasil simulasi WASIM-ETH dicirikan oleh ketidak pastian akibat struktur model, input data dan parameter serta kurangnya ketersediaan data. Hal-hal pokok yang penting adalah :

1) Ketidak pastian mengenai wilayah curah hujan berdasarkan pola ruang dan waktu yang sangat mempengaruhi keseluruhan penampilan model.
2) Data series selama dua tahun tidak mencukupi untuk memperoleh hasil yang dapat diandalkan.
3) Model hidrologi sangat sensitive terhadap pola ruang dari sifat fisik tanah.

Implikasi untuk kemungkinan iklim dan kondisi penggunaan lahan dimasa mendatang terhadap neraca air dari contoh Sungai Gumbasa telah diduga dengan analisis skenario, dengan mensimulasi sebuah bagian dari kemungkinan peristiwa mendatang. Skenario tersebut mengkuantifikasi perubahan neraca air bila iklim atau tata guna lahan berubah dari basis tahun 2003. Untuk membuat variabel ruang dan waktu yang disebabkan skenario anomali curah hujan sebagai data input model hidrologi untuk daerah tangkapan Sungai Gumbasa, pendekatan skenario secara statistik telah diterapkan. Untuk membuat skenario tata guna lahan dipilih skenario perubahan total yang tergantung pada elevasi. Kesimpulan dari analisa skenario dengan model hidrologi WASIM-ETH adalah :

1) Analisa skenario dengan model hidrologi WASIM-ETH membuktikan dan mengkuatifikasikan bahwa ENSO sebagai penyebab anomali curah hujan mengakibatkan meningkatnya variabilitas pengisian.
2) Hasil modeling menunjukkan bahwa disamping variabilitas iklim lokal, karakteristik daerah tangkapan mempunyai pengaruh terhadap besarnya pengaruh anomali curah hujan terkait dengan ENSO terhadap neraca air daerah tangkapan.
3) Mengingat ketersediaan data tanah dari contoh daerah tangkapan, tingkat gangguan permukaan tidak dipertimbangkan dalam skenario tata guna lahan. Oleh karena itu faktor yang sangat penting dari ketidak pastian skenario tata guna lahan adalah “problem aliran rendah”, karena laju infiltrasi tidak disimulasi secara tepat oleh skenario yang diterapkan.

Sebuah studi kasus, yaitu perhitungan areal irigasi potensial dari jaringan Irigasi Sungai Gumbasa menunjukkan bagaimana hasil analisis skenario model hidrologi dapat diimplementasikan lebih lanjut untuk menajemen dan evaluasi pertanian. Kerangka, metodologi, hasil dan implikasi dari riset studi pengaruh peristiwa ENSO terhadap ketersediaan sumber daya air dari daerah tangkapan sungai skala menenga daerah tropis di Sulawesi Tengah Indonesia yang telah dipaparkan ini menunjukkan dasar yang berguna untuk implementasi Manajenem Sumber Daya Air Terpadu.

INTRODUCTION

1.1 BACKGROUND AND MOTIVATION

The two most recent extreme El Niño (warm phase of ENSO) events of 1982/83 and 1997/98 severely hit the socio-economy of main parts of Indonesia. The El Niño/Southern Oscillation (ENSO) phenomenon is the strongest known natural interannual climate fluctuation [LATIF & ENDLICHER, 2001]. ENSO is a disruption of the ocean-atmosphere system in the tropical Pacific and has important impact on the global weather. During El Niño events pressure over Southeast Asia and the western Pacific rises, while it drops over the East Pacific. This loss of a pressure gradient across the Pacific is driven by a large-area warming of the upper layer of the equatorial eastern Pacific Ocean, causing a weakening of the trade winds in the central and western Pacific. Again this leads to a depression of the thermocline in the eastern Pacific, and an elevation of the thermocline in the west. Rainfall follows the warm water eastward, leading to floods in Peru and drought in Indonesia and Australia. Moreover the eastward displacement of the atmospheric heat source overlaying the warmest water indicates large changes in the global atmospheric circulation, which in turn forces changes of weather in regions far away from the tropical Pacific [NOAA, 2005]. El Niño is usually followed by La Niña (cold phase of ENSO), a time period which is characterized by unusually cold ocean temperatures in the Equatorial Pacific. The global climate impacts of La Niña events are contrary to those of El Niño impacts. Statistically ENSO events occur every second to seventh year [LATIF & ENDLICHER, 2001]. However, El Niño events are expected to increase in frequency and magnitude. Observations of the Sea Surface Temperature (SST) in the tropical Pacific for the last hundred years show an increased interannual variability during the most recent decades [LATIF& ENDLICHER, 2001]. TIMMERMANN *et al.* [1999] simulate a more frequent

occurrence of ENSO events if the global warming caused by CO_2 emissions will continue according to the IPCC (Intergovernmental Panel on Climate Change) scenario IS92a. The temperature change according to the IS92a forcing scenario for the 30-year average 2021 to 2050 compared with 1961 to 1990 is 1.3°C with a range of +0.8 to 1.7°C [IPPC, 2001].

Throughout the Archipelago of Indonesia the ENSO related droughts lead to water shortage, crop failure and forest fires of natural or human origin [LATIF & ENDLICHER, 2001]. Furthermore the population morbidity and mortality rates of affected countries increased dramatically due to undernourishment and bad drinking water quality. One main measure of climate impact research is to express the impacts of natural hazards like El Niño in socio-economic losses (e.g. costs or mortalitiy rates). Globally 21 706 deaths and an inflicted damage of $33 billion are attributed to the 1997-98 El Niño event [PHILANDER, 2004]. Table 1.1 lists the socio-economic consequences for Indonesia and Australia of the 1997-98 El Niño. Here it may be assumed that the morbidity and mortality cases are primary related to the underdeveloped conditions for the main population of the republic of Indonesia.

Table 1. 1: Socio-economic consequences of the 1997-98 El Niño [Source: VOITURIEZ & JACQUES 2000].

	Indonesia and Australia
Cost $_{\text{in billions of dollar}}$	4.45
Mortality	1316
Morbidity	124 647
Displaced	2 555 000
Area affected $_{\text{in hectars}}$	1 544 701

According to the World Water Assessment Programme [UNESCO, 2003] the probability of harmful consequences is results from interactions between natural or human hazards (e.g. ENSO caused droughts) and the vulnerability of the society. Societies in tropical developing countries are often most vulnerable, since population growth and economic development intensifies the pressure on water resources. To mitigate the consequences of drought, strategies to reduce vulnerability factors are required. These strategies might imply for example altering land use and agricultural

practices or modifying the severity of the drought by providing irrigation from reservoirs, wells or water imports from areas unaffected by drought.

As the climatic variability is not homogeneous over the whole Archipelago of Indonesia, El Niño events cause negative rainfall anomalies of diverse magnitude and duration in different regions [ALDRIAN, 2003]. Therefore possible mitigation strategies have to be developed on a regional scale and integrated into long term Integrated Water Resource Management (IWRM) strategies, which operate on a catchment scale [Global Water Partnership, 2000]. But hydrological catchment studies, which are the basis for Integrated Water Resource Management strategies, are still rare for mesoscale tropical catchments. With respect to the population number that is affected by ENSO caused droughts an urgent research need for tropical mesoscale catchment studies is obvious. For the Indonesian Archipelago already a few hydrological catchment studies to better implement water management strategies [e.g. ADI, 2003; PERANGINANGIN *et al*., 2004] exist, but still interdisciplinary surveys for IWRM strategies are lacking.

The following study investigates the impact of ENSO caused precipitation anomalies on the water resources of a mesoscale tropical catchment in Indonesia. The project is integrated into an interdisciplinary climate impact research project (IMPENSO), which is itself again embedded into the German Climate Research Group (DEKLIM, sponsored by the Ministry of Education and Research). The project IMPENSO consists of three integrated sub-projects investigating the impacts of ENSO events on climate variability, water resources availability and furthermore on socio-economy and policy implications on a catchment scale [KEIL, 2005]. Representative for the Archipelago of Indonesia the Palu River Watershed (2694 km²) located in Central Sulawesi was chosen as investigation area. The overall objectives of the project IMPENSO are: (1) to quantify the local and regional manifestations of global climate variability, (2) to analyze their implications for water resources and agricultural land use, (3) to assess the socio-economic impact of ENSO on rural communities living in agro-ecologically sensitive regions and (4) to develop participatory approach strategies and policy recommendations that help improve the capacity of developing regions to cope with ENSO events.

Understanding the hydrology of humid tropical catchments is an essential prerequisite to assess the impact of climate variability on the catchment hydrology. Three major aspects of tropical hydrology are of minor importance in temperate regions: (1) nonstationarity of the catchments, (2) macro-hydrological processes and (3) eco-hydrology [KLEMES, 1993]. Moreover, data availability is a major problem in the analysis of catchment processes. Especially in developing countries to which most of the tropical countries belong to, numerous basins are ungauged or poorly gauged. An appropriate database is urgently needed to enable the development and management of water resources [IAHS, 2003]. Long term records are required to study hydrological trends, but are often not available [MANLEY & ASKEW, 1993]. Furthermore, the vast majority of tropical catchment studies have been conducted at the micro spatial (<10 km²) and time (<5 years) scale [see BRUIJNZEEL, 1996]. It is not generally possible to upscale the understanding gained from these experiments to larger scales. Considering the increasing stress on water resources in humid tropical developing countries, there is an urgent global research need in humid tropical hydrology and its associated mesoscale catchment processes.

1.2 ENSO AND STREAMFLOW IN CENTRAL SULAWESI

River systems are comprehensive integrators of rainfall regimes over large areas [AMARASEKERA et al., 1996]. Hence, an accurate characterisation of the flow regime will increase our knowledge of the impact of ENSO caused rainfall anomalies on the river system, thus on the precipitation pattern of the watershed. Several studies in different regions that are teleconnected to ENSO events have shown distinct relations of ENSO events with inter-annual variations in stream flow [e.g. AMARASEKERA et al. 1996, ANDERSON *et al.* 2001, TERESHCHENKO *et al.* 2002, ELTAHIR 1996, SIMPSON *et al.*, 1993, GUTIERREZ & DRACUP 2001, DRACUP & KAYA 1994, CLUIS 1998].

To provide evidence on the impact of ENSO events on water resources in Central Sulawesi, the flow regime of two River catchments within the research area was analysed. The Wuno (190 km²) and the Miu (177 km²) catchment are sub-catchments of the Palu River watershed. Their catchment characteristics vary in topography and land use systems (Wuno = 44 % and Miu= 87 % forest cover). The two gauging

stations are run by the watershed department of the Forestry agency, which records the river stage since 1996 until present. So far these two data sets represent the longest available daily data records of stream flow for Palu Provincy. ALDRIAN [2003] has shown that a seasonal delineation is more preferable than a monthly temporal delineation to investigate the impact of ENSO events on rainfall anomalies. This seasonal delineation was also applied by BÖHNER [1996] to analyse the impact of ENSO events on air pressure anomalies of central/east Asia. Table 1.2 and 1.3 demonstrate the cross-correlation of stream mean seasonal discharge (Mq) with the Southern Oscillation Index (SOI) and the Sea Surface Temperature anomalie of the ENSO 3 region (SST3) of the Pacific. As the SOI and the SST 3 anomalie time series vary out of phase the seasonal SOI has a positive and the SST a negative correlation with the seasonal discharge of Miu and Wuno River. The analysis indicates a strong correlation with both ENSO indices. The impact is strongest from June until November and diminishes in November, which conforms to the seasonality of the impact of ENSO events in Indonesia [ALDRIAN, 2003]. Moreover even though the two sub-catchments belong to the same watershed, the Wuno River catchment is more vulnerable to rainfall anomalies than the Miu River catchment. In total for the strong ENSO year 1997/98 about 40% of the mean discharge was recorded for the Wuno catchment, whereas 60% of the mean discharge was recorded for the Miu catchment.

Table 1. 2: Correlation of SOI and average seasonal specific discharge for Wuno and Miu River, 1996-2002.

SOI / Mq in ($l \cdot s \cdot km^{-2}$)		**spring**			**summer**			**autumn**			**winter**		
		MAM			**JJA**			**SON**			**DJF**		
station	period	+1a	0a	-1a	+1a	0a	-1a	+1a	0a	-1a	+1a	0a	-1a
WUNO	1996-2002	0.19	0.52	-0.18	-0.53	0.7	-0.03	-0.2	0.68	0.25	-0.13	0.54	0.018
MIU	1996-2002	-0.19	0.26	-0.09	-0.24	0.85	-0.5	-0.24	0.69	-0.28	-0.29	0.38	-0.36
correlation with the SOI Index of the following (+1a), the previous (-1a) year, without adjustment (0a)													

Table 1. 3: Correlation of SST3 anomalie and average seasonal specific discharge for Wuno and Miu River, 1996-2002.

SST3 / Mq in ($l \cdot s \cdot km^{-2}$)		**spring**			**summer**			**autumn**			**winter**		
		MAM			**JJA**			**SON**			**DJF**		
station	period	+1a	0a	-1a	+1a	0a	-1a	+1a	0a	-1a	+1a	0a	-1a
WUNO	1996-2002	-0.34	-0.66	0.49	0.14	-0.76	0.14	0.24	-0.83	-0.11	0.12	-0.69	-0.08
MIU	1996-2002	0.01	-0.08	-0.09	-0.06	-0.62	0.65	0.28	-0.54	0.28	0.36	-0.21	-0.18

correlation with the SOI Index of the following (+1a), the previous (-1a) year, without adjustment (0a)

1.3 OBJECTIVES

The general objectives of the research study are to investigate and quantify the impact of ENSO caused precipitation anomalies on the water balance and furthermore to assess its implications for water resources of a mesoscale tropical catchment. As it was observed in the study within the Miu and Wuno catchment study the magnitude of the impact of ENSO events on a catchment level are spatially highly variable (see chapter 1.2). This spatial variability might be related to the high spatial variability of rainfall pattern within the watershed or on the other hand to the various catchment characteristics of the sub-catchments. Therefore catchment characteristics like e.g. land use might superimpose or compensate the impact of precipitation anomalies. FLEMING [1993] describes the water balance equation of a humid tropical catchment as follows:

$$P = E + SRO + IF + GWF + \Delta SS + \Delta MS + \Delta GWS \qquad (1)$$

with	P	precipitation
	E	evaporation
	SRO	surface runoff or rapid response
	IF	interflow
	GWF	baseflow
	ΔSS	change in surface storage which includes interception storage, surface depression store and free water surfaces
	ΔMS	change in mantle storage which includes root zone store, transitional zone store and perched groundwater store
	ΔGWS	change in the regional groundwater

In tropical regions with tropical rain forest as main land cover ΔSS can reach quite high values because of a high storage in the canopy and the litter layer. If tropical rain forest is converted to crop, ΔSS is strongly reduced, which leads to an intensification of hydrographical peaks. During dry periods a crop vegetation cover raises the total discharge in comparison with tropical rain forest vegetation cover, because ΔSS has a low storage and therefore a higher proportion of precipitation can infiltrate [FLEMING, 2003].
KLEINHANS [2004] investigated the impact of deforestation on the water balance of a small tropical catchment in Central Sulawesi, Indonesia. He concludes that deforestation leads to an increase of the low water discharge and to a significant increase of the peak flows. Hence for a comprehensive analysis of the impact of land use change on water resources during ENSO years, besides the drying conditions also the wetting up conditions have to be considered.

By means of a scenario analysis the following hypotheses are going to be analysed and assessed with regard to the impact of ENSO events on water resource availability:

(1) ENSO caused precipitation anomalies lead to an overall increase of the discharge variability of a mesoscale catchment, which is due to a decrease of the low and mean discharge during the ENSO affected period.

(2) ENSO caused precipitation anomalies are characterised by a high spatial variability.

(3) The impact magnitude of ENSO related rainfall anomalies on the water balance of a mesoscale catchment strongly depends on the catchment characteristics.

(4) Extensive land use change like deforestation compensates the amplitude of hydrological response to ENSO related rainfall anomalies, but leads to an overall increase of high water discharge during storm events.

PALU RIVER WATERSHED

CASE STUDY

2.1 LOCATION AND OVERVIEW

The case study area Palu River watershed is located in the humid tropics in Central Sulawesi, Indonesia (1°10`S, 120°05`E). The total area of the watershed amounts to 2694 km² (Figure 2.1). The elevation ranges from sea level at the estuary mouth of the Palu River to 2491 m.a.s.l. at the Peak of the Nokilalaki Mountain, which is located in the complex of steeply folded mountains and rift valleys in the south eastern part of the watershed. Up to 41 % of the basin area is covered by the protected tropical montane forest of the Lore Lindu National Park (LLNP) (Figure 2.1). The National Park, which stretches over 2310 km² was founded in 1977 and in the same year has been declared a Man and Biosphere Reserve by the United Nations Educational, Scientific and Cultural Organization. The National Park serves as an important habitat for endemic and endangered fauna and flora of Sulawesi. Approximately 16 % of the total watershed area is covered by the major local land use systems that are predominantly located in the valleys and alluvial plains. Peasants use these plains for agricultural cultivation of paddy rice, maize and perennial crops like cacao and coffee. The population of the research area comprises approximately 300.000 people of whom 237000 (census 1995) live in the province capital Palu. As the region has been subject to different transmigration programs and additionally due to spontaneous migration people especially from South Sulawesi settled within the catchment area over the past two decades, the population has grown by 66% [MAERTENS et al., 2004]. One implication of this rapid population growth is an increase of conflicts about natural resources, which result in massive deforestation along the border of the National Park. Moreover the clearing of forested areas causes ecological and economical problems such as erosion and a higher risk of flash floods. One demonstrative example of the effects of deforestation

is the Dongi - Dongi case, located in the north–eastern part of the research area. In the year 2001 the plains along the Dongi - Dongi valley have been illegally logged. This massive forest conversion of the virtual protected National Park area covers an area of 2200 ha [ERASMI et al., 2004]. Besides resulting in a higher sedimentation load of the Gumbasa River, in December 2003 these logged areas of the valley might have intensified a flash flood, which destroyed bridges, streets and agricultural fields of the valley and the vicinal Palolo valley.

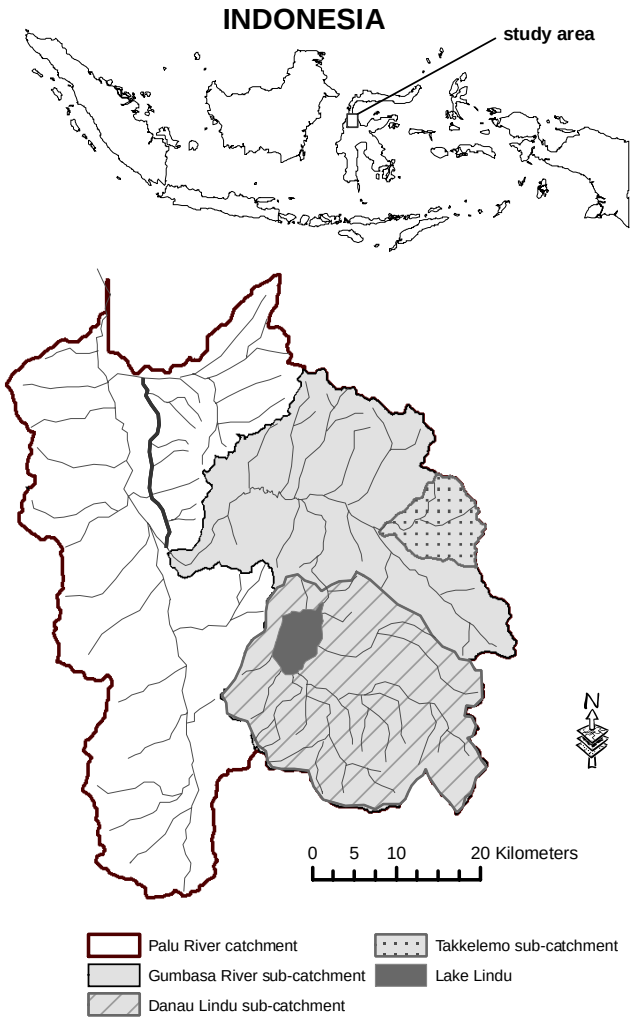

Figure 2. 1: Location of the Palu River Watershed (2694 km²), Central Sulawesi, Indonesia

2.2 CLIMATE

Due to the tropical conditions in Central Sulawesi the yearly temperature variation is relatively low. Whereas other climate variables such as wind velocity, evaporation and humidity depend highly on local conditions, the climate of Central Sulawesi is best characterised with reference to yearly rainfall pattern [WHITTEN et al., 2002]. According to ALDRIAN & SUSANTU [2003], the Palu River watershed is located in an intermediate zone of the main Indonesian climate regions with a yearly rainfall regime that is strongly influenced by the Asian–Monsoon–System. Between March and June variable, humid south-easterly winds reach eastern Sulawesi, causing the first rainy season of the year. Then the south-easterly winds from the dry and wintery Australian landmass prevail, initiating the dry season from August to October. The second shorter, but even stronger rainy season from November to December is generated by humid north-westerly winds from Kalimantan [WHITTEN et al., 2002]. As a result of the watersheds vicinity to the equatorial through of low pressure the area is influenced by convective rainfall during the whole year. The total amount of yearly rainfall is spatially highly variable and depends largely on topography and elevation. Valleys like the Palu valley, which are situated in a north–south direction, are in the rain shadow of the steep surrounding mountains. With a total annual amount of rainfall of around 600 mm, Palu is one of the driest cities in Indonesia, whereas the mountain regions have a gross annual rainfall of up to 2500 mm.

Table 2. 1: Mean yearly precipitation [mm] within the Palu River Watershed, Dutch colonial meteorological and geophysical survey, Source: BERLAGE [1949].

station	period	Lat / Lon	Elevation (m a.s.l.)	Precipitation (mm)
Palu	1908 - 1941	00°55`S 119°54`E	30	547
Kal. Napoetih	1919 - 1941	01°12`S, 119°56`E	80	1576
Bora	1923 - 1941	01°02`S, 119°57'E	90	1042
Kulawi	1916 - 1941	01°26`S, 119°59`E	735	2446
Lindu	1931 - 1941	01°18`S, 120°05`E	+/- 1000	2371

Table 2.1 shows the spatial variability of the mean yearly precipitation depending on location and elevation of five meteorological stations of the Dutch colonial meteorological and geophysical survey. Figure 2.2 demonstrates the mean yearly rainfall pattern of the above named stations, indicating a bimodal rainfall pattern for the stations at higher elevation (Lindu, Kulawi) and an all–season influence of the rain shadow effect for the Palu valley.

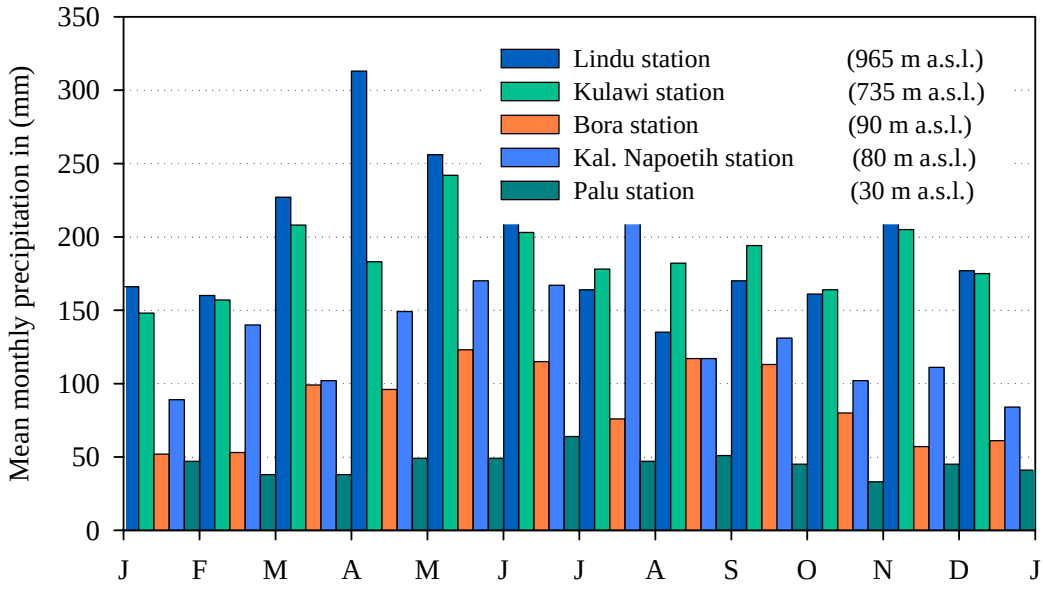

Figure 2. 2: Mean monthly precipitation in (mm), Palu River Watershed, Dutch colonial meteorological and geophysical survey, Source: BERLAGE [1949].

Climate variables like temperature, humidity and radiation vary according to elevation and topography. For the year 2002 the meteorological station Palu that is run by the Institute of bioclimatology (IBK), Göttingen recorded a mean air temperature of 27.9 °C, a mean relative humidity of 75.4 % and a mean daily global radiation of 20.0 MJm^{-2}. In comparison the meteorological station Nopu located at 660 m.a.s.l at the edge of the Palolo valley, recorded for the same year a mean air temperature of 24.5 °C, a mean relative humidity of 85.6 % and a mean daily global radiation of 19.1 MJm^{-2}.

2.3 GEOLOGY AND SOILS

The distinct geological zones of Sulawesi are strongly related to plate tectonics. Supposably during the Miocene (13 – 19 Mio years ago) the northward drifting Australian plate collided with the Banda Arc, resulting in the present shape of Sulawesi. Correspondingly the geological zones East and West Sulawesi are divided by the still active left lateral Palu Fault, which is apparently the western boundary of a lithospheric plate that is overriding the Sulawesi sea floor to the north [HAMILTON, 1979]. The Palu Fault is marked by a continuous rift valley, the present river bed of the Palu River. According to the geomorphologic study of Central Sulawesi by GARRELTS [2000] the two basins Sopu and Lindu of the watershed are the results of the mainly horizontal deformations along secondary faults, shaping characteristically rhombohedral pull-apart basins. Lake Lindu and its surrounding flood plain are one of the youngest formations of these pull-apart basins. Similarly for the Sopu basin (Palolo valley) a lake stage during the landscape genesis is assumed. This theory is verified by definite lake sediments that were detected in the Sopu basin. In general alluvial fill is associated with pull-apart basins where alluvial fans are an important point of this fluvial depositional environment [KARTEKAAS, 2000]. Within the research area of this work the geological terrains are defined by the Palu Fault and are described by diverse lithological characteristics and tectonic histories. The Systematic Geological Map of Indonesia, Quadrangle Poso, Sulawesi-2114 of 1997 (1:250000) differentiates between the geological formation of the Kambuno Granite, Napu Formation and Tineba Volcanics for the Western Sulawesi Terrain and Intrusive rocks in the Eastern Sulawesi Terrain. During the Quaternary the basins were filled with lake deposits. Table 2.2 describes the dominant geological formations of the watershed. Although the research area is located in the humid tropics the dominant soil types are not classified as deeply weathered soils characteristic for the tropics. The relatively weak soil development is a result of the young age of the diverse parent material [MACKENSEN et al., 2000]. MACKENSEN et al. [2000], who carried out a soil survey of the Sopu and Nopu basin in 2000, estimates that on up to 80 % of the surveyd area Cambisols can be found. The parent material was either of granitic or andesitic origin. On less developed soils Leptosols can be found. Furthermore azonal Fluvisols and Gleysols occur, which are related to a high water table in depression zones.

Table 2. 2: Dominant Geological formations of the Palu River watershed according to the Systematic Geological Map of Indonesia, Quadrangle Poso, Sulawesi-2114, 1997 (1:250000).

Symbol	Name	Description	Age
Ql	Lake deposits	Clay, silt, sand, showing horizontal beds, several meters to tens of meters thick	Quaternary
Qpn	Napu Formation	Sandstone, siltstone conglomerate, shallow marine environment	Plio –Pleistocene
Tmpi	Intrusive rocks	Granite	Miocene
Tpkg	Kambuno Granite	Granite, diorite	Pliocene
Tmtv	Tineba vulcanics	Andesite, breccia	Middle-late-Miocene

Unfortunately the soil survey by MACKENSEN was conducted only in the main basin of the research area and little is known about the dominant soil types of the montane forested areas. An analysis of the dominant soil types of a catena at the southern slope of the Sopu valley (605-1423 m.a.s.l.) is reported by KLEINHANS [2004]. On the uniform Andesite parent material of the catena mainly Cambisols of different subclasses are developed. The alluvial soils close to the stream at the bottom slope are characterised as fluvic Cambisols that are partly associated with gleyic Cambisols. The moderate steep area of the slope is dominated by eutric Cambisols, whereas the upper steep slope is covered by dystric Cambisols that are partly associated with young shallow Leptosols. Though the main parent material of the research area is of granitic origion it can be assumed that the slope succession of soil types desribed by KLEINHANS [2003] can be transferred as a leitcatena for other slopes with similar topographic attributes.

2.4 VEGETATION AND LAND USE

The vegetation cover of the research area is highly affected by the topography and therefore by the associated agricultural availability. The lowland of the Palu valley which would be naturally covered by rainforest, is totally deforested and at present covered by paddy fields, pasture and coconut plantations. Also the entire basin of the

Sopu valley is utilized for agricultural production, such as paddy, perennial crops like cacao and annual crops like maize and cassava. The agricultural use of the Lindu basin that is located at higher elevation is dominated by paddy fields and perennial crops like coffee. A great part of the Lindu basin is covered by a swampy area with dominant reed vegetation. Figure 2.3 illustrates the fractions of the main land use types of the Palu River watershed after the Landsat/ETM+ land-use classification of the year 2001 (SFB-552).

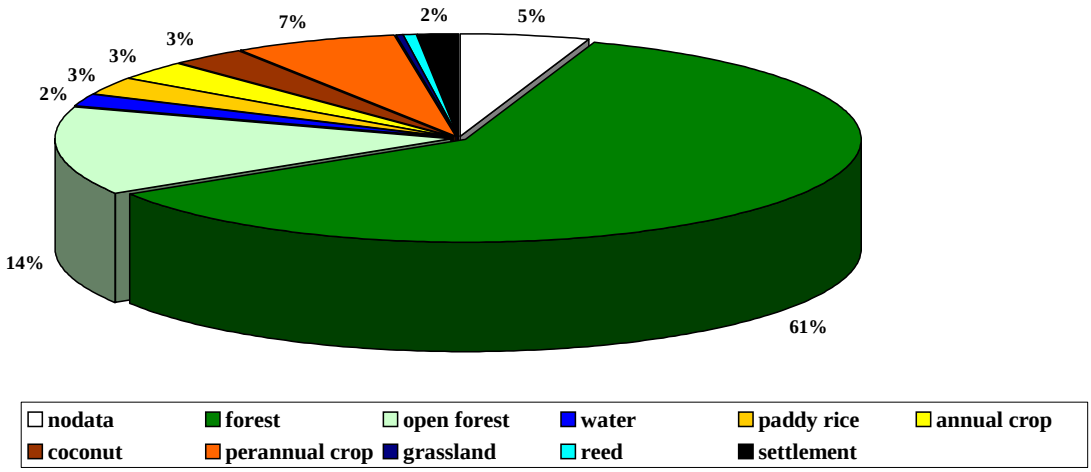

Figure 2. 3: Main Land-use types of the Palu River watershed after the Landsat/ETM+ land use classification 25th August, 2001, Source: (SFB 552).

The Landsat/ETM+ based land-use classification distinguishes between forest and open forest. This differentiation of forest types might be correlated with the occurance of dense primary forest and open secondary forest. According to WHITTEN [2002] the forest types of Sulawesi can be classified by their altitude zonation into lowland and hill forest (0-1200 m.a.s.l.), lower montane forest (1200-2400 m.a.s.l.), upper montane forest (2400-3000 m.a.s.l.) and subalpine forest (+3000 m.a.s.l.). In the undisturbed area of the LLNP, hill and lower montane forest can be found according to elevation range. The main forest vegetation characteristics regarding the elevation are associated with the canopy height, leaf size class and the occurance of epiphytes and creepers [WHITTEN, 2002]. Ecologically, the primary

forest is characterised by high species diversity. In a primary forest of this region KESSLER [2002] identified up to 150 tree species per hectar. As a result of slash and burn practice and deforestration along the slopes of lower elevation (600 –1200 m.a.s.l.) the percentage of hill forest is constantly diminishing.

2.5 HYDROLOGY AND WATER RESOURCES

The Palu River Watershed is divided into five sub-catchments: (1) The Lake Lindu sub-catchment, (2) the Sopu River sub-catchment, (3) the Miu River sub-catchment, (4) the Wuno River and (5) the Palu River sub-catchment. Figure A (Appendix) describes the stream network of the Palu River watershed and its tributary sub-catchments. The hydrology of the Palu River watershed is described by a fast responding rainfall-runoff system which is typical for a tropical watershed with a high topographic variation. Therefore, the runoff regime of the tributary streams is highly associated with the spatial variability of the yearly rainfall. Characteristic water discharges are fundamental for any hydrological analysis. Since no long-time discharge records of the research area are available the analysis is related to the Palu River record (1981-1986), two records of the tributary streams Wuno and Miu (1996-2003) and discharge measurements of two tributary streams of this work (2002-2004). For a better comparison of the sub-watersheds the characteristic water discharges are presented as a daily mean of the runoff per unit area ($ls^{-1}km^{-2}$). Table 2.3 summarizes the characteristic water discharges at the outlet of the watershed (Palu) and at different tributary streams. It should be noticed that due to the poor and timely variable record the following characteristic water discharges are statistically not directly comparable. Nevertheless, they give a first impression of the hydrological characteristics of the watershed and its tributary sub-basins. The values for characteristic water discharges indicate that the watershed is divided into zones of runoff per unit area with diverse magnitude and variability. At the outlet of the Palu River much of the discharge is already withdrawn from the system for irrigation use. Shortly before the confluence of the Gumbasa and Palu River, discharge water is extracted for the main irrigation scheme that supplies ca. 10000 ha of paddy fields along the eastern Palu valley. Located within the LLNP, Lake Lindu with a size of 35

km², a mean depth of 60 m and an estimated storage capacity of $2.8^{*}10^{9}$ m³, plays a significant role in the low water discharge generation of the tributary Gumbasa River during dry seasons and hence for the water supply of the main irrigation scheme. Besides this main irrigation scheme, small technical irrigation schemes are located along the Sopu and Kulawi valley. A further possible explanation for the relatively low mean discharge of the Palu River, is a high groundwater recharge that might results from a high permeability of the lake deposits of the Sopu and Palu valley. A catchment is never a closed system, since groundwater may be lost due to a geological connection to the deeper groundwater layer. BRUIJNZEEL [1996] states that bedrock underlying valley fills are leaky itself. Especially, volcanic terrains show significant leakage. Because no geohydrological research has been conducted for the research area, it can be only assumed that a significant amount of the water balance is lost due to leakage of the lower boundary of the watershed. The high spatial rainfall variability of the area leads to a balanced discharge at the outlet with moderate maxima and minima.

Table 2. 3: Characteristic water discharges in ($ls^{-1}km^{-2}$) of the Palu river outlet and of tributary streams.

station	**period**	**watershed area (km^2)**	**MNQ_{month} ($ls^{-1}km^{-2}$)**	**MQ ($ls^{-1}km^{-2}$)]**	**MHQ_{month} ($ls^{-1}km^{-2}$)**
Palu	1981-1985	2694	14.5	22.7	38.8
Miu	1996-2003	177	32.4	45.2	87.3
Wuno	1996-2003	190	40.9	51.5	74.8
Takkelemo	2002-2004	79	13.0	20.82	44.0
Lindu	2002-2004	582	27.0	35.62	45.0

Basis of a classification of hydrological river types is the river discharge regime [KELLER, 1962]. The river discharge regime is a resultant reflection of a composite catchment hydrologic response to discharge producing processes [CUNDERLIK & BURN, 2002]. It is described by the coefficient of the mean monthly and the mean yearly discharge. The seasonal regime of a river indicates the dry and wet seasons of tropical catchment areas. The Pardé or runoff coefficient after PARDÉ [1933] which describes the seasonal regime of discharge is calculated with the following equation:

$$k_{Pardé} = \frac{MQ_{month}}{MQ_{year}} \tag{2}$$

with MQ_{month} mean monthly discharge ($m^3 \cdot s^{-1}$)

MQ_{year} mean yearly discharge ($m^3 \cdot s^{-1}$)

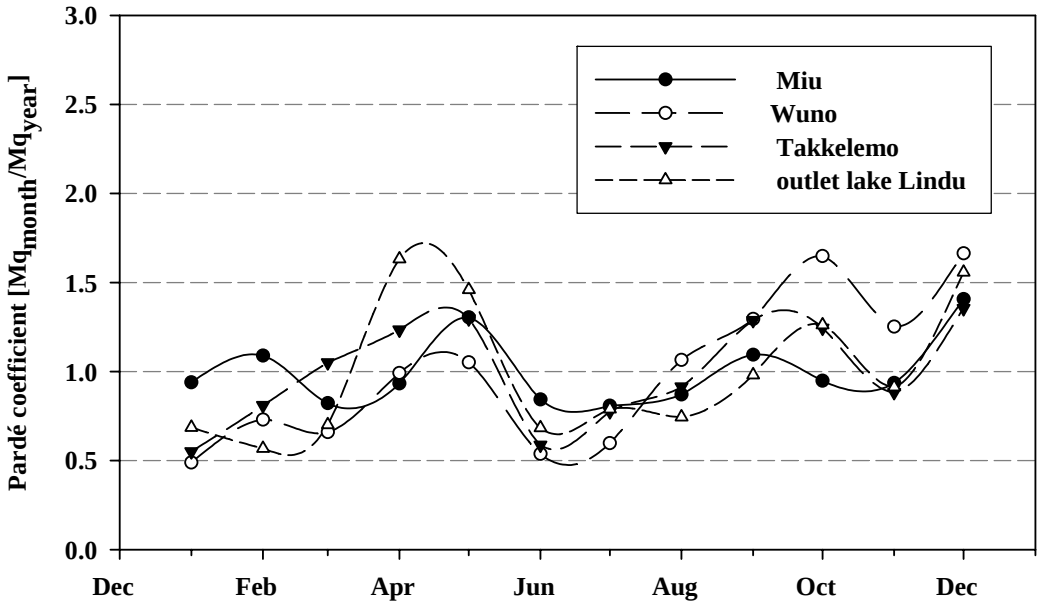

Figure 2. 4: Seasonal regime (2003) after Pardé [1933]of four different rivers within the Palu River watershed

Figure 2.4 describes the seasonal regime after Pardé for four tributary catchments of the Palu River watershed for the year 2003 with a range of 0.5 – 1.6. On equatorial islands like Sulawesi monthly Pardé or runoff coefficients usually exceed 0.6 [CHANG, 1993]. A seasonal regime with two peaks that strongly corresponds with the rainy seasons is specified for all tributary catchments. Equatorial rivers with two peaks are characteristic for tropical forest areas and are produced by a yearly precipitation distribution with monthly totals over 100 mm. Rivers that are located in monsoon regions show a great variation of seasonal and annual flow [OYEBANDE & BALEK, 1987]. A wide variation of magnitude of the discharge peaks is observed for the different tributary catchments, which stresses the high spatial variability of rainfall pattern and catchment characteristics within the Palu River watershed. For example the regime of the Lindu catchment has a high peak during the first rainy season from March until May, the regime peak during the second rainy season from November until December is less pronounced and the yearly regime of the Wuno River shows the opposite behaviour. The same yearly trend is reflected by the historical precipitation data for the Lake Lindu catchment (see Figure 2.2). The Lindu station is situated close to the outlet of the catchment records a mean seasonal (1931-1941) precipitation peak for the first rainy season from March until May.

METHODOLOGY

3.1 BASIC CONCEPT

The main research focus of this work is the investigation of the impact of ENSO caused rainfall anomalies on the water balance of a mesoscale catchment. As discussed in Chapter 1, ENSO caused rainfall anomalies form a distinguished pattern in space and time. A representation of the catchment hydrology with regard to space and time resolution is essential to analyse the research question. After ABBOT & REEFSGARD [1996] the spatially-distributed and time-dependent hydrological model becomes the conditio sine qua non for investigations in this area. The aim of distributed hydrological modelling is to make the fullest use of spatial and timely data, like geological data, satellite data, stream discharge etc. and furthermore to apply supplementary information that is available about soil physics, plant physiology, meteorology etc. that is relevant within this context. “Certainly, no matter how much data we have and no matter how much we know, it will never be enough to represent the real-world water balance of a catchment, but in this way we do the best that we possibly can.” [ABBOT, REEFSGARD, 1996]. A modelling protocol includes an order of steps in hydrological model application that should be adapted to the research question. In general such a protocol is flexible, adaptive and open to new insights. Figure 3.1 shows the modelling protocol that was developed for the purpose of this work. In the following sections each step of the modelling protocol is first explained and then applied to the research question.

3.1.1 Define purpose

In a first step the purpose of a model application is defined. Furthermore a first assessment of the desired time and spatial resolution and the accuracies are made. The objectives of this work are discussed in Chapter 1.5. Concerning the time and spatial resolution a first rough estimation is related to the potential users of the hydrological model application and the physical characteristics of the watershed. The

potential users are represented by the local authorities of the research region. In case of a predicted ENSO event, the simulated scenarios of the hydrological model assist the local water authorities to work out water management concepts for the catchment area. The responsible local authority usually operates with weekly resolution. On the other hand the spatial climate variability of the research area has to be considered. Thus, it is more appropriate to foremost apply a daily resolution and later on aggregate daily to weekly sums.

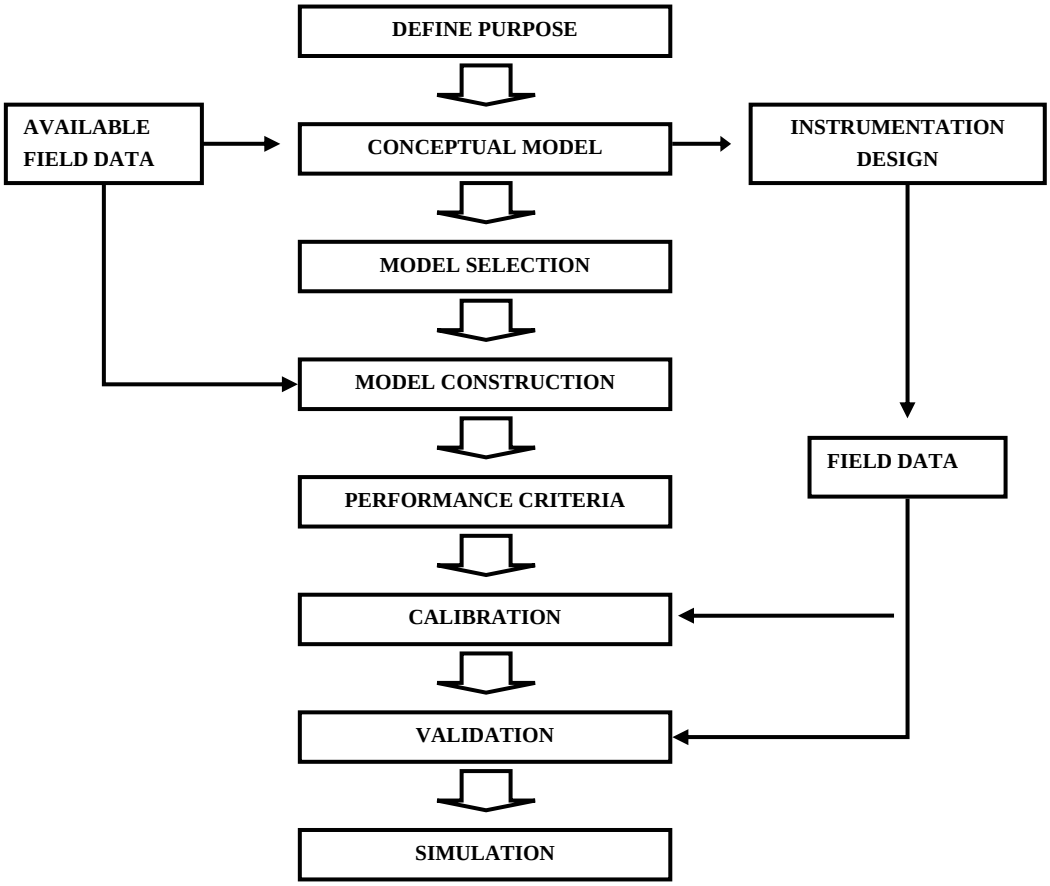

Figure 3. 1: Modelling protocol for the analysis of the impact of rainfall anomalies in a mesoscale catchment in Central Sulawesi, Indonesia. (modified after Anderson and Woessner, 1992).

3.1.2 Conceptual model

The conceptual model implies the user's perception of the key hydrological processes in the catchment with regard to the purpose of the specific problem. The whole process is based on an analysis of the available field data. As a result of this protocol step the available field data set should be evaluated regarding its application for hydrological modelling.

The impact of ENSO events on the hydrology of a mesoscale watershed in Central Sulawesi, Indonesia are discussed in Chapter 1.6. Furthermore an analysis of the specific catchment hydrology is described in chapter 2.6. Essential for the performance of any hydrological model is a sufficient representation of the areal precipitation. According to BEVEN [2002] no model will be able to simulate accurate predictions if the areal precipitation is not adequately represented. The available meteorological field data set of the research area comprises only one long time record of a single climate station (MUTIARA AIRPORT) that does not allow any further interpolation of areal precipitation. The available discharge data set includes a 4 year record (1981-1985) at the outlet of the Palu River watershed and a 7 year record (1996-2003) of two small sub-catchments. Instead of using this poor available field data for the application of the hydrological model, a new coarser instrumentation design should be set up. Within the time frame of this work only a two year time series (2002-2004) could be recorded.

3.1.3 Model selection

On the basis of the defined conceptual model a suitable hydrological model has to be selected. The two classical types of hydrological models are the stochastic and the deterministic model [REFSGAARD, 1996]. The latter are classified into empirical models (black box), lumped conceptual models (grey box) and distributed physically-based or process-based models (white box). Black box models integrate mathematical equations, which are not related to physical processes, but rely on analysis of concurrent input-output time series. Within grey box models all parameters and variables represent average values over the entire catchment. They operate with different storages, which represent the physical elements in a catchment. The description of the hydrological processes are based on semi-empirical equations,

therefore a number of model parameters have to be assessed by model calibration. They are especially applicable for the simulation of the rainfall-runoff process when long hydrological time series exist.

White box models are physically or process-oriented and describe the natural system using the basic mathematical representations of the flows of mass, momentum and various forms of energy. On a catchment level, a process-based model has to be fully distributed, which implies that they take account of spatial variations in all variables and parameters. Due to their process-based distributed attributes they provide a more detailed description of the hydrological processes within the catchment. For the prediction of the impact of land use changes or rainfall anomalies on the water balance of a catchment, a hydrological model based on physical parameters allows a direct estimation. But even the state of the art process-based distributed models are an extreme simplification of reality [SCHELLEKENS, 2000]. The uncertainty of the representation of hydrological processes on a catchment scale is related to scaling problems in hydrological modelling and due to the problem of regionalisation of hydrologic variables [BLÖSCHEL, 1996]. All physical equations, which the process-oriented distributed models are based on, were developed on a local scale (scale of the laboratory soil column or the experimental plot), but are applied on a catchment or regional scale. BLÖSCHL [1996] states that if Darcy's law is upscaled for saturated flow, it is not certain that it describes the average behaviour of the spatial pattern. Further BEVEN [1996] argues that with a complex model many combinations of parameter values can lead to the same result.

Also the simulation of different hydrological processes may represent the same output. SCHELLEKENS [2000] concludes that the predictive value of these models strongly relys on a good knowledge of the main hydrological processes within a catchment. Despite of all uncertainties of process-based distributed models, there is no other alternative if we want to simulate the spatial variability of the water balance and furthermore simulate rainfall anomalies and land use scenarios.

With regard to this study`s objectives, the process-based distributed Waterbalance-Simulation-Model WaSiM-ETH [SCHULLA & JASPER, 1999], using the Richard-

Equation for the unsaturated zone, was chosen. WASIM-ETH was developed to assess "the impact of climate change on the hydrological regimes and water resources in Europe" and tested successfully for the Thur basin (1700km^2), located in north-east Switzerland [SCHULLA, 1997]. WASIM-ETH is a complex modularly and raster based water balance simulation model, which can be applied on different hydrological scales and time resolutions. Up to now it has been successfully applied to various catchments with diverse climatological and morphological characteristics [e.g. JASPER *et al.*, 2002; NIEHOFF, 2001; GURTZ *et al.*, 2002; VERBUNT *et al.*, 2002]. KLEINHANS [2004] applied WASIM-ETH successfully on the Nopu catchment (2.3km²), which is a small sub-catchment of the Palu-River-Watershed. For the application he used a 30*30 m grid scale with a daily resolution. Additionally he calculated the evapotranspiration rate using an experimental approach. The comparison of the simulated and calculated evapotranspiration rate demonstrated that the evapotranspiration module of WASIM-ETH is capable to simulate the evapotranspiration rate of a humid tropical catchment. His work also showed that already with a daily temporal resolution satisfactory results for the simulation of the water balance can be obtained. This application of WASIM-ETH on a tropical catchment is encouraging to test the models performance on a larger hydrological scale with a coarser spatial resolution. The concept of the hydrological model WASIM-ETH is described in more detail in Chapter 4.

3.1.4 Model construction

After having selected a suitable hydrological model, the model is adjusted for the catchment of investigation. In this step, a selection of the spatial resolution for the model application is made that is related to catchment size, altitude dependence of the input variables (e.g. temperature, humidity) and required output accuracy of the hydrological processes. In general, a suitable spatial resolution should be balanced between model efficiency and a reasonable computer run time [SCHULLA & JASPER, 1999]. Furthermore, the boundary and initial conditions of the model are set. Values for the physical parameters are obtained either from field or literature data sets (see chapter 6.3.4). The construction of the applied hydrological model WASIM-ETH is described in detail in chapter 6.

3.1.5 Performance criteria

Performance criteria involve the definition of the accuracy that should be achieved during the following calibration and validation steps. A specification of realistic performance criteria requires an estimation of the accuracy desired for the specific problem, the catchments heterogeneity and the available field data.

The choice of suitable performance criteria is described in detail in Chapter 4. Chapter 6 discusses the application of the hydrological model with regard to the achieved model efficiency.

3.1.6 Calibration

The aim of model calibration is to determine values for the calibration parameters that cannot be assessed directly from field or literature data. Calibration itself is an iterative process to find a parameter set that optimally reproduces the catchment behaviour. The accuracy of the model is mainly assessed by comparing observed hydrograph or soil moisture values versus the simulated ones. They can be compared either graphically or with an objective function, e.g. using the model efficiency by NASH & SUTCLIFFE [1970]. Furthermore, a predictive uncertainty analysis to evaluate the uncertainty in the assessment of parameter estimation should be carried out. In general, the calibration procedure is carried out either by trial-and-error adjustment, by automatic parameter estimation or by a combination of the two methods.
The chosen calibration method is explained in Chapter 4, the calibration of the applied hydrological model is discussed in Chapter 6.

3.1.7 Validation

During the validation process the model’s capability for site specific for sufficiently accurate predictions is tested. One of the regular applied methods is the split sample test. Here the time series is split into a period for calibration and a following period of validation. This procedure involves the application of the calibrated model without changing any parameter value for another period. Again the model’s performance is evaluated and should correspond with the models accuracy achieved during the

calibration period. The model is regarded as validated and can be used for predictive analysis.
The used validation method is specified in Chapter 4, the validation results of the applied hydrological model can be found in Chapter 6.

3.1.8 Simulation

The model simulation of future scenarios with a validated model is the overall goal of hydrological modelling. Here the effect of the uncertainties in parameter values on future catchment conditions should be assessed by carrying out a predictive analysis. It is common that there are often many different sets of parameters for which the objective function is at its minimum. Therefore for the simulation of scenarios many different optimum sets of parameters should be applied. The predictive uncertainty analysis tests if the model simulates different values for key model outputs when different optimum parameter sets are applied [DOHERTY, 2000].

The application of scenarios is described in Chapter 7. A further description of the predictive uncertainty analysis can be found in Chapter 4.

INSTRUMENTATION AND MEASUREMENT

4.1 INSTRUMENTATION DESIGN

In order to obtain a feasible data set of hydrological calibration and validation data to set up a distributed hydrological model, a network of six automatic stage recorders was installed in August 2002. Furthermore, eight additional climate stations have been added to the ten climate stations run by the IBK (Institute of Bioclimatology) Göttingen, existing since 2001, to establish a high resolution area precipitation for the research area. Data collection started in September 2002 and the operation of the measurement network continued until present.

4.1.1 Climate stations and meteorological instrumentation

The locations of the climate stations were selected according to various criteria. On the one hand the site should fulfil all meteorological criteria for an effective measurement network to determine areal precipitation, areal temperature and areal humidity. This implies well distributed stations located at a range of different elevations. On the other hand an effective and safe data acquisition should be ensured to minimise the risk of data loss. As the main part of the research area is covered by protected rainforest, which coincides with elevations > 800 m.a.s.l. it is not possible to set up any climate station within this part of the research area. A climate station in these forested areas would be difficult to access moreover the setup of a station would also imply a clearing of forest, which is not appropriate and legal within the border of a National Park. The final decision on site location for the climate stations was based on the already existing climate station network of the IBK Göttingen, and suitable places close to villages where the station could be guarded by local workers (FIGURE 4.1) were chosen. Precipitation (P) was recorded continuously using a 0.1 mm resolution precipitation pulse transmitter with datalogger *(Theodor Friedrichs & Co, Schenefeld).* Air temperature and humidity

were determined with a 2 channel datalogger *(Onset HOBO, Bourne).* To protect the instrument against rain and sunlight the air temperature / humidity logger is installed inside a standardised weather instrument shelter. Precipitation, air temperature and humidity data were stored at 5 min. intervals. Table 4.1 lists the IMPENSO run climate stations within the Palu River watershed.

Table 4. 1: Distribution of climate stations within the Palu River watershed.

station	lat / lon	elevation[m.a.s.l.]	period
Maranata	01°02`30 S; 119°54`32 E	85	01.09.2002 - present
Sidondo II	01°05`26 S; 119°53`35 E	65	01.09.2002 - present
Salua	01°21`13 S; 119°58`11E	375	01.09.2002 - present
Bolapapu	01°26`31 S; 119°59`05 E	570	01.09.2002 - present
Berdikari	01°07`27 S; 120°05`01 E	650	01.09.2002 - present
Sintuwu	01°09`35 S; 120°03`10 E	560	01.09.2002 - present
Tongoa	01°11`42 S; 120°10`10 E	670	01.09.2002 - present
Tomado	01°19`34 S, 120°03`9 E	965	01.09.2002 - present

4.1.2 Gauging sites and hydrologic instrumentation

The accuracy of the record from a gauging station is generally controlled to a large extend by the physical and hydraulic characteristics of the channel in which it is placed [HERSCHY, 1978]. According to DYCK & PESCHKE [1989] the main criteria for the selection of a gauging site are a high accuracy of the measurement and a risk less monitoring of the water level. Besides these physical and safety requirements for a gauging site selection the specifications for the hydrological model of the watershed should be considered. For an optimal calibration and validation of the hydrological model the gauging sites should be well distributed within the watershed. Within the natural river system of the Palu River watershed gauging site locations, which provide all physical and hydraulic criteria and could be built within the project budget, were scarce. Due to an already existing weir construction and therefore a stable cross-section only the Takkelemo gauging site (Appendix A.1) fulfilled most criteria. The choice of final site locations of the

gauging sites was dependent on the sum of the lowest limitations of all criteria. The water levels at the chosen gauging sites were predominantly recorded with a float operated shaft encoder with integral data logger *(OTT, Kempten)*. The water level is sampled by a value every 10 min. and the resolution of the instrument amounts to 1 mm. For the monitoring of the lake water level (station Danau Lindu) also a float operated shaft encoder with integral data logger with a one hour temporal resolution was used.

In both cases the shaft encoder was installed safely inside a stilling tube that is fixed at the cross-section. For the construction of the lake station a stationary platform for the stilling tube and the staff gauge was built inside the water close to the shore of the lake (Appendix A.3). Due to a high current of the river at one gauging site (station Sopu), an installation of a stilling tube was not possible. Instead a level sensor using the touchless radar principle *(OTT, Kempten*) was set up at a bridge construction (Appendix A.2). The sensor has an integrated software filter that averages wave motion. The accuracy of the sensor lies in the range of 1 cm over the complete measuring range. Water level data are stored by a mean value every 10 minutes with a multi-channel datalogger *(OTT, Kempten).* Both water level monitoring systems were calibrated by stationary installed vertical staff gauges.

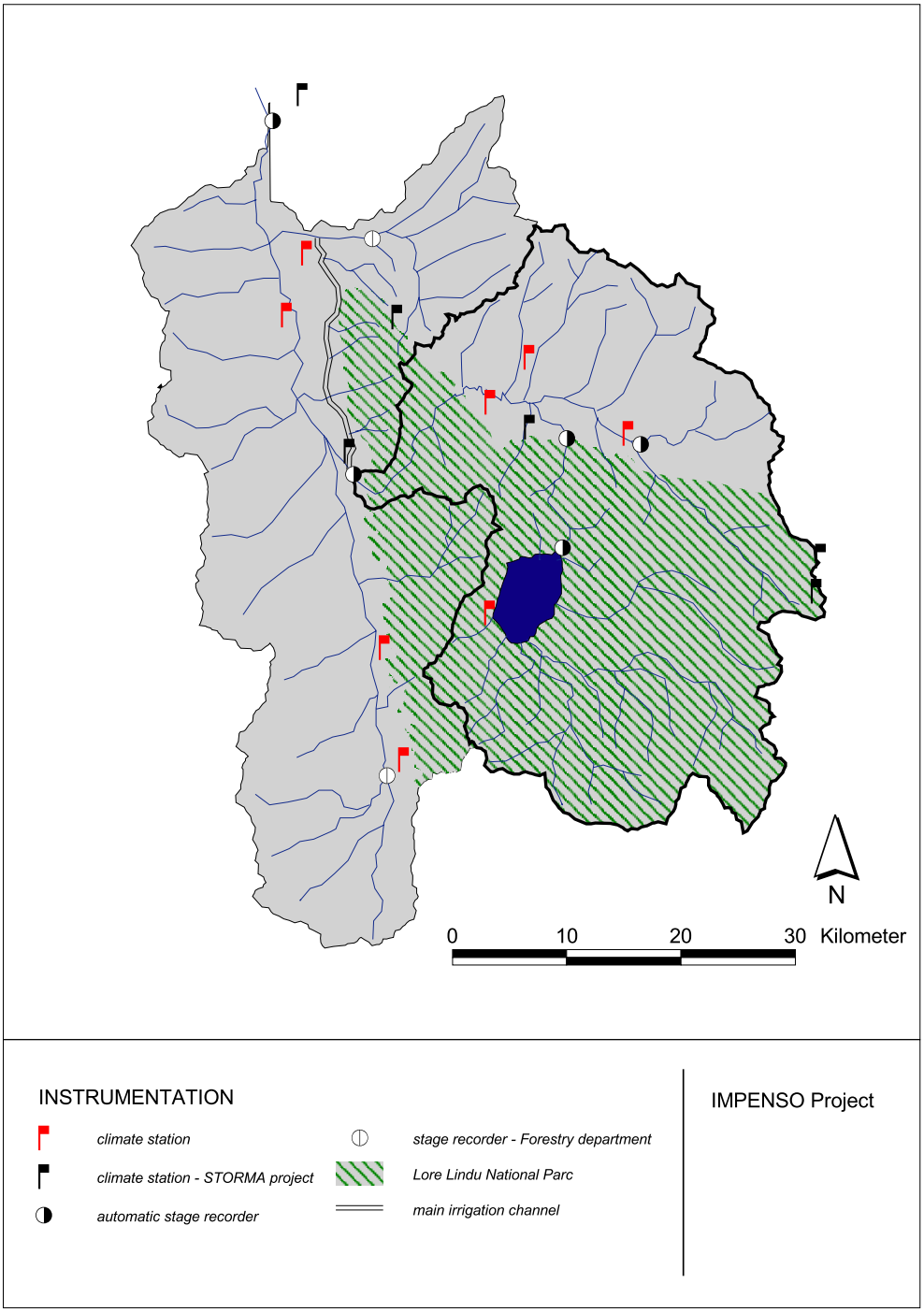

Figure 4. 1: Location of the climate and hydrological stations within the Palu River watershed, Central-Sulawesi, Indonesia.

4.2 RIVER DISCHARGE CALCULATION

4.2.1 Methods

4.2.2 Velocity-area method

The velocity-area method for the determination of discharge in open channels consists of measurements of stream velocity, depth of flow and distance across the channel between observation verticals [HERSCHY, 1995]. The mean velocity of each river profile segment is derived by flow velocity measurement at varying depths in each segment with an electromagnetic current meter *(SEBA, Kaufbeuren).* The electromagnetic current meter measurement technique employs the Faraday principle of electromagnetic induction, i.e. a magnetic field induces an electropotential in a moving conductor (water) [HERSCHY, 1999]. In order to describe the bed shape and the horizontal and vertical velocity distribution the cross-section is divided into segments by spacing verticals at a sufficient number of locations across the channel to ensure an adequate sample of velocity distribution and bed profile. In order to achieve an accurate measurement of discharge, a number of 20 - 30 segments is recommended.

For the computation of the flow velocity measurements the mid-section method is used. The method assumes that the velocity sampled at each vertical represents the mean velocity in a segment. The mean velocity is determined by electromagnetic current meter applying the 0.2 + 0.8 depth method. This method implies velocity observations on each segment at 0.2 + 0.8 m depth below the water surface. Then the average of the two readings is taken as the mean for the vertical. Finally the discharge is derived from the sum of the product of mean velocity, depth and width between verticals. According to HERSCHY [1999] the 0.2 + 0.8 depth method is universally used and gives acceptable results. A gauging station is calibrated by the velocity-area method when continuous flow velocity measurements at various water levels have been conducted. Then the discharge measurements can be transformed into a stage-discharge relationship [HERSCHY, 1978]. The analytic type of the stage-discharge relation is usually expressed by the potency equation:

$$Q = C(h + a)^n \tag{3}$$

with	Q	discharge	(m³/s)
	a	stage at zero flow	(m)
	h	stage height	(m)
	C, n	constants	

A good definition of the rating curve is dependent on the physical stability of the cross-section and the measuring conditions. It is essential to keep an established stage-discharge relationship under review in order to ascertain that its validity is maintained and to redetermine the relationship if the physical properties of the channel have been significantly altered. The accuracy of the stage discharge relationship is expressed by the mean square relative error $m_{Q(h)}$ as follows:

$$m_{Q(h)} = 100\sqrt{\frac{1}{n-1}} \cdot \sum_{i=1}^{n}\left(\frac{Q_i - \overline{Q_i}}{\overline{Q_i}}\right)^2 \tag{4}$$

with	Q_i	observed discharge	(m³/s)
	$\overline{Q_i}$	calculated discharge after stage relationship	(m³/s)
	n	number of measured values	(m)

4.2.3 Slope-area method [MANNING]

The slope-area method relates the surface slope and cross-section area to discharge [HERSCHY, 1999] and computes the discharge as follows:

$$Q = A \cdot k_{st} \cdot R^{2/3} \cdot I^{1/2} \tag{5}$$

with	Q	discharge	(m³/s)
	A	cross-section area	(m²)
	k_{st}	roughness coefficient after Strickler	

R	hydraulic radius	(m)
I	slope of water surface	(%)

This method is used especially when flow velocity measurements are not applicable [HERSCHY, 1978] as for instance by the occurrence of peak flows. The slope-area method represents in comparison to the velocity-area method a less accurate calculation of discharge.

4.2.4 Applied combined method

A stage-discharge relation is verified if discharge measurements of at least 10% of all possible ranges of water levels are available [DYCK & PESCHKE, 1989]. The operation of flow velocity measurements for the set up of a stage-discharge relationship implies measurements over a wide range of water levels. This is often not feasible for tropical catchments due to their fast rainfall-runoff relationship and their often remote location. For the calculation of discharge of the hydrological stations a combined velocity-area / slope-area method is applied in this study. In a first step all flow-velocity measurements that could be applied during the time of operation are analysed and a stage-discharge relationship is set up. Flow velocity measurements are only available for a small section of possible stages. Thus, an extrapolation of the stage discharge relationship might be incorrect. In a second step the discharge is calculated using the slope-area method where the empirical roughness coefficient k_{st} (see equation 5) is determined iteratively from discharge measurements (Chapter 4.22). HERSCHY [1999] states that in selecting a value for the roughness coefficient k_{st} (see equation 5), it is always better and more accurate to calculate these coefficients from discharge measurements on the site rather than from tables where the values could have significant uncertainties.

4.3 Uncertainties in hydrometric and meteorological measurements

In order to assess the reliability of hydrometric and meteorological measurements it is important to assess the uncertainty of the conducted measurements. The result of a measurement is only complete when accompanied by a statement of its uncertainty [HERSCHY, 1999]. In general the uncertainty is given as the range in which the

"true value" is expected to lie within specified limits. For precipitation measurements the true value of a catch at a gauge location cannot be fully assessed. The uncertainties arise mainly from the gauge design and exposure and furthermore for the calculation of the areal precipitation from the geographic extent of the network and spatial aggregation techniques. According to SEVRUC and KLEM [1989] up to 20 % of precipitation uncertainties are due to wind field deformation. Also in hydrological measurement there are many different sources of errors. In general the overall uncertainty of a measurement depend upon the standard of construction of the gauging station, the correct application of the design specifications and a number of other factors. Unlike precipitation measurement streamflow measurements are amenable to statistical analyses. Due to precise measurements the true value lies within the relative small uncertainty limits which can be almost negligible. The uncertainty of the stage-discharge relationship is expressed by the prementioned mean square relative error $m_{Q(h)}$ (see equation 17). The following threshold values of $m_{Q(h)}$ should not be exceeded [DYCK & PESCHKE, 1989]:

low water	20%	$(Q \leq 0.5MQ)$
mean water	5%	$(0.5MQ < Q \leq 2MQ)$
high water	10%	$(Q > 2MQ)$

The threshold values for the different parts of the stage-discharge relationship differ due to diverse hydrological processes and measurement methods. The comparative high threshold value for low flow is related to a higher percentage of possible measurement errors due to the relative higher weight of sedimentation and erosion effects compared to the cross-section of average and high water discharges.

4.4 Discharge calculation for IMPENSO gauging sites

The discharge calculation of the different gauging sites cross sections are conducted with different methods and therefore accuracy. Finally the applied discharge calculation method mainly depends on the physical and hydraulic characteristics of the cross section for each gauging site. These determine if the flow-velocity area method can be applied with the available hydrometric equipment. As for instance in

case of very strong river current when flow velocity measurements, involving wading or a boat on the river are not possible. Here cableway gauging or bridge measurements that require a winch or a reel mounted on a portable crane are indispensable. This equipment unfortunately exceeded the project's budget. The available electromagnetic current meter can only be used for wading or boat measurements. A statistical error analysis of discharge calculation can only be applied if the velocity-area method is feasible for the cross section, because the calculated discharge is presumed as the "true value". The exclusive set up of a stage-discharge relationship for the calculation of discharge is not sufficient for the gauging sites of the research area, because the small range of level fluctuations, where measurements are possible, do not allow any extrapolation of the stage-discharge relationship. Finally, the discharge was calculated by the slope-area method with an iterative calibration of the roughness coefficient k_{st} (equation 5). The following tables (Tables 4.2-4.7) list the IMPENSO gauging sites and the corresponding methods and evaluations of discharge calculation.

Table 4. 2: Detailed description of discharge calculations, Takkelemo gauging site

TAKKELEMO GAUGING SITE	
Location	1°11`42S, 120°10`10E; 650 m.a.s.l
Physical and hydraulic characteristics of cross-section	Rectangular cross-section, 20 m bed width, constructed weir with concrete bed profile
Sensor	Float operated shaft encoder with integral data logger (OTT, Kempten)
Monitoring period	01.09.2002 - present
Velocity-area method	20 segment measurements by wading, due to the low stage of mean water only one flow velocity measurement per section
$m_{Q(h)}$ **stage-discharge relation**	11.84 %
combined method	Calibrated roughness coefficient k_{st} : 19
$m_{Q(h)}$ **combined method**	13.23 %
Uncertainties	Flow velocity measurements only carried out at low stage

Table 4. 3: Detailed description of discharge calculations, Sopu gauging site.

SOPU GAUGING SITE	
Location	1°11`12S, 120°06`46E; 632 m.a.s.l.
Physical and hydraulic characteristics of cross-section	Parabolic cross-section, 30 m bed width, natural bed profile with detritus, steep slope, high flow velocity
Sensor	Radar level sensor *(OTT. Kempten)* with a multi-channel datalogger *(OTT, Kempten)*
Monitoring period	01.09.2002 - present
Velocity-area method	Due to the high flow velocity and the mean stage wading not possible, no adequate equipment for bridge measurement available, control flow velocity measurements at a control cross-section downstream with boat
Slope-area method	k_{st} [ACHTEN, 1991]
Uncertainties	Because no control flow velocity measurements could be conducted a statistical validation was not possible

Table 4. 4: Detailed description of discharge calculations, Gumbasa Irrigation gauging site

GUMBASA IRRIGATION GAUGING SITE	
Location	1°12`54S, 119°56`42E, 121 m.a.s.l.
Physical and hydraulic characteristics of cross section	Rectangular cross section, 11 m bed width, constructed irrigation channel with concrete bed profile
Sensor	Float operated shaft encoder with integral data logger (OTT, Kempten)
Monitoring period	01.09.2002 - present
Velocity-area method	no adequate equipment for measurements
Slope-area method	k_{st} [ACHTEN, 1991]
Uncertainties	Because no control flow velocity measurements could be conducted a statistical validation was not possible

Table 4. 5: Detailed description of discharge calculations, Gumbasa gauging site.

GUMBASA GAUGING SITE	
Location	1°12`54S, 119°56`42E, 121 m.a.s.l.
Physical and hydraulic characteristics of cross section	Rectangular cross-section, 40 m bed width, constructed weir with paved bed profile
Sensor	Float operated shaft encoder with integral data logger (OTT, Kempten)
Monitoring period	01.09.2002 - present
Velocity-area method	no adequate equipment for bridge measurement available
Slope-area method	k_{st} [ACHTEN, 1991]
Uncertainties	Because no control flow velocity measurements could be conducted a statistical validation was not possible

Table 4. 6: Detailed description of discharge calculations, Danau Lindu gauging site.

DANAU LINDU GAUGING SITE	
Location	1°19`34S, 120°03`9E; 965 m.a.s.l.
Physical and hydraulic characteristics of cross-section	Cross-section located at the outlet of lake Lindu (01°16`23S, 120°06`32E), triangular cross-section, 35 m bed width, natural bed profile with lake sediments, moderate slope
Sensor	Float operated shaft encoder with integral data logger (OTT, Kempten)
Monitoring period	01.09.2002 - present
Velocity-area method	17 segments measurements by boat
$m_{Q(h)}$ **stage-discharge relation**	6.2 %
Combined method	Calibrated roughness coefficient k_{st} : 20
$m_{Q(h)}$ **combined method**	7.7 %
Uncertainties	No stable cross section, limited range of flow velocity measurements

Table 4. 5: Detailed description of discharge calculations, Palu River gauging site.

PALU RIVER GAUGING SITE	
Location	0°54`95S, 119°54`33' E, 74 m.a.s.l.
Physical and hydraulic characteristics of cross section	Trapezoidal cross section, 60 m bed width, constructed channel with natural river bed, high sedimentation rate
Sensor	Float operated shaft encoder with integral data logger (OTT, Kempten)
Monitoring period	01.09.2002 - present
Velocity-area method	no adequate equipment for measurements
Slope-area method	k_{st} [ACHTEN, 1991]
Uncertainties	Due to sedimentation problems of shaft encoder no recording of low flows = stagnant level for low flows Because no control flow velocity measurements could be conducted a statistical validation was not possible

For the Gumbasa (Tables 4.4/6) and Sopu (Table 4.3) gauging sites flow velocity measurements with the available equipment were not feasible. They do however represent key locations for the set up of the hydrological model. Therefore they produce useful reference data for the calibration and validation of the hydrological model, even if the calculated discharge by the slope area method without any statistical evaluation is less accurate.

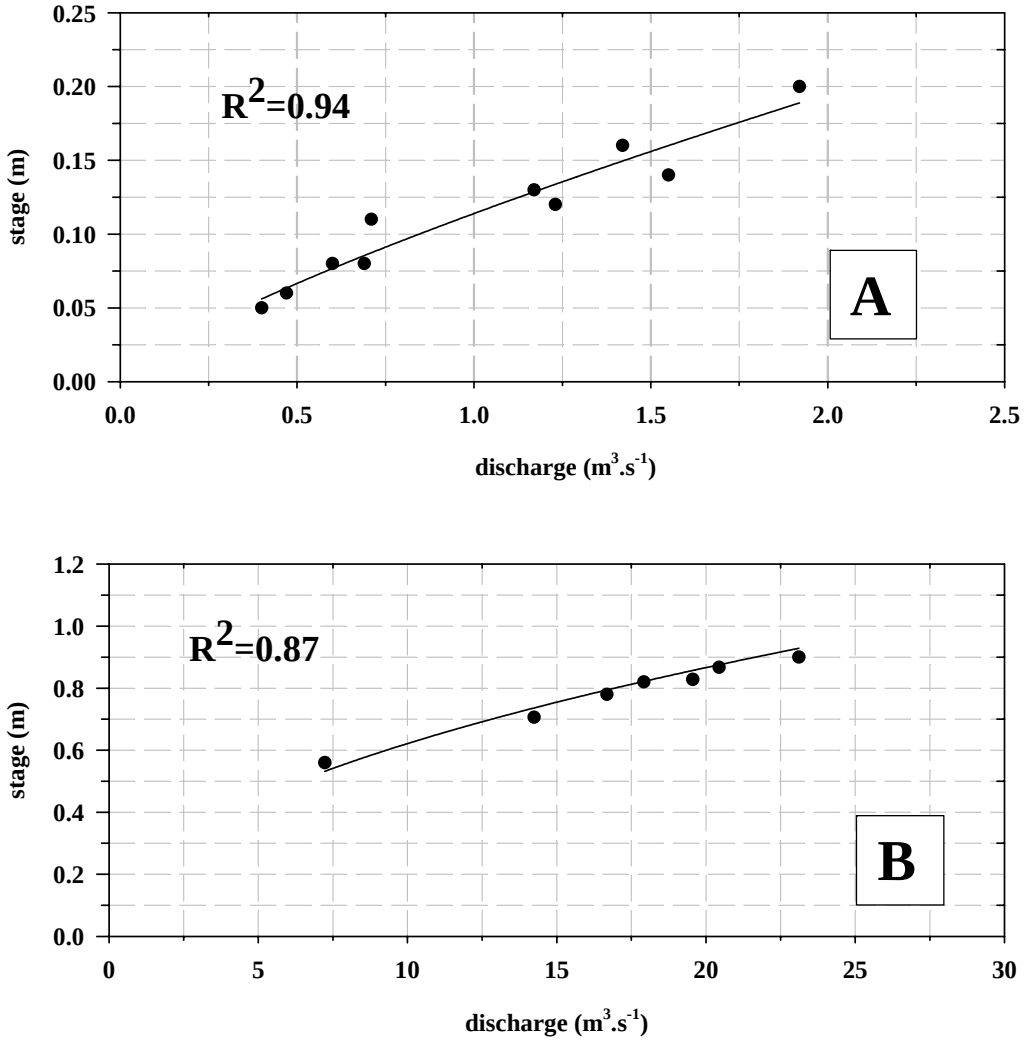

Figure 4. 2: Stage-discharge relationship for the Takkelemo gauging site (A): $Q = 14.28 * stage^{1.2295}$ and the Lake Lindu gauging site (B): $Q = 24.46 * stage^{1.4427}$.

In order to derive an analytic form of the stage-discharge function basically a power function is assumed [DYCK & PESCHKE, 1983]. Figure 4.2 describes the stage-discharge relationships for the Takkelemo and the Lake Lindu gauging sites (see Table 4.2/5), both stage–discharge relationships describe a power function. The Takkelemo gauging site has a mean daily level fluctuation from 0.03-0.43 *m* with a mean stage of 0.11 *m* for the period 01.09.2002-31.08.2004, whereas the Danau Lindu gauging site has a mean daily level fluctuation from 0.44-1.59 *m* with a mean stage of 0.88 *m* for the same period. The intervals between discharge measurements were conducted describe a too small range to prove the stage-discharge relationship. This means that even if a satisfying coefficient of agreement is derived for both stage-discharge relationships the stage-discharge relationship is limited to low water and mean discharges due to measurement restrictions. Therefore the stage-discharge relationship is extrapolated by means of the slope-area method after Manning-Strickler (equation 5) for the calculation of high water discharges. Here, the roughness coefficient k_{st} is determined iteratively on the basis of the stage-discharge relationship.

HYDROLOGICAL MODEL WASIM-ETH

5.1 MODELLING CONCEPT

The Water Flow and Balance Simulation Model (WaSiM-ETH) is a process-based fully distributed catchment model. The spatial resolution is given by a grid and the time resolution can vary from minutes to days. The main processes of water flux, storage and the phase transition of water are simulated by physically-based simplified process descriptions [SCHULLA, 1997]. The meteorological input data of the model are interpolated for each grid cell and is followed by the simulation of the main hydrological processes like evapotranspiration, interception, infiltration and the separation of discharge into direct flow, interflow and base flow. These calculations are modularly built and can be adapted to the physical characteristic of the catchments area. If for example the catchment is situated in a tropical area, modules for snow accumulation and snow melt can be deactivated. The generated discharge of all discharge components of each grid cell are then transferred by river routing into total discharge of each subcatchment, and finally of the whole catchment. The horizontal boundary condition of the model is the surface watershed divide of the catchment. The vertical boundary condition is represented by an impermeable layer in the soil. This implies that the hydrological model is a closed system, where deep percolation is not considered. The upper boundary of the hydrological model is represented by the vegetation cover. A feedback of the simulated hydrological processes on the meteorological processes is not incorporated in the modelling system, as for instance a change of the relative humidity by evapotranspiration. Hence, the model is not fully accounting for the energy conservation law.

5.2 DATA REQUIREMENTS WASIM-ETH

5.2.1 Spatial data

All spatial data is required in a raster data set (grid) with unique resolution and extension. Essential grid data include the topography land use, and soil types (Figure 5.1). Starting from the primary grid of the topography secondary grids were generated with a topography analysis program.

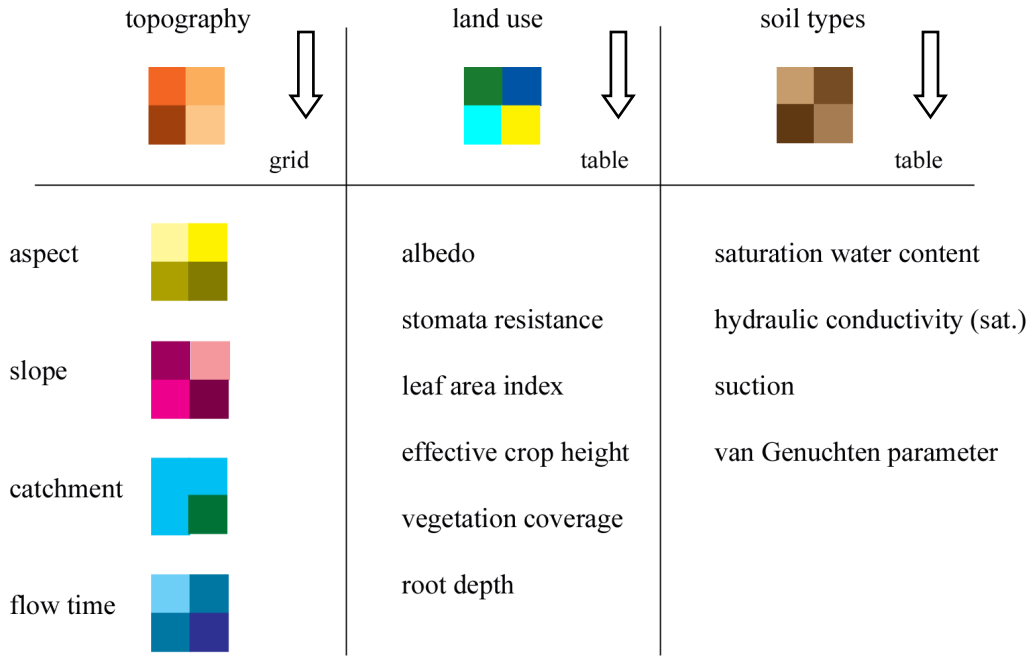

Figure 5. 1: Needed spatial data for the hydrological model WASIM-ETH (after NIEHOFF, 2001).

The WASIM-ETH package includes the topography analysis program TANALYS, which performs a complex analysis of the Digital Terrain Model (DTM), calculating secondary grids like local slope and aspect. Furthermore, it determines the automatic delineation of flow directions, sub-basin structure, flow accumulation, and the river network. The flow directions are calculated by the steepest slope of neighbouring

grid cells. Artefacts like sinks are filled interactively. After the flow directions are determined the flow accumulation is calculated. The flow accumulation represents the catchment area for each grid cell. The river network is then extracted by setting a threshold of grid cells for the flow accumulation. The flow orders identified according to *Strahler* are essential to outline artefacts like parallel rivers. A detailed description of TANALYS can be found in SCHULLA & JASPER [1999]. The land use and soil type's grids are parameterised with a land-use and a soil type table (Tables 5.4/5.5) that describes each grid cell with a parameter data set according to the grid classification.

5.2.2 Temporal data

For the simulation of the water balance in the optimum configuration within WASIM-ETH the following time series are needed:

- precipitation ($mm \cdot time\ step^{-1}$)
- air temperature (C°)
- relative humidity (%)
- wind speed ($m \cdot s^{-1}$)
- global radiation (Wh/m^2)
- relative sunshine duration (h)

If not all of the meteorological variables are available, the potential evapotranspiration can be either calculated on a daily resolution with a reduced data set after *Hamon* or *Wendling*. For the calibration and validation of the model a time series of specific discharge data *($mm \cdot time\ step^{-1}$)* for each sub-basin is required. The resolution of the temporal data sets depends on the objective of the hydrological research and the size of the watershed. During storm events an hourly resolution is essential for the simulation of the discharge dynamics [NIEHOFF, 2001]. If the long term water balance within a mesoscale catchment is the main research focus, a daily resolution is appropriate.

5.3 SPATIAL INTERPOLATION OF METEOROLOGICAL DATA

A precise interpolation of the meteorological input data is crucial for a successful simulation of the water balance. Especially the distribution of the areal precipitation has a strong effect on the simulation of the hydrological dynamics of the catchment (see Chapter 6.4.1). Before WASIM-ETH starts with the simulation of the water balance within a preprocessing routine, an interpolation of the point meteorological input data for each grid cell of the modelling catchment is conducted. With regard to the meteorological input variables three different statistical methods can be used: (1) Inverse distance weighting (IDW), (2) altitude dependent regression or (3) a weighted combination of the IDW and altitude dependent regression.

(1) Inverse distance weighting (IDW)

For the IDW-method all stations within a specified search radius are included into the interpolation. The interpolation result is the sum of all contributing weighted station data. The maximum distance and two parameters specifying the anisotropy need to be defined.

(2) Altitude dependent regression

Within this method the altitudinal dependence of meteorological variables is considered. The altitudinal gradient of each variable is defined by a physical relationship. Then the value of the variable’s time series is interpolated for each grid cell with regard to its elevation.

(3) IDW / Altitude dependent regression

Both interpolation methods are combined with respect to a specified weight of the proportion of both methods. This method allows an adaptation of the variable to the specific catchments characteristics, which might be important e.g. for the calculation of the areal precipitation.

5.4 MODEL MODULES

5.4.1 EVAPOTRANSPIRATION

Evapotranspiration (ET) is a combined term for the transfer of water vapour to the atmosphere from land surfaces with and without vegetation. It is influenced by climate, availability of water and vegetation [WANG *et al*, 2001].

Potential Evapotranspiration

The potential evapotranspiration (ETP) is the maximum amount of water that is evaporated and transpired from a reference crop when water availability is not limited. For the calculation of the potential evapotranspiration the equation after *Penman-Monteith* [MONTEITH, 1975; BRUTSAERT, 1982] is used:

$$\lambda E = \frac{3.6 \cdot \frac{\Delta}{\gamma_P} \cdot (R_N - G) + \frac{p \cdot c_p}{\gamma_p \cdot r_a}(e_s - e) \cdot t_i}{\frac{\Delta}{\gamma_p} + 1 + r_s / r_a} \qquad (6)$$

with

λ	latent vaporization heat $\lambda = (2500.8 - 2.372 \cdot T)$; T: temperature in °C	(KJ˙Kg^{-1})
E	latent heat flux in	(kg˙m^{-2})
Δ	tangent of the saturated vapour pressure curve	(hPa˙K^{-1})
R_N	net radiation, conversion from Wh˙m^{-2} to KJ-m^{-2} by factor 3.6	(Wh˙m^{-2})
G	soil heat flux (here: 0.1˙ R_N)	(Wh˙m^{-2})
p	density of dry air $p/(R_L \cdot T)$ (at 0°C and 1013.25 hPa: p =1.26)	(kg˙m³)
c_p	specific heat capacity of dry air at constant pressure c_p = 1.005	(KJ˙(Kg˙K)$^{-1}$)
e_s	saturation vapour pressure at temperature T	(hPa)
e	actual vapour pressure (observed)	(hPa)
t_i	number of seconds within a time step	(-)

γ_p	psychrometric constant	(hPa˙K^{-1})
r_s	bulk-surface resistance	(s˙m^{-1})
r_a	bulk-aerodynamic resistance	(s˙m^{-1})

In general the *Penman-Monteith* equation represents a “top-down” scaling approach. It assumes that the canopy is reacting as if it is a “big leaf” [BONELL & BALEK, 1993]. Even though steady state conditions are assumed, the evaporaration-rate can be calculated with any temporal resolution. For the calculation of the transpiration of water bodies (e.g. lake), the approach is an approximation since the temperature of the water body also controls the transpiration rate [MENZEL, 1999].

Real Evapotranspiration

For the calculation of the real evapotranspiration (ETR) the relation between the actual soil water content θ and the actual capillary pressure ψ , which is described by the *van Genuchten* parameters of the actual soil is used. This implies that besides a reduction as a result of dry soils also the impact of too wet soils is accounted for. Some parameters of the *Penman-Monteith* equation are not obtained from measurements, but can be derived from secondary parameters. The secondary parameters, which are needed as input data for the evapotranspiration module are the following:

R_C	surface resistance	(s˙m^{-1})
LAI	leaf area index	(-)
v	vegetation coverage degree	(-)
α	albedo	(-)
z_0	effective crop height	(m)
z_w	root depth	(m)
p	root distribution	(-)
ψ_g	minimum suction for reducing ETR compared to ETP	(hPa)

For daily calculation of potential evapotranspiration the temperature is modified by a subdivision of the *Penman-Monteith* approach into day and night. The calculation of the potential evapotranspiration with secondary parameters and the used equations

for a model run with daily time steps are described in detail in SCHULLA [1997].

5.4.2 INTERCEPTION

Interception (EI) is the storage of precipitation on the foliage of vegetation or other surfaces. Within WASIM-ETH only a single storage is used, which integrates all interception effects. After SCHULLA [1997] the interception is calculated as follows:

$$SI_{\max} = \nu \cdot LAI \cdot h_{SI} + (1-\nu) \cdot h_{SI} \qquad (7)$$

with	$SI_{\max}$	maximum interception storage capacity	(mm)
	ν	degree of vegetation coverage	($m^2 \cdot m^{-2}$)
	LAI	leaf area index	($m^2 \cdot m^{-2}$)
	h_{SI}	maximum height of water	(mm)

The capacity of the storage is regulated by the Leaf area index (LAI), the vegetation coverage degree, and the maximum height of water on the leaves. For the latter it is assumed that the height of water on the foliage is constant for different kind of land use and various types of precipitation. The extraction of the interception storage is simulated with the potential evapotranspiration after equation 1. The storage content is reduced by the potential evapotranspiration, but when the storage content is smaller than the potential evapotranspiration rate, the remaining rate will be taken from the soil.

EI = ETP	(for SI ≥ ETP in mm),	ETR = 0	(8)
EI = SI	(for SI < ETP in mm),	ETR = ETP-SI	

with	EI	interception evaporation	(mm)
	ETP	potential evaporation	(mm)
	ETR	remaining evaporation from soil and vegetation	(mm)
	SI	content of the interception storage	(mm)

If the interception storage is filled, further precipitation is defined as throughfall, which is the input for the infiltration and soil model.

5.4.3 INFILTRATION

The infiltration capacity of a soil determines the generation of storm runoff. The calculation of the infiltration is carried out after the approach of PESCHKE [1977, 1987], which is based on the theory of GREEN & AMPT [1911]. This approach assumes that the soil is a homogeneous and unlayered matrix, where the matrix flow dominates over the makroporeflow. Further it is assumed that the wetting front is a step function, which is separated with initial moisture θ_0 from the saturated soil with the saturated moisture θ_S. For the calculation of the infiltration this approach is divided into two phases. During the first phase, also defined as the saturation phase, the time until all precipitation is infiltrated is calculated. Afterwards in the next phase the cumulated infiltration until the end of the time step is calculated. The part of precipitation, which exceeds the infiltration, is generated as direct runoff.
The first phase (saturation time) is calculated by:

$$\text{if } PI > K_S \qquad t_S = \frac{l_S \cdot n_a}{PI} = \frac{\frac{\psi_f}{PI/K_S - 1}}{PI} \tag{9}$$

with	t_S	saturation deficit from the beginning of the time step	(h)
	l_S	saturation depth	(mm)
	n_a	fillable porosity ($n_a = \theta_S - \theta$)	(-)
	ψ_f	suction of the wetting front ($\approx 1000 n_a$)	(mm)
	PI	precipitation intensity	($mm \cdot h^{-1}$)
	K_S	saturated hydraulic conductivity	($mm \cdot h^{-1}$)

Then the infiltrated amount of water to the time F_S is calculated:

$$F_S = l_S \cdot n_a = t_S \cdot PI \tag{10}$$

At last within the second phase the cumulated amount of infiltration after saturation for one time step is determined after PESCHKE [1989]:

$$F = \frac{A}{2} + \left[\frac{A^2}{4} + AB + F_S{}^2 \right]^{1/2} \tag{11}$$

with $A = K_S (t - t_S)$

$B = F_S + 2 \cdot n_a \cdot \psi_f$

In reality barely a soil matrix does not exist, and generally the water that infiltrates exceeds the calculated amount. This effect is considered deterministically by the implementation of parameter $x_{f,}$ which controls the amount of reinfiltrating water. Especially if larger grid cells are applied, this correction might be important to take into account inhomogenities of the soil properties.

5.4.4 SOIL MODEL

For modelling of the vertical fluxes within the unsaturated zone WASIM-ETH uses the *Richard Equation* [RICHARDS, 1931; PHILIPS, 1969] that is given by:

$$\frac{\delta\theta}{\delta t} = \frac{\delta q}{\delta z} = \frac{\delta}{\delta z}\left(- K(\theta) \frac{\delta \Psi(\theta)}{\delta z} \right) \tag{12}$$

with			
	θ	water content	($m^3 \cdot m^{-3}$)
	t	time	(s)
	k	hydraulic conductivity	($m \cdot s^{-1}$)
	Ψ	hydraulic head (Σ suction ψ and geodetic altitude h)	(m)
	q	specific flux	($m \cdot s^{-1}$)
	z	vertical coordinate	(m)

The soil is discredited into several layers that show the same thickness and soil properties. If the soil is saturated the equation for saturated flow after *Darcy* is used.

The parameterisation of the needed soil physical properties for unsaturated flow can be carried out by the application and adjustment of the soil water retention curve, which is described by the empirical equation of *van Genuchten* [VAN GENUCHTEN, 1980]:

$$\theta(\psi) = \theta_r + \frac{\theta_s - \theta_r}{\left(1 + (\alpha|\psi)^n\right)^m} \tag{13}$$

with	θ	actual water content	(-)
	ψ	suction	(hPa)
	θ_r	residual water content at $k(\theta) = 0$	(-)
	θ_s	saturation water content	(-)
	α, n	empirical parameter (m=1-1/n)	(-)

The calculated empirical parameters α, n, and the saturated hydraulic conductivity are then used for the calculation of the unsaturated conductivity function $K(\psi)$. Within WASIM-ETH the soil hydraulic parameters for the water retention curve and the conductivity function are essential input parameters for the soil model.

Calculation of interflow

Interflow is a result of conductivity, river density and hydraulic gradient:

$$q_{ifl} = k_s(\theta_m) \cdot \Delta_z \cdot d_r \cdot \tan\beta \tag{14}$$

with	k_s	saturated hydraulic conductivity	($m \cdot s^{-1}$)
	θ_m	water content in the actual layer matrix	(-)
	d_r	river density (scaling parameter)	(-)
	β	local slope angle	(°)
	Δ_z	layer thickness	(m)

Calculation of baseflow

If WASIM-ETH is run without the groundwater module, baseflow is generated in a conceptual way, because no lateral exchange between grid cells is possible:

$$q_b = Q_0 \cdot k_s \cdot e^{\left(h_{gw} - h_{geo,0}\right)/k_b} \tag{15}$$

with	Q_0	scaling factor for baseflow	(-)
	k_s	saturated hydraulic conductivity	($m \cdot s^{-1}$)
	h_{gw}	groundwater table	(m.a.s.l.)
	$h_{geo,0}$	soil surface	(m.a.s.l.)
	k_b	recession constant for baseflow	(m)

Adjustable parameters for calibration

Using the Richards equation within WASIM-ETH the empirical adjustable calibration parameters are:

d_r	(scaling parameter river density for the calculation of interflow)
k_{rec}	(recession constant for the saturated hydraulic conductivity with increasing soil depth)
Q_0	(scaling factor for baseflow)

5.4.5 DISCHARGE ROUTING

For the simulation of the discharge routing the drainage structure and hydraulic parameters as well as geometric data of the channels is required. The method is conducted by routing each tributary through a separate channel to the outlet where all discharges are summed up. The routing description includes a definition of the tree structure of the catchment until the outlet of the entire basin is reached. Further external and internal inflows, abstraction and reservoirs can be added. Further the description specifies the sub-basin for which the tributaries are routed, the sub-basin area, zone code of the tributary, external or internal inflows, geometry of the channel and the flood plain, mean slope angle of the channel, Manning-Strickler roughness

parameters for mean channel and flood plains, and length and sub-basin area of the tributary. Basis for the calculation of flow times is the flow equation after Manning-Strickler:

$$v_l = M \cdot R_h^{2/3} \cdot I^{1/2} \tag{16}$$

with	v_l	flow velocity	$(m \cdot s^{-1})$
	M	roughness parameter after Manning Strickler	$(m^{1/3} \cdot s^{-1})$
	R_h	hydraulic radius	(m)
	I	slope	$(m \cdot m^{-1})$

For the calculation of R_h a definition of the river depth and width for each routing channel is needed. It is assumed that the channels have a rectangular shape and are divided into the main river channel and the flood channel. Flow velocity will increase following a raise of the river stage due to a changing hydraulic radius. The discharge for each stream link of the river number grid is the product of the calculated flow velocity and the flow cross section. The flow time *t* is linked to the calculated flow velocity and is defined as the time the water needs to cross each grid cell of the actual river link.

5.4.6 Reservoir

Within WASIM-ETH reservoirs are considered as storages. The abstraction rule or a single linear storage approach describes the reservoir retention impact within the routing structure.

5.4.7 Irrigation

Irrigated paddy fields within the catchment are represented by ponded areas. A pond depth grid is created which contains for each grid cell the maximum storage capacity of the pond in mm. During the simulation of the water balance evaporation is firstly taken from ponding water before unsaturated zone flow is started.

5.5 CALIBRATION OF WASIM-ETH

The calibration of the hydrological model WASIM-ETH is carried out by a combination of the trial-and-error adjustment and an automatic parameter estimation method. The first step of calibration implies a manual parameter assessment through a number of calibration runs. A combination of a graphical and statistical assessment of the simulated versus the observed hydrograph is conducted. REFSGAARD & STORM [1996] recommend that in a calibration numerical criteria should only be used for guidance. Even if the graphical comparison is more subjective, it provides a good overall indication of the models capabilities. In a second step the automatic parameter estimation method takes the advantage from the earlier carried out trial- and error method, because realistic lower and upper limits of the adjustable parameters are determined by the first method. Within this second phase of calibration a fine adjustment of calibration parameters is made. This method involves the use of a numerical algorithm, which finds the extreme of a given numerical objective function [REFSGAARD & STORM, 1996]. The combination of these two widely used methods uses the advantage of the fast optimization of the automatic parameter estimation method for the fine adjustment of the beforehand manually calibrated adjustable parameters. Therefore the definition of clear adjustable parameter boundaries for automatic parameter estimation is essential to minimise the risk that the optimization process results in a local instead of a global optimum.

5.5.1 Numerical evaluation of model performance

With the simulation run of WASIM-ETH the coefficient of efficiency R^2 after NASH & SUTCLIFFE [1970] is calculated:

$$R^2 = 1 - \frac{\sum_{i=1}^{N} \varepsilon_i^{\,2}}{\sum_{i=1}^{N} \left(x_i - \bar{x}\right)^2} = 1 - \frac{\sum_{i=1}^{N} \left(y_i - x_i\right)^2}{\sum_{i=1}^{N} x_i^{\,2} - \frac{1}{N\left(\sum_{i=1}^{N} x_i\right)^2}} \qquad (17)$$

with	i	time step	(-)
	y_i	simulated value	(mm · time step^{-1})
	$x_i, \bar{x}$	observed value, mean observed value	(mm · time step^{-1})
	ε_i	derivation observed/modelled at time step i	(mm · time step^{-1})
	N	number of time steps used for calculating R^2	(-)

The coefficient of efficiency R^2 ranges from minus infinity to 1.0 with higher values indicating better agreement. The performance criterion R^2 represents the most common statistical technique in hydrological modelling for quantitative assessment of the degree to which the model simulation matches the observation. For model evaluation purpose the coefficient of efficiency represents an improvement over the widely used coefficient of determination, because it is sensitive to differences in the observed and model-simulated means and variances [LEGATES & McCABE, 1999]. For a further assessment of the model performance the index of agreement *d* after WILLMOT [1981] is calculated:

$$d = 1 - \frac{\sum_{i=1}^{N} (x_i - y_i)^2}{\left(\left| y_i - \bar{x} \right| + \left| x_i \bar{x} \right| \right)^2} \tag{18}$$

The index of agreement overcomes the insensitivity of correlation-based measures to differences in the observed model-simulated means and variances. The index of agreement *d* lies in the range of 0.0 – 1.0 with higher values indicating better agreement. Both the coefficient of efficiency and the index of agreement are sensitive to extreme values, owing to the squared differences. This implies sensitivity to outliers and high values in both statistical methods. To quantify the occurrence of outliers in terms of units, the mean absolute error *(MAE)* and the mean square error *(RMSE)* are calculated:

$$MAE = N^{-1} \sum_{i=1}^{N} \left| x_i - y_i \right| \tag{19}$$

$$RMSE = \sqrt{N^{-1}\sum_{i=1}^{N}(x_i - y_i)^2} \tag{20}$$

The degree to which *RMSE* exceeds *MAE* serves as an indicator of the extend to which outliers (or variance in the difference between the modelled and observed values) exist in the data [LEGATES & McCABE, 1999]. LEGATES and McCABE [1999] conclude that a complete assessment of model performance should include one "goodness-of-fit measure" (e.g. R^2, *d*) and at least one absolute error measure (e.g. *RMSE*, *MAE*).

In order to evaluate the general model performance of the distributed hydrological model ANDERSEN *et al*. [2001] suggest the following graduation of the achieved model efficiency.

Table 5. 1: Model performance criteria after ANDERSEN *et al.* [2001].

performance	D_v	R^2
very good (1)	<5	>0.95
good (2)	5-10	0.85-0.95
fair (3)	10-20	0.70-0.85
poor (4)	>20	<0.70

D_v describes the volume error and R^2 the coefficient of efficiency after NASH & SUTHCLIFFE [1972]. Because the volume error might balance negative and positive deviations of the whole calibration period in this study, it is not considered as a statistical measure of model efficiency. In general these specified model performance criteria can only serve as a rough guide to classify the achieved model performance.
The overall model performance should be assessed by a combined evaluation of statistical and graphical performance. Additionally a qualitative analysis of the simulated components of the water balance should be carried out. Even if a very good statistical accordance of observed and simulated discharge is achieved, it does

not necessarily mean that the components of the water balance are simulated equally well.

5.5.2 Automatic calibration

Generally automatic calibration implies software that makes use of a certain algorithm to determine an optimum of adjustable parameters. PEST *(Parameter ESTimation)* is a commonly used model-independent parameter estimation software, which was developed by DOHERTY [1994]. In general PEST can be coupled to any nonlinear simulation model and assists in data interpretation, estimation of adjustable parameters and predictive analysis tasks. When running PEST in a parameter estimation mode, it takes control of the model and runs it as many times as necessary in order to determine the optimal parameter set [DOHERTY, 1994]. Within a control file it is possible to define the lower and upper limit of the adjustable parameters of the model. For parameter estimation PEST uses the nonlinear *Gauss-Marquardt-Levenberg algorithm*. [DOHERTY, 1994]. This method requires that the dependence of model-generated observation counterparts on adjustable parameters is continuously differentiable. Parameter estimation is an iterative process. At the beginning of each iteration the derivatives of all observations are calculated with respect to all parameters. This implies that the relationship between model parameters and model-generated observations is linearised by formulating it as a Taylor expansion about the currently best parameter set. New parameters are tested by running the model again. Then the parameters changes and objective function improvement are compared with those achieved in previous iterations. If no further parameter optimization can be achieved, PEST stops the parameter optimization process and records the optimized values of each adjustable parameter. A detailed description of the parameter estimation algorithm used by PEST can be found in DOHERTY [1994].

5.6 VALIDATION AND PREDICTIVE UNCERTAINTY ANALYSIS

For the validation of the calibrated hydrological model the common used split-sample test is applied and the statistical outcomes are compared with the achieved model efficiencies of the calibration run. Besides the validation of the hydrological model, also the overall parameter uncertainty should be analysed. During the calibration of the model various suitable optimum parameter sets are determined. Once a parameter set has been determined that shows best model and system behaviour, it should be tested whether another parameter set exists which also results in reasonable simulation by the model of the system under study [DOHERTY, 1994]. The ramifications of different used parameter sets are extremely important for further predictions, as for example a scenario analysis. The classical “sensitivity analysis” is not feasible to assess parameter uncertainties because the model is immediately uncalibrated as soon as any parameter is varied from the calibrated value. To fully explore the repercussions of parameter nonuniqueness the parameters must therefore be changed in such a way that the objective function hardly changes.

PEST assists to identify parameter uncertainty with the application of a predictive uncertainty analysis. The range of parameter values, which can be considered to calibrate the model, can be quite large. In most instances of model calibration only a single set of parameters lying within the calibration range of the objective function is applied for predictive analysis. The applied analysis generates a couple of optimal parameter sets by defining a range ($\Phi_{min} + \delta$) around the minimum objective function (Φ_{min}). Within this range the model can be considered to be calibrated. The predictive analysis determines iteratively the critical-point, where maximum model prediction is compatible with calibration imposed constraints on parameter values (Figure 5.2). Thereafter PEST calculates the model prediction that is associated with the determined critical point.

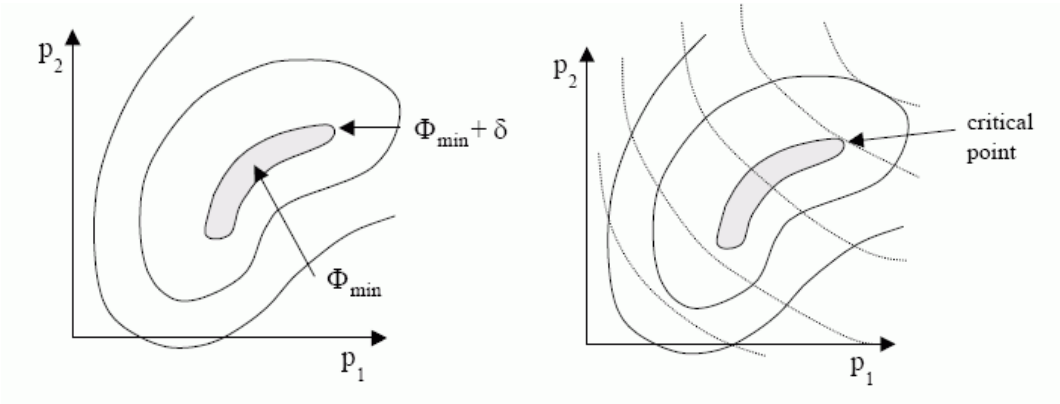

Figure 5. 2: Objective function contours in parameter space for a nonlinear model and the critical point in parameter space (DOHERTY, 1999).

MODEL APPLICATION:

GUMBASA RIVER CASE STUDY

The modelling approach focuses on the tributary Gumbasa River catchment which covers an area of 1275 km². The limitation of the application of the hydrological model to this tributary catchment is due to several reasons. First of all the Gumbasa River catchment represents the catchment area of the greatest irrigation scheme of the Palu River catchment. The diversion of the irrigation scheme is located shortly before the confluence of the Gumbasa and Palu River. Therefore at the same time the water availability of the Irrigation scheme is simulated, which allows to formulate water availability scenarios for agricultural water use of ca. 10000 ha of irrigated paddy fields. Further downstream along the Palu valley several hydraulic constructions regulate the distribution of the irrigation water, and are mainly regulated by the water demand of the different farmers due to the actual water availability situation. Therefore the simulation of the water balance of the Palu valley would be restricted by a lack of knowledge about the settings of the hydraulic irrigation constructions. A second limitation of the hydrological model application of the whole Palu river catchment is related to the potential leakage of the lower boundary layer of the Palu valley which might lead to major miscalculations of the simulated water balance of the applied hydrological model. Even if a geological connection to the deeper groundwater layer can not be excluded for the Sopu and Lindu valley, this influence might be more significant for the Palu valley. The river bed of the Palu River marks the line of the major Palu fault, whereas the secondary faults of the Sopu and Lindu basin [GARRELTS, 2000] might have a weaker connection to the deeper groundwater layers. Due to a lack of geohydrological research within the Palu River catchment these conclusions are only based on the broad geological knowledge of the research area, but serve as an important consideration for the selection of the catchment area of the applied hydrological model. In general vertical leakage can not be excluded for most of the hydrological model applications, but a careful selection of

the catchment area can mitigate this effect. In a first step the adaptability of the chosen hydrological model WASIM-ETH has been tested and evaluated on a small tributary catchment of the Gumbasa River catchment. The selected Takkelemo catchment covers an area of 79 km². Here, the special focus of the hydrological model was on the parameterisation of the soil and land use parameters and the choice of grid size of the raster cells. Further the performance of all components of the water balance was analysed and evaluated. On the basis of ideal conditions for discharge measurements for calibration and validation purpose and a manageable modelling size the Takkelemo catchment serves as an adequate test catchment site.

6.1 SPATIAL DATA AVAILABILITY

Table 6. 1: Details of spatial data for the Gumbasa River case study.

Theme	Derived from	Grid resolution	Source
DTM	TK50 (1980) 1:50,000	50, 250, 500 m	SciLands GmbH
SOIL MAP (PHA)	DTM	50, 250, 500 m	SciLands GmbH
LAND USE	Landsat/ETM+ 24th August 2001 28th September 2002	30 m	SFB-552

The needed spatial data like the Digital Terrain model (DTM), Soil and Land Use Map is derived from various sources. Table 6.1 gives an overview of the spatial data of the study area and its sources. The particular data sets are described in detail in the following sections.

6.1.1 Digital Terrain Model

The basis for most of the needed spatial data for the application of a hydrological model is the Digital Terrain Model (DTM). The DTM of the Palu River catchment is generated from digitised contour lines from topographic maps (TK50, 1:50,000) with the SAGA (**S**ystem for Automatic Geoecological Analysis) software and has a grid cell size of 50 m. Due to the relatively high equidistance of the counter lines (25m) artefacts might occur in the smoothly sloped basins [SCILANDS, 2003]. This effect leads to an overall uncertainty of the DTM especially in smoothly sloped areas like e.g. basins or valleys.

6.1.2 Soil Map

The only available soil map of the research area is the soil map of Indonesia (1:1,000,000), which is based on available exploration soil maps that were published in various years [PUSAT ATLAS NATIONAL, 2000]. The application of this unique soil type map as input spatial data is limited by its coarse scale. Furthermore a regionalization of the conducted soil research data of the SFB-552 within the research area is not feasible. The soil samples were mainly taken in the accessible Sopu and Napu valley. This lumped representation of soil data without any scattered elevation distribution does not allow a meaningful statistical regionalisation of soil types. Therefore instead of using this inadequate source of spatial soil data a more general topographic based approach that classifies potential homogeneous areas (PHA) has been applied [see SCILANDS, 2003]. This topographic approach assumes that texture classes and bulk density mainly affect the soil physical properties and depend on slope degree and geomorphologic location (basin, valley, slope, summit area). For the classification of PHA`s complex morphometric terrain factors are calculated on the basis of the DTM. The relevant classification factors are the relative altitude above channel line (a.a.c.l.), catchment area and slope angle. Table 6.2 lists the classified PHAs and its corresponding morphometric terrain factors.

Table 6. 2: PHA classification and its corresponding morphometric terrain factors.

	Morphometric description	**mean values**		
		m.a.s.l. (m)	a.a.c.l. (m)	slope (°)
I	Intramontane basin (low altitude above channel line)	591.46	2.68	1.60
II	Intramontane basin (moderate altitude above channel line)	453.80	8.00	2.50
III	Valleys outside the intramontane basin catchment (large catchment area)	802.05	5.17	9.31
IV	Valleys outside the intramontane basin catchment (moderate catchment area)	1154.31	3.71	12.14
V	Slope with moderate inclination	1191.37	88.13	17.43
VI	Slope with strong inclination	1143.57	121.84	30.77
VII	Summit area with low inclination	1337.96	87.88	5.31
VIII	Summit area with moderate inclination	1340.72	168.00	12.74

6.1.3 Land use

The main land use classification was derived from a Landsat/ETM+ classification from 2001 and 2002 respectively, both generated by the Department of Cartography, GIS & Remote Sensing, Institute of Geography, University Göttingen. The main difference between the two classified Landsat/ETM scenes is the applied classification technique. The first land use classification map of the research area was generated from a Landsat/ETM+ Scene of 24th August 2001 by a supervised maximum likelihood classification. The second classification map was generated from a Landsat/ETM+ Scene of 28th September 2002. Here an object oriented image classification technique (ecognition®) with defined rules was conducted. The use of different classification techniques results in variable land use classifications. For example the land use classification of 2001 distinguishes between annual crops (maize, cassava etc.) and perennial crops (cacao, coffee), whereas the 2002 classification integrates these two classes as plantations. Another difference between the two classifications is the applied preprocessing routine. The 2001 scene was only geometrically corrected, whereas the 2002 scene additionally was atmospherically and topographical corrected. Though the research area undergoes rapid land use changes, the 2002 land-use classification at first seemed to be more suitable as spatial

input data for the application of the hydrological model. On the other hand major land use misclassifications could be identified for the land-use classification derived from the object oriented image classification (2002 scene). Furthermore the distinction of the land-use classes in annual and perennial crops is meaningful for the simulation of interception and evapotranspiration. The 2002 land use classification map became available in late October 2004. At that time the hydrological model of the Gumbasa catchment was already calibrated. To start a complete new calibration with a possibly partly imprecise land-use classification was not reasonable, and the classification of 2001 was taken as a base land use map (see Appendix B.6). But in the long run it is recommended to apply both land use classifications and thereafter analyse the impact on the choice of land use classification technique and date on the model performance. Land use classification maps based on satellite data as spatial input data represent a source of uncertainty for hydrological model application. The final classification depends on the used technique and the research area knowledge of the producer.

6.2 TEMPORAL DATA AVAILABILITY

The source of temporal data is based on own measurements (see Chapter 3; 4) and climate station data of an associated project (IBK, Göttingen University). For the regionalisation of the climate variables wind speed and solar radiation the station network is limited to the available meteorological data, because these climate variables were not recorded by the station network that was set up within this work.

6.3 PREPROCESSING

The preprocessing for hydrological model application comprises the normalisation of all spatial data and its parameterisation [SCHULLA, 1999]. In addition the initial values for the adjustable parameters are estimated. For WASIM-ETH all spatial data is required in a raster data set (grid) with unique resolution and extend. All spatial data sets have to be refined to the applied grid resolution and extend of the hydrological model. The choice of grid size mainly is related to the spatial variability of the modelling parameters. Furthermore the characteristic morphological length, which describes the length of slope, should be considered. Because the altitude dependence determines most of the meteorological input variables, an appropriate

choice of grid size should consider the length of slope. SCHULLA [1999] has investigated the sensitivity of grid size on model efficiency for the mountainous Thur basin, which covers an area of 1700 km². He concludes that for mountainous catchments the grid size threshold value for an acceptable performance of the hydrological model ranges between 1000*m**1000*m* till 2000*m**2000*m*. If a coarser grid size is chosen, the model efficiency declines rapidly. To account for the spatial variability of the modelling parameters he recommends a grid size of 500*m**500*m*.

6.3.1 Topographic analysis of DTM

The topographic analyse model TANALYS [SCHULLA, 1997] was applied to derive secondary grids needed as spatial input data for the hydrological model WASIM-ETH. On the basis of the DTM secondary grids were calculated, like aspect, slope, stream network, flow direction, flow accumulation, stream numbers, and stream orders. Additionally the drainage structure and the geometry of the cross-sections were determined. According to the gauge-coordinates the sub basins were delineated. Table 6.3 lists the morphological parameters of the determined sub-basins based on the original 50 m raster of the DTM.

Table 6. 3: Morphological parameters of the Gumbasa River watershed and its sub-basin (DTM 50 m raster grid).

(sub) /basin	**area** (km²)	**min. elevation** (m.a.s.l.)	**mean elevation** (m.a.s.l.)	**max elevation** (m.a.s.l.)	**mean slope** (°)
Takkelemo	79	693	1149	2053	9.16
Danau Lindu	547	939	1310	2325	9.11
Sopu	592	730	1305	2325	9.45
Gumbasa	1275	99	1199	2491	10.37

6.3.2 Soil Texture

The parameterisation of soil hydraulic properties is crucial for any hydrological model application. Soil hydraulic properties, basically saturated and unsaturated hydraulic conductivity and water retention, control the main hydrological processes [ELSENBEER, 2001]. The soil hydraulic properties values can be either obtained from direct laboratory-or field measurements. To describe the varying soil hydraulic

characteristics would require a large number of samples, because the temporal and spatial variability of hydraulic characteristics is high [WOESTEN, *et al.*, 2001]. Therefore it is virtually not possible to determine the soil hydraulic properties of a large area (e.g. catchment) by laboratory or field measurements. BOHNE [1993] suggests determining soil hydraulic properties approximately from available data of soil type and textural classes. The basis for this approach is the *van Genuchten* equation [VAN GENUCHTEN, 1980], which describes the hydraulic conductivity function. Its parameters are estimated from typical water retention data of soil types and textural classes. This indirect parameter estimation approach is commonly referred to as Pedotransfer Functions (PTF's). PTF's are the most widely used method to estimate soil hydraulic properties for larger areas [HODENETT & TOMASELLA, 2002]. SOBIERAJ *et al.* [2001] evaluated the performance of nine published PTF's of worldwide tropical soils for estimating the soil hydraulic properties of a rainforest catchment for modelling stormflow generation. They conclude that the published PTFs are inadequate to model stormflow generation, because runoff was overestimated for all events. The main differences between *van Genuchten* soil water-retention parameters for temperate and tropical soils were investigated by HODENETT & TOMASELLA [2002]. Their survey showed that most of the PTF's have been developed using databases for the soils of temperate regions and are non-transferable to tropical soils. Their finding is mainly due to the significantly different bulk density and van Genuchten parameters of tropical and temperate soils that are described by the same soil texture. Better results for the determination of soil hydraulic properties by PTF's for tropical soils were achieved when only a small soil data base of the region was used. Because no soil texture map exists for the research area the PTF based approach for the parameterisation of soil hydraulic properties could not be applied at all. Therefore the classified PHA's were parameterised according to the PHA's of equal topographic properties of the catena, which was analysed by KLEINHANS [2004]. KLEINHANS [2004] conducted his research in the Nopu catchment (2.3 km²), which is a small headwater catchment of the Gumbasa River catchment. The catena surveyed by KLEINHANS serves as a leitcatena for the whole catchment area. A similar soil hydraulic behaviour was assumed for equal PHA's. It should be noted that the parameterisation of soil hydraulic properties using the PHA approach can only serve as a rough estimation for

soil hydraulic parameters. Nevertheless it describes a clear topographic based soil hydraulic trend, which again is reflected in the hydraulic behaviour of a catena. Table 6.4 lists the required soil hydraulic parameters for the soil model of WASIM-ETH according to the PHA's classes. The layer thickness and layer numbers are estimated values and determine the layer thickness of the whole soil column. Instead of using the measured values of the saturated hydraulic conductivity k_s, KLEINHANS [2004] increased the value consistently. He argues that using the initial measured saturated hydraulic conductivity values no satisfactory calibration modelling results can be achieved. This effect is related to the modelling concept of the soil model using the *Richards Equation*. Here the soil is represented by a homogeneous matrix and therefore the flux of water through the matrix is characterised by a homogeneous matrix flow. But in reality the soil has an inhomogeneous structure, which implies a heterogeneous flux of water with preferential flow through makropores. If we assume a flux of water through a homogeneous soil matrix, the saturated soil hydraulic conductivity is therefore higher than the measured value. The recession constant k_{rec} represents an adjustable calibration parameter that determines the varying saturated hydraulic conductivity with increasing soil depth. Initially this parameter is set to 0.1. The parameter values of the suction ψ were transferred from the study of NIEHOFF [2001]. The parameters describing the van Genuchten equation were computed from measured values. Empirical studies [WOESTEN *et al.*, 1990] showed a good parameter adjustment if the residual water content θ_r was set to zero. Accordingly θ_r was set to zero for all PHA's classes. It should be considered that soil physical parameters no longer describes the measured point value but rather an effective parameter that represents the average value for the element [GRAYSON, 2000]. Hence they reproduce the bulk behaviour of a finite volume and cannot directly be related to point measurements at all.

Table 6. 4: Determined PHA classed and its associated soil physical parameters.

PHA	Pot. texture	θ_s	θ_r	α	n	ψ	k_s	k_{rec}	l_t	l_n
		(-)	(-)	(-)	(-)	(hPa)	($m \cdot s^{-1}$)	(-)	(m)	(-)
I	sand	0.45	0	7.36	1.23	385	9.0E-4	0.1	1.0	10
II	sand	0.45	0	7.36	1.23	385	5.0E-4	0.1	1.0	10
III	loamy sand	0.41	0	1.86	1.26	375	4.0E-4	0.1	0.9	10
IV	loamy sand	0.41	0	1.86	1.26	375	5.0E-4	0.1	0.9	10
V	sandy loam	0.45	0	4.01	1.2	345	1.5E-3	0.1	0.9	10
VI	loam	0.49	0	4.01	1.2	350	5.3E-3	0.1	0.7	10
VII	sandy clay loam	0.51	0	2.0	1.13	290	5.0E-4	0.1	0.3	10
VIII	sandy clay loam	0.51	0	2.0	1.13	290	4.0E-4	0.1	0.9	10

6.3.3 Land use

Quantitative research on vegetation parameters for the research area is scarce. The required vegetation parameters were therefore mainly derived from literature studies conducted in the humid tropics or world wide data sets (Table. 6.5). In order to differentiate between varying vegetation physical characteristics of forest of different altitude [WHITTEN, 2002] the vegetation class forest was divided into the classes: forest < 1200 m.a.s.l. and forest > 1200 m.a.s.l. According to this altitude classification the vegetation height and the Leaf Area Index LAI decreases and the minima stomata resistance increases in higher altitudes. The values of the albedo of the land use classes were mostly derived from COPPIN [1977], and from a data set from global vegetation guides by MATHEWS [1999]. The parameterisation of the LAI was mainly derived from a comprehensive data set of worldwide historical estimates of the LAI from 1932 – 2000 [SCURLOCK, 2001]. Further single parameter estimations of LAI from GARDIOL *et al.* [2003], HÖLSCHER *et al.* [2004] and MO *et al.* [2004], DIJK & BRUIJNZEEL [2001] were included. The parameter values of the minima stomata resistance R_C, the effective crop height z_0, and the vegetation coverage degree v were mainly taken from global vegetation data by MATHEWS [1999]. The estimation of the minima stomata resistance R_C and the effective crop height z_0 also results of the studies by KÖRNER [1994] and two local study conducted in Central Sulawesi by BOHMAN [2004] and FALK [2004].

Table 6. 5: Derived land use classes and its vegetation physical parameters.

land use class	α	R_C	LAI	v	z_0	z_w	p	ψ_g
	(-)	($m \cdot s^{-1}$)	(-)	(-)	(m)	(m)	(-)	(m)
forest<1200 m.a.s.l.	0.39	150	7	1	24	1.0	0	3.55
forest>1200 m. a.s.l.	0.39	200	6	1	20	1.0	0	3.55
open forest	0.39	150	6	0.9	20	1.0	0	3.55
water	0.05	20	1	0.1	0	0.1	-1	3.55
paddy rice	0.12	100	1	0.2	0.5	0.3	-1	3.55
annual crops	0.18	100	1.5	0.3	2.0	0.3	-1	3.55
coconut	0.32	200	4	0.6	10	1.0	-0.5	3.55
perennial crops	0.15	270	5	0.6	5	1.0	-0.5	3.55
grassland	0.26	200	1	0.2	0.5	0.2	-1	3.55
reed	0.18	250	2	0.1	2.0	0.4	-1	3.55
settlement	0.15	150	1	0	0	0.1	-1	3.55

The root depth z_w was derived from a global study of root distributions for terrestrial biomes [JACKSON *et al.*, 1996]. Within WASIM-ETH the root density distribution p describes the geometrical shape of the root system and is defined by: $-1 < p < 0$ (concave shape), $p = 1$ (linear decrease of extraction with depth) and $p > 0$ (convex shape**)** [SCHULLA&JASPER, 1999]. The main values of the root density distribution were taken from LANDON [1984]. The model assumes an ideal regular distribution and a complete root-soil contact. In reality root distribution in soils is non-homogeneous and the root-soil contact may be incomplete [NOORDWIJK *et al*, 1993].

6.3.4 Catchment characteristics

The total area of the Gumbasa catchment is 1275 km². The elevation ranges from 99-2491 m.a.s.l with a mean elevation of 1119 m.a.s.l. According to this steep gradient the slope degree averages to 10.37°. Table 6.6 lists the percentage of the potential homogeneous areas within the catchment.

Table 6. 6: Percentage of morphometric potential homogeneous areas (PHA) within the Gumbasa watershed.

PHA	Morphometric description	[%]
I	Intramontane basin (relatively low altitude above channel line)	10
II	Intramontane basin (relatively moderate altitude above channel line)	6
III	Valleys outside the intramontane basin (large catchment area)	4
IV	Valleys outside the intramontane basin (moderate catchment area)	5
V	Slope with moderate inclination	39
VI	Slope with strong inclination	30
VII	Summit area with low inclination	3
VIII	Summit area with moderate inclination	2

About two-thirds of the catchments area is classified as slope with moderate and strong inclination (69%), which emphasizes the mountainous character of the watershed. Due to its morphology the Gumbasa catchment can be subdivided into three main hydrological response units: (1) Lake Lindu catchment, (2) headwater catchments of different scale draining into the Gumbasa River and (3) the Palolo valley basin. Especially the headwater catchments are described as fast responding hydrological systems, whereas Lake Lindu catchment with its 35 km² lake Lindu serves as a hydrological retention area. All tributary rivers of the adjacent mountains confluence in the Palolo valley [204 km²] and form the main Gumbasa River. The Gumbasa River meanders through this wide and geologically highly permeable valley which has a mean altitude of 600 m.a.s.l. At the end of the valley the river confluences through a narrow and steep gorge into the Palu River, that is situated at an elevation of 99 m.a.s.l. The irrigated paddy fields and other agricultural land use systems are situated mainly in the valleys. Figure 6.1 describes the allocation of land use types within the Gumbasa watershed after the Landsat classification of 2001 [INSTITUTE OF CARTOGRAPGY, GIS & REMOTE SENSING, 2002]. Forests form the main general land-use type within the watershed with a total percentage of 86%.

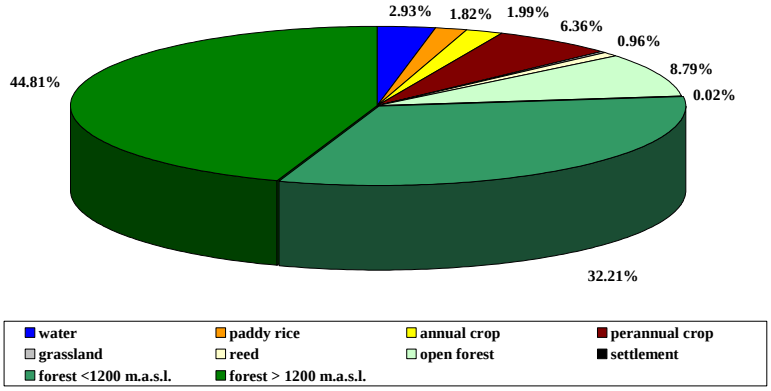

Figure 6. 1: Allocation of the main land use types within the Gumbasa River watershed after Landsat / ETM+ classification 24th August, 2001 [SFB].

6.4 SMALL MESOSCALE TEST APPLICATION: TAKKELEMO

At first WASIM-ETH was applied for the TAKKELEMO test catchment with a 250*m** 250 *m* resolution. Thereafter the applicability of a 500*m** 500*m* resolution on the same catchment was tested and analysed. The use of a 500*m** 500*m* grid for the GUMBASA catchment would result in far less computing time for the run of the hydrological model.

6.4.1 Calibration

The calibration period was set to the period 01.09.2002-31.08.2003, which corresponds to the first year of the measurement period. In order to achieve realistic soil moisture conditions for the initial conditions of the calibration run the start of the whole model run was predated to the 01.09.2001. The required temporal data for this period of model initialisation was copied from the first year of measurements. Thus the first year of measurements was simulated for two years in a row. The calibration period started in real time after one year of the simulation run.

Besides the adjustable calibration parameters of the soil model (see Chapter 5.4.4) the two adjustable parameters of the interpolation of precipitation *prec* and *precp* were added for the calibration of the hydrological model. The area precipitation was calculated within WASIM-ETH by a weighted combination of the IDW and the altitude dependent regression (see Chapter 5.3). Here the weight of the reciprocal distance for the IDW calculation and the relative weight of the IDW interpolation in the result of the interpolation method were adjusted. First the model was calibrated by manual parameter assessment through a number of calibration runs. The results were assessed by a combination of graphical and statistical assessment. For this first statistical evaluation the coefficient of efficiency R^2 [NASH & SUTCLIFFE, 1970] was used (equation 17). Based on these first calibration runs the lower and upper limits of the adjustable parameters were determined. Thereafter the control file of the automatic parameter estimation model PEST was created. The PEST control file sets the weight of each observation for the calibration period. The measured discharge (01.09.2002-31.08.2003) was used as observation data. The model was calibrated for three different types of observation data: (1) daily resolution, (2) weekly resolution, and (3) exceedance flow duration curve. The calibration was optimised following four

optimisation iterations after the lowest value for the objective function was achieved. Figure 6.2 shows the results of the achieved objective function for the calibration period on a daily resolution. For a better comparison with all components of the water balance the discharge is specified in $mm \cdot d^{-1}$. The observed versus the simulated discharge demonstrate a satisfying agreement (Figure 6.2). The displayed simulated baseflow indicates that the water balance component baseflow is slightly overestimated during periods of low flow conditions. The observed versus the simulated discharge on a weekly resolution (Figure 6.3) shows a more precise agreement. The observed trend is confirmed by the statistical analysis of the calibration results (Table 6.7). The coefficient of efficiency R^2 [NASH & SUTCLIFFE] increases from $R^2 = 0.62$ for a daily to $R^2 = 0.79$ for a weekly resolution. In general the achieved model efficiency suits the expected model accuracy according to the performance criteria after ANDERSEN [2001] (see Table 5.1).

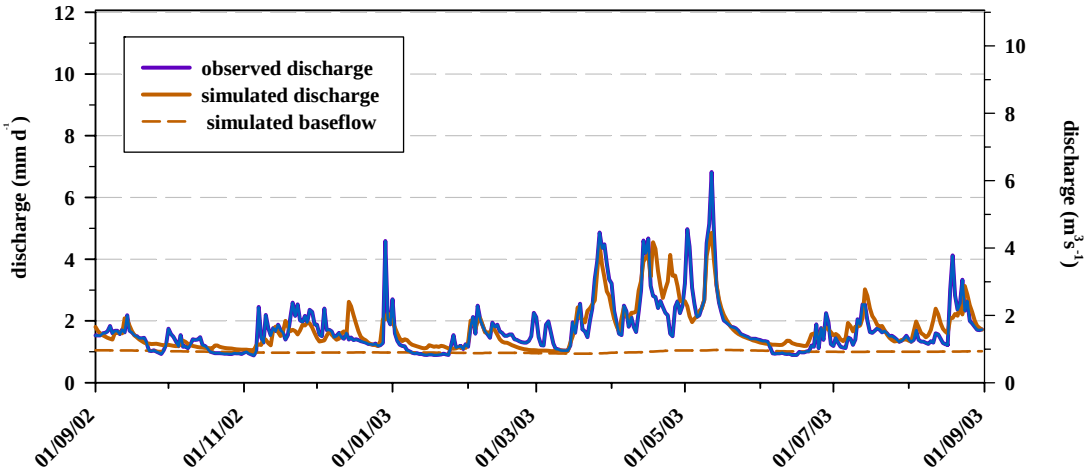

Figure 6. 2: Results of the calibration (01.09.2002-31.08.2003) of the Takkelemo test catchment (daily resolution): comparison between observed and simulated discharge ($R^2 = 0.62$) and simulated baseflow.

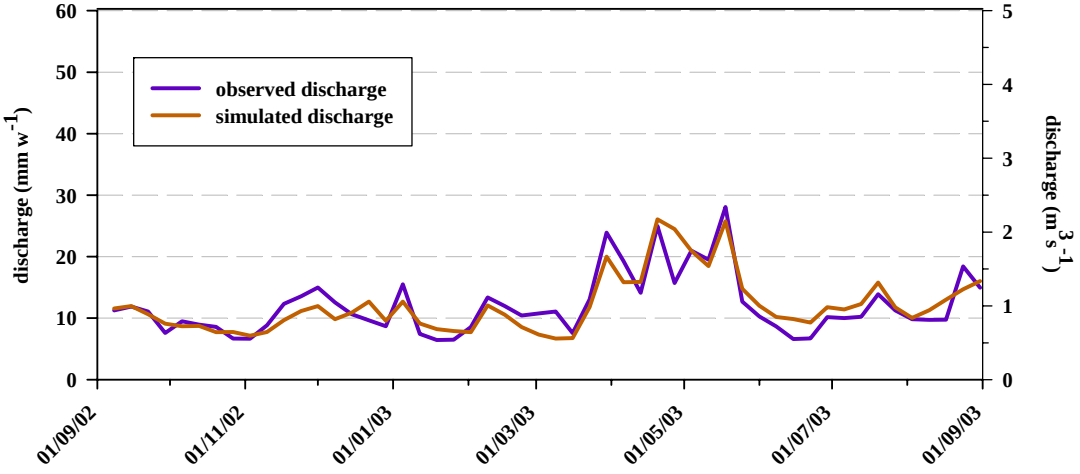

Figure 6. 3: Results of the calibration (1.09.2002-31.08.2003) of the Takkelemo test catchment (weekly resolution): comparison between observed and simulated discharge (R^2 = 0.79).

Table 6. 7: Displayed is the coefficient of efficiency R^2 **,** the index of agreement *d* and the ratio of the for the mean square error MSE and the root mean square error RMSE **(**∆RMSE/MSE) for the calibration period (01.09.2002-31.08.2003) for a daily and weekly resolution.

calibration period (01.09.2002 – 31.08.2003)	**R²**	**d**	**∆RMSE/MSE**
daily resolution	0.62	0.88	0.18
weekly resolution	0.79	0.94	0.51

Concerning the temporal resolution the index of agreement *d* (equation 18) shows a similar but alleviated trend. The increase of model efficiency by a coarser temporal resolution might be related to the smoothing of extreme daily values by a weekly sum. This effect corresponds to the compensation of negative and positive extreme values over a long period. The degree to which MAE (equation 19) exceeds RMSE (equation 20) indicates the occurrence of outliers or extreme values. The ratio of the calculated MSE and RMSE values for daily and weekly resolution proves the existence of extreme values within the observed and simulated discharge data. On closer examination of extreme values, which were not simulated correctly, it shows

that an over- or underestimated area precipitation does not correspond adequately with the simulated discharge. For example the interpolated strong precipitation event mid of December 2002 (Figure 6.4) was not recorded by the discharge gauge station. SCHULLA [1997] explains the over- or underestimation of area precipitation with the present climate station density. Particularly small-range spatial variability of convective strong precipitation events are hardly represented by the interpolated areal precipitation. BEVEN [2001] states that an inadequate estimation of rainfall inputs results in an increase of model uncertainty. Insufficient interpolation of areal precipitation leads to a lower model efficiency especially for tropical regions, where spatial area precipitation pattern due to small-scale convective rainfall are highly variable

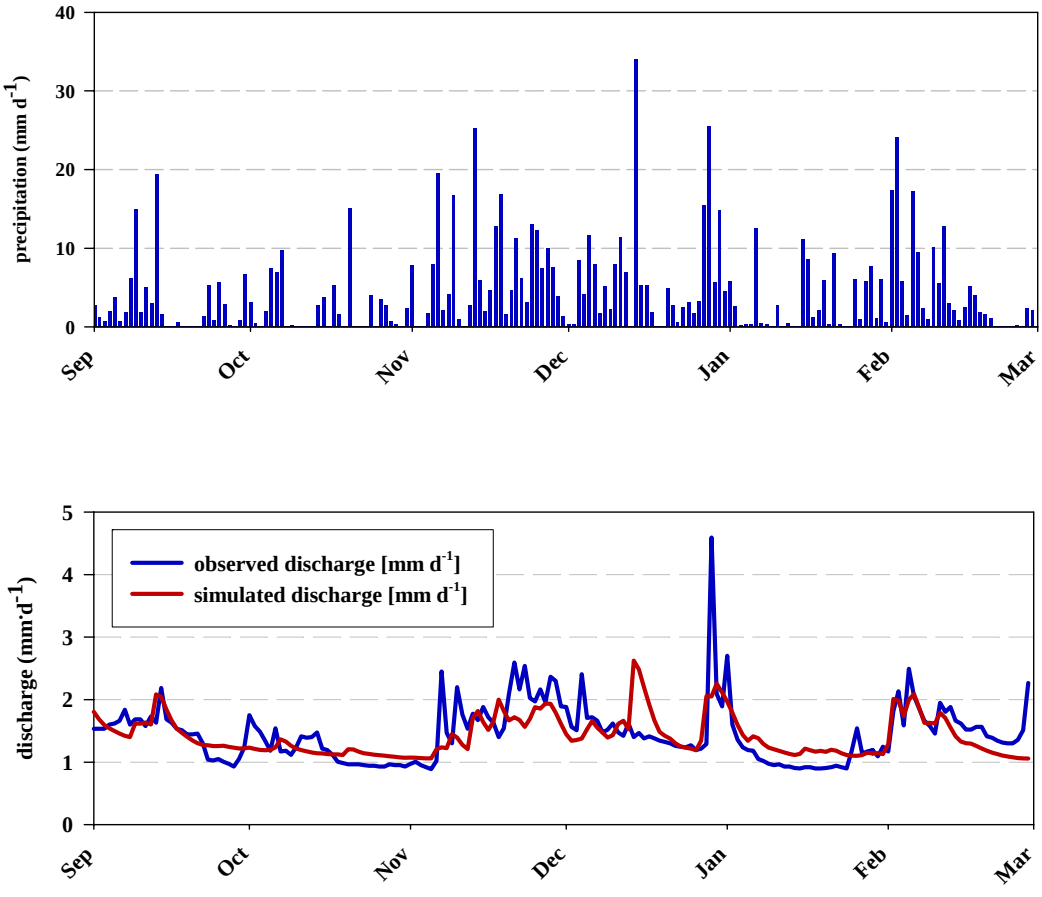

Figure 6. 4: Areal precipitation and observed versus simulated discharge for the calibration period 01.09.2002 – 28.02.2003 (daily resolution), Takkelemo subcatchment.

None of the climate station used for the interpolation of areal precipitation is situated within the Takkelemo sub-catchment. This insufficient station density for the Takkelemo subcatchments leads to a miscalculation of several small-scale precipitation events. But the well simulated run-off of several precipitation events (Figure 6.2) shows the overall influence of the regional precipitation pattern on the areal precipitation. NOORDWIJK [2003] concludes that at a landscape or regional scale patchy rainfall leads to a more homogeneous riverflow. A study by ANDREASSIAN *et al.* [2001] showed that smaller watersheds require more precise areal rainfall estimates to achieve good modelling results. Hence it can be assumed that patchy rainfall has a minor effect on the model efficiency for the application of WASIM-ETH for the whole Gumbasa River watershed (1275 km²) than for the smaller Takkelemo test-catchment (79 km²).

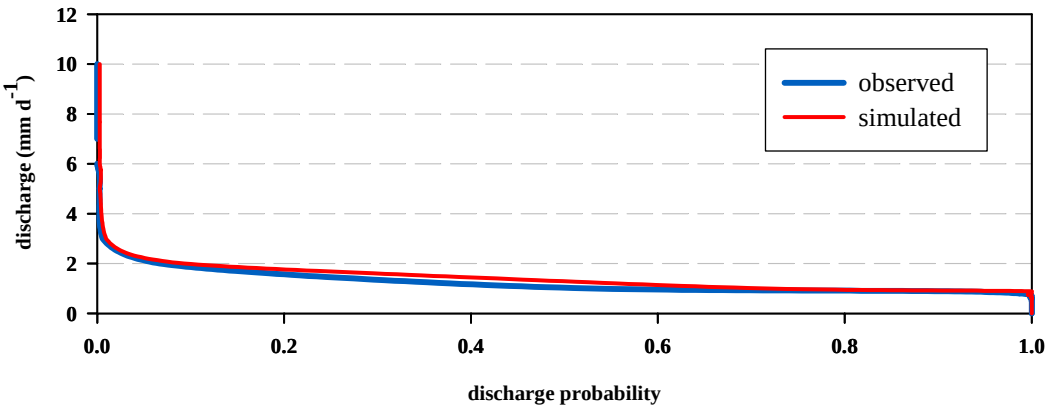

Figure 6. 5: Simulated and observed exceedance flow duration curve for the calibration period 01.09.2002-31.08.2003.

PEST also calibrates the hydrological model with respect to the flow duration curve of the observed discharge. The flow duration curve describes the probability that the discharge falls below or above a certain value [DYCK & PESCHKE, 1989]. The comparison of observed and simulated flow duration indicates the ability of the calibrated hydrological model to reproduces the discharge variability. Figure 6.5 displays the observed and the simulated flow duration curve for the calibration period 01.09.2002-31.08.2003. The x-axis records the exceedance of the discharge probability. The comparison of the observed and simulated flow duration curve

reveals an overall good performance of the hydrological model. But to a small extend in the range of $2 - 4\ mm \cdot d^{-1}$ the simulated discharge is overestimated. Furthermore an overestimated simulation of a discharge peak could be compensated by an underestimation of another event. Nevertheless the performance of the flow duration curve indicates that the baseflow is well reflected by the hydrological model.

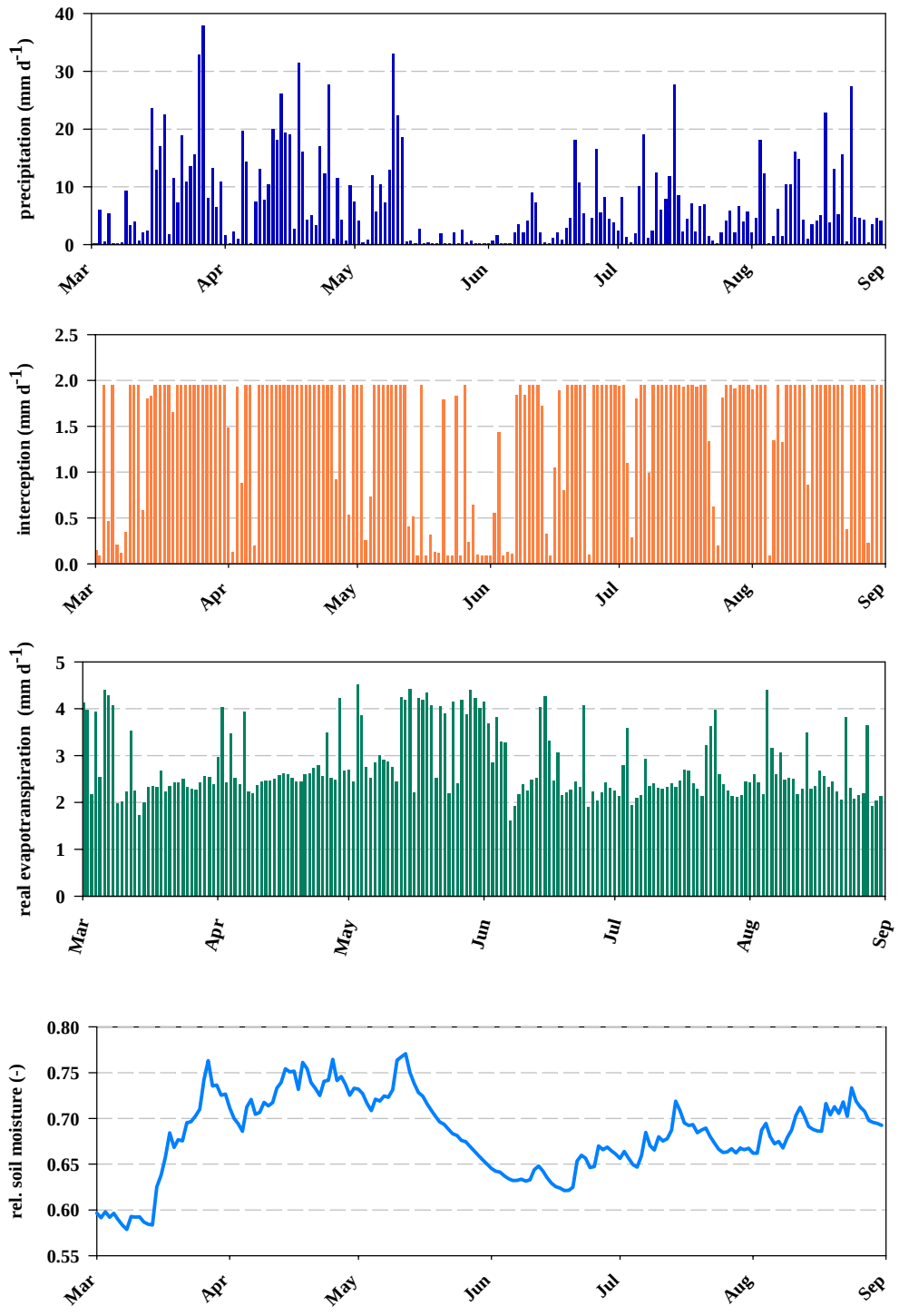

Figure 6. 6: Plotted is the daily simulated areal precipitation, interception, real evapotranspiration and relative soil moisture, Takkelemo catchment 01.09.2002-31.08.2003.

Figure 6.6 describes the performance of the simulated dynamics of the interception and evapotranspiration models with regard to the areal precipitation and the relative soil moisture change. The simulated dynamics show that during dry periods (e.g. May- June) a low interception rate and a high evapotranspiration rate were simulated. At the same time the relative soil moisture declines, which is induced by the high evapotranspiration activity. Correspondingly during wet periods the interception rate increases and the evapotranspiration rate decreases, which causes an increase in the relative soil moisture content. During rainy periods approximately 1-2 mm of water may be stored within the canopy. Although the transpiration rate of this intercepted water is not limited by the stomata resistance like the evaporation rate of the vegetation, it is transpirated first [MONTEITH & UNSWORTH, 1990]. Furthermore the reduction of the evapotranspiration rate during rain periods is linked to a decline in available net radiation and an increase in actual vapour pressure.

Additionally the dynamics of the interpolated areal precipitation, the simulated relative soil moisture, the simulated depth to water table and the corresponding simulated discharge for the calibration period were analysed (Figure 6.7). The displayed values refer to a mean value for the entire Takkelemo catchment. The soil model determines the infiltration, the vertical water fluxes and the change of relative soil moisture. The comparison of the displayed soil model components demonstrates a fast responding precipitation-discharge hydrological system. The simulated processes of relative soil moisture variation and groundwater fluctuation could not be validated, because no real data have been measured. KLEINHANS [2004] evaluated the performance of the WASIM-ETH soil model by an analysis of the model efficiency for simulated and observed relative soil moisture. His results show that the soil model simulates the overall dynamic of the relative soil moisture satisfactorily, but under-or overestimates some events. Although his study was conducted in a small head-water catchment of the Gumbasa watershed and the parameterisation of the soil model refers to the soil-morphological classification of the corresponding catena, the same behaviour can be assumed for the Takkelemo catchment.

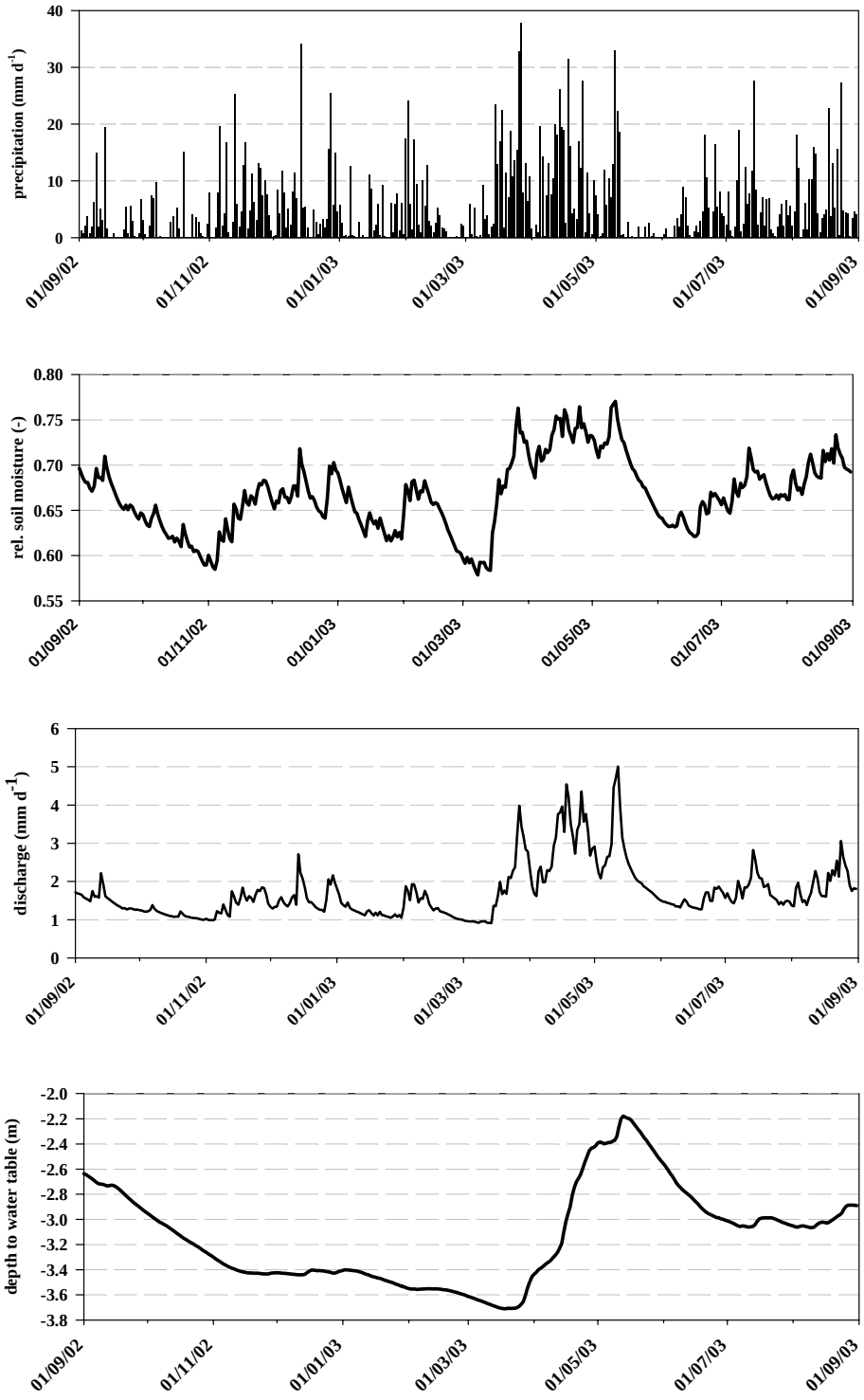

Figure 6. 7: Plotted is the daily simulated areal precipitation, relative soil moisture, depth to ground water table and discharge, Takkelemo catchment 01.09.2002-31.08.2003.

6.4.2 Analysis of residuals

In order to assess parameter uncertainties further statistical measures of weighted residuals were calculated. The weighted residuals should have a mean of zero and be randomly distributed after the parameter estimation process [DOHERTY, 1994]. Figure 6.8 shows the histogram of the daily weighted residuals of the calibration for the Takkelemo test catchment. The number of non-zero weighted residuals amounts to a total of 338 and they have a mean of 0.0216. The analysis of weighted residuals demonstrates that the residuals are randomly distributed around a mean of zero, which indicates that the chosen hydrological model itself is consistent.

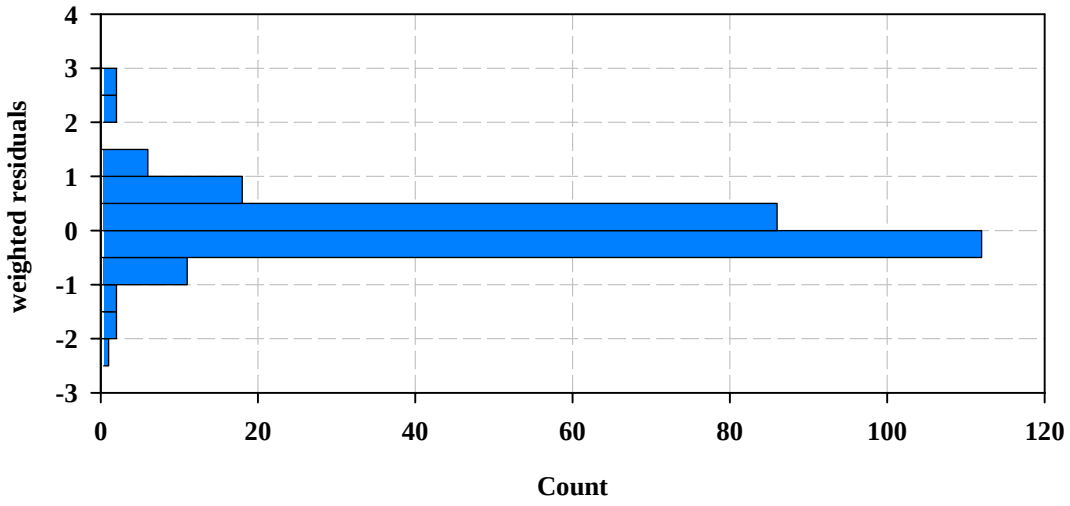

Figure 6. 8: Histogram of the daily non-zero weighted residuals for the calibration period 01.09.2002-- 31.08.2003 for the Takkelemo test catchment.

6.4.3 Validation

For the validation of the hydrological model the commonly used split sample test [ABBOT & REEFSGARD, 1996] was applied for the validation period: 01.09.2003-31.08.2004. In the following the model was validated for the whole period of available measurements (01.09.2002-31.08.2004). Table 6.8 lists the statistical assessment of the calibration and validation run for daily and weekly resolution.

Table 6. 8: List of the statistical measures (coefficient of efficiency R^2, index of agreement d, and the ratio of the root mean square error and the mean square error ΔRMSE/MSE) for the calibration, validation-split sample and validation-whole period, Takkelemo test catchment, daily & weekly resolution.

	R^2		**d**		**Δ RMSE/MSE**	
	daily	weekly	daily	weekly	daily	weekly
calibration period	0.62	0.79	0.88	0.94	0.18	0.51
validation period - split sample	0.49	0.63	0.82	0.92	0.24	0.7
validation period	0.56	0.72	0.86	0.89	0.21	0.84

Both the daily and the weekly resolution plot show a slight decline of the model efficiency for the various validation runs. This degradation of model efficiency is accompanied by a rise of outliers within the data set, which is demonstrated by an increase of the RMSE /MSE difference. Again this effect is most likely related to a miscalculation of local precipitation events. Furthermore, the adjustable parameters for the calculation of the areal precipitation *prec* and *precp* were calibrated only for the calibration period and thereafter taken as fixed parameters for the validation run. The results of the validation run demonstrate that in general the calibration period of one year is not adequate for a reliable calibration of the adjustable parameters for the areal precipitation calculation, and that miscalculated local precipitation events decrease the model effiency to certain extend.

6.4.4 Evaluation of the simulated water balance

Figure 6.9 illustrates the simulated components of the water balance for the first year of available measurements (01.09.2002-31.08.2003), Takkelemo subcatchment.

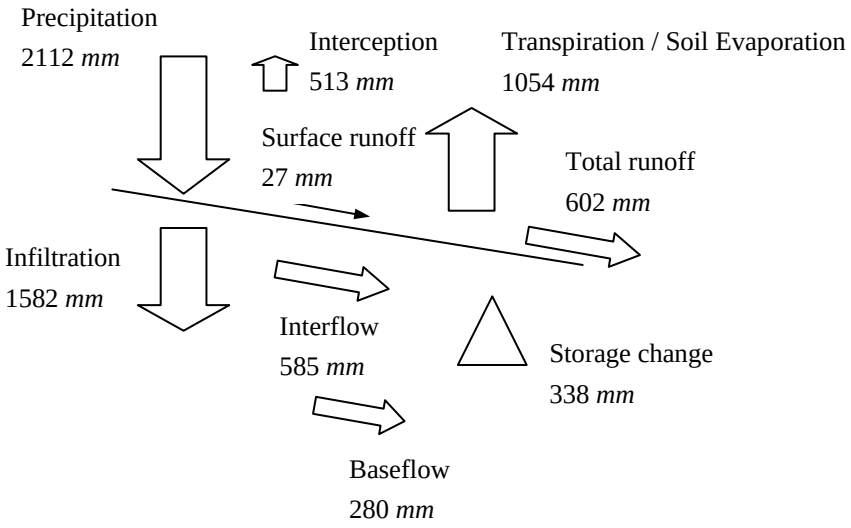

Figure 6. 9: Components of the simulated water balance, Takkelemo subcatchment 01.09.2002-31.08.2003 (after FALKENMARK & CHAPMAN, 1989).

Only the observed discharge at the outlet of the subcatchment is available for the calibration and validation of the hydrological model. Further components of the simulated water balance were assessed by a comparison with the results of diverse tropical catchment studies. Assessing the simulated water balance with other diverse tropical catchment studies is problematic due to the variety of catchment characteristics, catchment scale and applied methods. The commonly used water catchment method is one source of uncertainty [MOTZER, 2003], because especially different measurement techniques and possible leakage of the catchment may influence the results. Therefore the following reference values should only serve as a rough guidance for the assessment of the water balance modelling results.

BRUIJNZEEL [1996] carried out a comprehensive review on tropical catchment studies. In particular annual precipitation and evapotranspiration rates were investigated for lowland forest and montane forest. Values for precipitation and

evapotranspiration of a number of studies for South-East Asia are given in Figure 6.10. Additionally the results of the Nopu catchment study by KLEINHANS [2004] and the results of the water balance simulation of the Takkelemo catchment are shown. Figure 6.10 shows the compared water balance components and demonstrates the great variety of the calculated values for yearly precipitation and evapotranspiration rates. This is mainly due to the diversity of regional climate and vegetation types [MOTZER, 2003]. In comparison with continental tropical forest BRUIJINZEEL [2000] indicates high observed evapotranspiration rates (2000 – 2400 $mm\ year^{-1}$) for forests at continental edge and island locations of high rainfall.

Furthermore the period of observation, the catchment size and topographic type influence the components of the water balance. Except the montane Cidiwey catchment with an average altitude of 1740 m.a.s.l., most of the catchments are classified as tropical lowland forest. The Nopu catchment (2.4 km²) as well as the Takkelemo catchment (79 km²) are classified as lower montane forest, but vary strongly in catchment scale. Therefore the simulated yearly precipitation and evapotranspiration rate of the Takkelemo subcatchment is not directly comparable with the other catchment studies. The relation of the simulated rates to the other studies indicates that the simulated yearly precipitation and evapotranspiration rate lies absolutely in the range of other catchment studies within South-East Asia, even though WASIM-ETH uses a simple bucket approach for the calculation of the interception rate. BRUIJNZEEL [1996] specifies a mean interception rate of 19-20% of the total precipitation for lower montane forest. The simulated interception rate in this study amounts to 24% of the total precipitation, which exceeds slightly the findings by BRUIJNZEEL. But with regard to the small sample size (n=6) and the great variety of catchment conditions again this value can only serve as a rough indication for the order of magnitude.

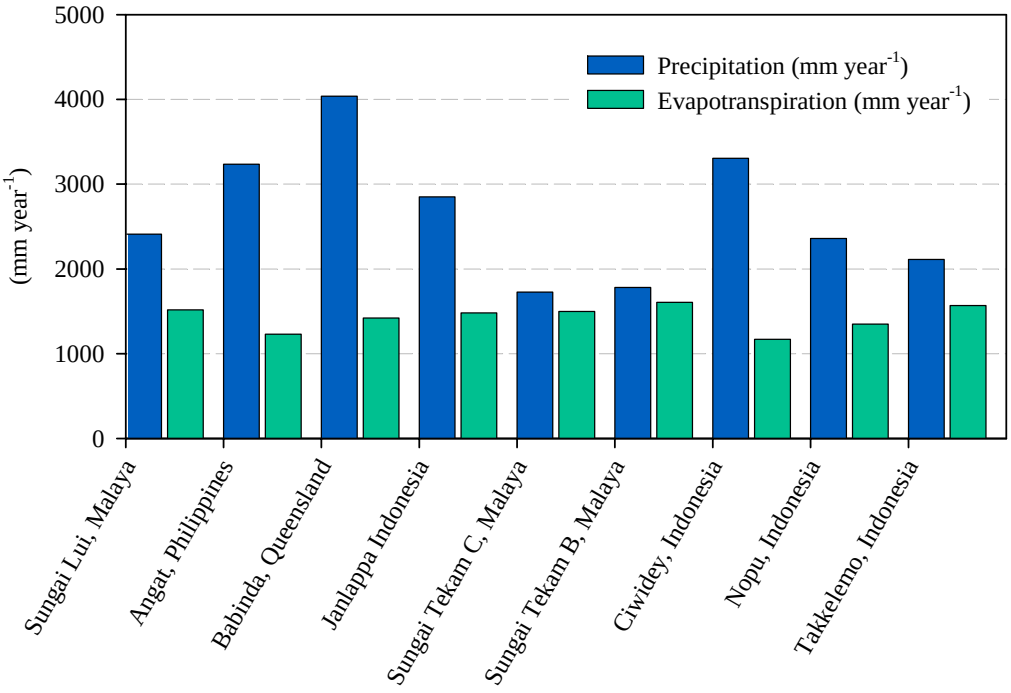

Figure 6. 10: Yearly precipitation and evapotranspiration rates (mm) of various catchment studies in South-East Asia (Source: BRUIJNZEEL, 1996).

SCHELLEKENS [1999] measured an interception loss of 50% of the gross precipitation, which emphasizes the great variety of interception rates. Stemflow with a rate of 1-2% of the incident rainfall is regarded as negligible. ASDAK [1998] determines a mean stemflow of 1.4% of the gross precipitation for an unlogged forest in Central Kalimantan, Indonesia. A catchment study in a lower montane forest in Ecuador [FLEISCHBEIN *et al.*, 2005] calculated a mean stemflow of 1% of the gross precipitation and ROLLENBECK [2002] determined a mean stemflow rate of 0.8 % for a lowland tropical forest in Venezuela.

Studies quantifying discharge separation in tropical catchments are rare. This complicates the evaluation of the simulated discharge components. An analysis of the simulated components of the discharge shows that the simulated direct runoff (55 mm $year^{-1}$) is negligible compared to the simulated interflow. KLEINHANS [2004] on the other hand simulates a considerable higher rate of direct runoff (245 mm $year^{-1}$) with a similar model parameterisation The underestimation of direct runoff compared to

the simulation study of KLEINHANS [2004] might be due to several scale related processes. Strong convective precipitation is the main meteorological process, which induces high water discharge [BRONSTERT & NIEHOFF, 2003]. An underestimated areal precipitation causes a decrease of the peak discharge. Fast surface runoff and interflow are the leading processes of flood events. Therefore the underestimation of surface runoff is related to the spatial miscalculation of areal precipitation. The representation of precipitation variability is directly related to the climate station density. Especially in tropical catchments, where strong small scale convective rainfall events prevail, a high climate station density would be required to display the areal precipitation variability. Another reason of the underestimated surface runoff in comparison to the simulation by KLEINHANS [2004] is the uncertainty of the subscale variability of the initial parameters [STEPHAN & DIEKKRÜGER, 2003]. If the slope is aggregated from a 30 m resolution to a 500 m resolution the slope parameter value of the 500 m grid cell represents a combined value of the subscale information. Though the slope also determines the generation of fast surface runoff an aggregation of slope values leads to a decrease of surface runoff, because the aggregation process is not linear with the surface runoff generation. Furthermore it should be noticed that not the same periods were calculated. KLEINHANS [2004] simulated the water balance for the period 01.01.02-31.12.02, which had different precipitation pattern and intensities. Other studies on deep porous volcanic deposits in Java have surface runoff coefficients less than 5 % of incident rainfall [RIJSDIJK & BRUIJNZEEL, 1990, SINUKABAN & PAWITAN, 1998; PURWANTO, 1999]. Though the infiltration capacity of the Gumbasa River catchment soils is likely to be slightly less than deep porous volcanic deposits the simulated surface runoff coefficient of 2.6 % most likely underestimates the real surface runoff.

CHANG [1993] states that the groundwater runoff of tropical catchments underlain by impervious granite amounts to 10 – 20 % of the total. For areas with highly permeable rocks it may account for half of the total. The Takkelemo catchment is a headwater catchment which is underlain by granite. The total simulated baseflow of 17 % corresponds with CHANGS [1993] conclusions.

6.4.5 Grid resolution sensitivity

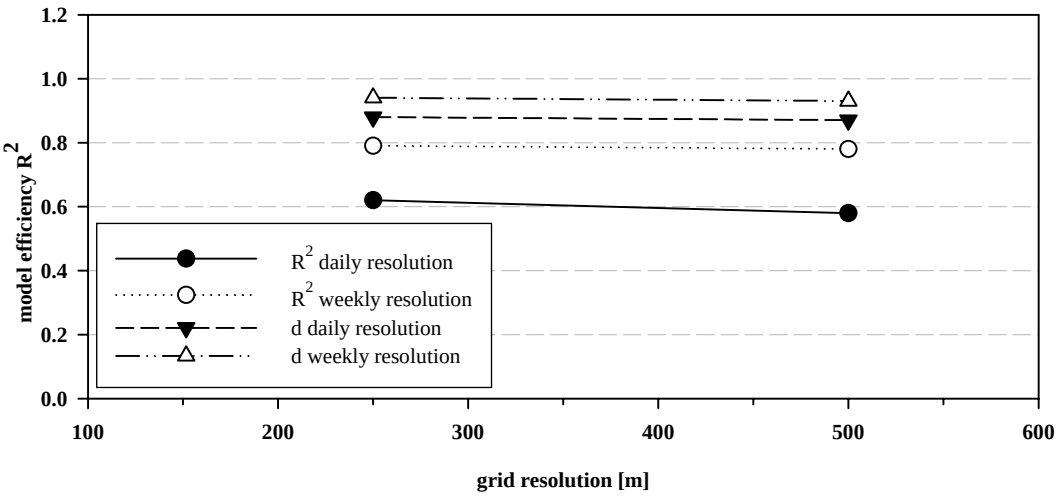

Figure 6. 11: Sensitivity of grid resolution on the model performance for a daily and weekly resolution for the Takkelemo test catchment (79 km²).

SCHULLA [1996] recommends a grid resolution of 500*m** 500*m* for the application of WASIM-ETH in mountainous catchments. In order to verify his conclusions for the application of WASIM-ETH for the Gumbasa catchment the Takkelemo catchment was used as a test site. Figure 6.11 describes the achieved model performance of a 250*m** 250*m* and a 500*m** 500 *m* resolution respectively on a daily and weekly resolution. With a coarser grid the model performance declines slightly for both temporal resolutions. The total number of grid cells for the Gumbasa catchment (1275 *km²*) drops rapidly from 21,250 for a 250*m** 250*m* to 5,100 for a 500*m** 500*m* resolution. The final choice of grid size is a compromise between model performance and manageable number of grid cells. The number of grid cells determines the run time of the simulation and therefore the run time of the whole calibration. With regard to the considerably shorter model run, and accepting a slight decline of model performance, the 500*m** 500*m* grid resolution was chosen for the Gumbasa catchment. The slight loss of accuracy is compensated by a gain of simulation runs for the calibration procedure.

6.5 MESOSCALE APPLICATION: GUMBASA CATCHMENT

The application of WASIM-ETH on the Takkelemo test catchment has proven the suitability of the chosen hydrological model for a mesoscale tropical catchment area like the Gumbasa River catchment. Moreover after consideration of all possible coefficients, a reasonable grid resolution of 500*m**500*m* was chosen for the simulation run.

6.5.1 Model construction

The relevant catchment areas were delineated with the software Tanalys according to the location of the observation gauging sites. In order to analyse the sensitivity of ongoing rapid forest conversation in the Dongi-Dongi valley on the hydrological model application this particular valley (148 km²) was defined as a separate catchment. Furthermore the Nopu catchment [KLEINHANS 2004] was defined as a small reference headwater catchment (2.4 km²). Here the effect of the calibration of gauged catchments on adjacent ungauged headwater catchments was analysed. The Gumbasa-River sub-catchments map (Appendix B.2) shows the delineated subcatchment for the simulation run.

Within WASIM-ETH Lake Lindu is defined as a reservoir. An abstraction rule specifies the reservoir content in m^3 and the corresponding discharge. The irrigated paddy fields are represented by a pond depth grid which defines the maximum storage capacity of the pond in *mm*. The parameterisation for the soil and land use table was transferred from the Takkelemo test catchment, which has been validated before (see Chapter 6.3).

6.5.2 Calibration

In general the calibration of Gumbasa River catchment is similar to the calibration of the Takkelemo test catchment. Corresponding to the Takkelemo test the calibration period for the Gumbasa catchment was set to 01.09.2002-31.08.2003. Also the simulation start was predated to the 01.09.2001, which means a repetition of the measurement period to achieve realistic soil moisture conditions for the calibration start. After a first manual calibration the following adjustable parameters of the soil submodel for the classified subbasins respectively were calibrated within defined limits with the automatic parameter estimation model PEST:

- d_r drainage density for interflow (m^{-1})
- Q_0 scaling factor for baseflow ($mm\ h^{-1}$)
- k_s hydraulic conductivity recession constant (-)

The calibration with PEST was optimised after four optimisation iterations and was elapsed since the lowest objective function was achieved after 372 total model calls. Table 6.9 demonstrates the statistical assessment of the model performance for the different sub-catchments for a daily and weekly resolution.

Table 6. 9: List of the statistical measures (coefficient of efficiency R^2, index of agreement d, and the ratio of the root mean square error and the mean square error △RMSE/MSE) of the subcatchments of the Gumbasa catchment for the calibration period *(1.09.2002-31.08.2003)*.

catchment	R^2		d		△ RMSE / MSE	
	daily	weekly	daily	weekly	daily	weekly
Danau Lindu (547 km²)	0.83	0.86	0.96	0.96	0.10	0.57
Sopu (592 km²)	0.79	0.77	0.94	0.93	0.15	0.88
Takkelemo (79 km²)	0.58	0.77	0.85	0.93	0.23	0.70

The comparison of the achieved model efficiency of the Sopu catchment and the much smaller Takkelemo proves the previously stated hypothesis that due to the low density of climate stations a better model performance is achieved for the larger catchments. According to the model performance criteria by ANDERSEN *et al.* [2001] the achieved coefficient of efficiency R^2 of the different subcatchments would be classified as poor to fair performance on a daily resolution and fair to good on a weekly resolution. The index of agreement *d* shows in general a satisfactory performance for all subbasins. The difference of RMSE and MSE *(△ RMSE/MSE)* indicates the occurrence of outliers or extreme values within the simulation for all subbasins. Before the general performance is evaluated, also the graphical performance and the simulated water balances of the different subcatchments with regard to the whole Gumbasa catchment were analysed.

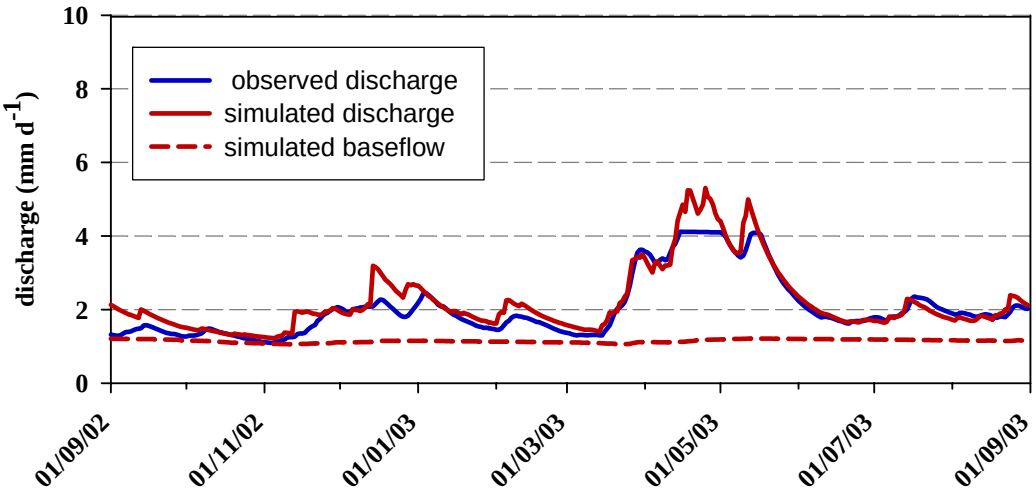

Figure 6. 12: Results of the calibration (01.09.2002-31.08.2003) of the Danau Lindu subcatchment (daily resolution): comparison between observed and simulated discharge (R^2=0.83) and simulated baseflow.

The graphical evaluation of observed and simulated discharge for the Danau Lindu catchment (Figure 6.12) shows a very good agreement. The baseflow is simulated within realistic values and also the discharge fluctuation during the rainy season from March till May is well reproduced. The flat hydrograph of observed discharge, which occurs end of April, is due to a faulty design of the hydrological station. Before the hydrological station at Lake Lindu was built, nothing was known about the maximum possible yearly lake level fluctuation, because no historical lake level data was available. For the construction of the gauging station the length of the stilling tube for the lake gauging site at Danau Lindu was restricted to 2 m, because the transport horses could not carry any longer material along the relatively small and winding path to the remote lake. During the rainy period the rising lake water level reached the top of the stilling tube and the shaft encoder was flooded. As a consequence the observed lake water level was recorded as stagnant till the water level again decreased beneath the top level of the installed shaft encoder. It is assumed that the simulated discharge within this period of instrument failure represent the real peak discharges. If the actual discharge was recorded for the rainy period, a better coefficient of efficiency would have been calculated accordingly.

Figure 6.13 displays the observed versus the simulated discharge and the simulated baseflow for the Sopu catchment. Again the baseflow is simulated well, whereas the simulation of discharge during the rainy seasons indicates a slight variance. The peak discharge in April is well reconstructed by the simulation and in general the graphical evaluation of the simulation indicates a good performance of the hydrological model.

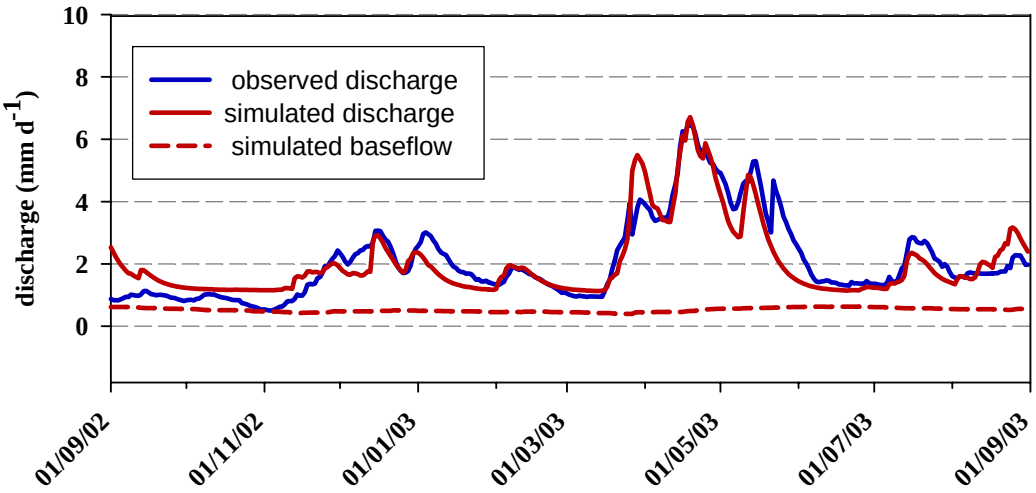

Figure 6. 13: Results of the calibration (01.09.2002-31.08.2003) of the Sopu subcatchment (daily resolution): comparison between observed and simulated discharge (R^2=0.79) and simulated baseflow.

The graphical assessment of the Takkelemo subbasin (Figure 6.14) shows a predominately good performance (R^2=0.58) of the hydrological model, but an incorrect simulation for singular flood events. Like previously stated (see chapter 6.4.1) the lower model performance for the Takkelemo subbasin is related to the smaller catchment size and the low climate station density.

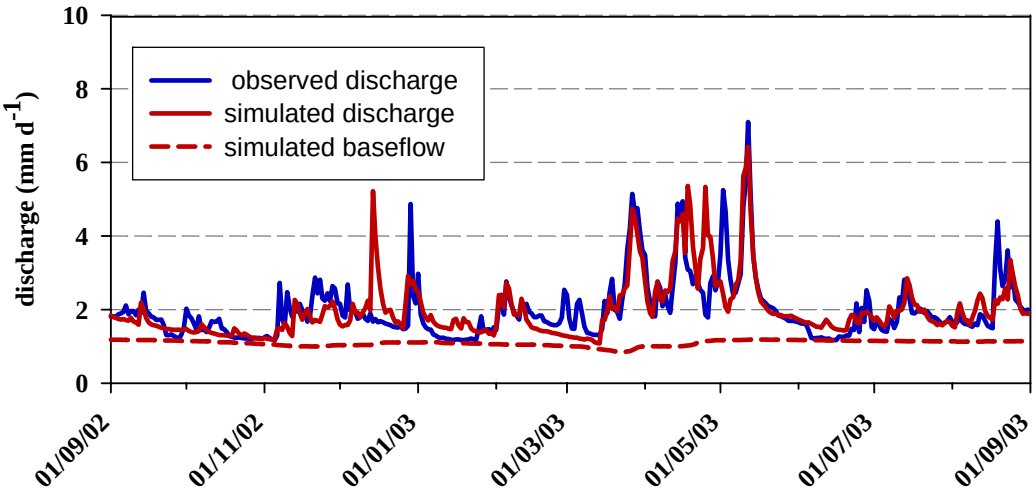

Figure 6. 14: Results of the calibration (01.09.2002-31.08.2003) of the Takkelemo subcatchment (daily resolution): comparison between observed and simulated discharge (R^2=0.58) and simulated baseflow.

Finally the performance of the simulation run was evaluated for the outlet of the whole catchment, the Gumbasa River gauging site. Unfortunately the installed float operated shaft encoder with integral data logger had some major technical problems during the period of operation, so that no continuous time series was recorded for this particular gauging site. Therefore no complete statistical assessment could be conducted for the Gumbasa River gauging site. Instead only the period of trustful measurements, which are of a patchy characteristic were used for the evaluation of the model performance. The applied evaluation procedure comprises no graphical comparison of the simulated and observed discharge was, but a statistical residual analysis of the trustful measurement periods, which will be discussed in the following section. Table 6.10 lists the results of the residual analysis for the Gumbasa River gauging site.

Except for the Gumbasa gauging site, the total number of 365 residuals, which corresponds with the complete calibration period *(01.09.2002-31.08.2003)* was taken for the residual analysis for all remaining gauging sites. First of all the calculated residuals for all gauging sites were compared and evaluated. The only statistical evaluation for the performance of WASIM-ETH for the Gumbasa River gauging site is the applied residual analysis. Therefore the model performance for the calibration period already has been proven by a statistical and graphical analysis and the classification of the Gumbasa residual analysis among the other stations assesses the overall model performance for the Gumbasa River gauging station. Table 6.10 lists the residual analysis for all gauging stations.

Table 6. 10: Analysis of weighted residuals for all gauging stations.

Residual analysis	Danau Lindu	Sopu	Takkelemo	Gumbasa
Number of residuals	365	365	365	104
Mean value of residuals	-0.18	0.39	0.03	0.37
Maximum residual	0.38	2.49	2.83	1.07
Minimum residual	-1.12	-1.16	-3.48	-0.66
Variance of residuals	0.11	0.44	0.30	0.27
Standard error of residuals	0.33	0.66	0.55	0.52

The results of the residual analysis for the Gumbasa River gauging site correspond with the achieved results of the other gauging sites. The mean is close to zero (0.37), and the maximum and minimum residuals don't show any extreme outliers. Also the variance and the standard error lie within the range of the other gauging stations. It can be concluded that even though the number of residuals is minimised by two thirds of the total number of the whole calibration period, the performance of the hydrological model WASIM-ETH for the Gumbasa River station is classified with a similar goodness of fit as for the remaining stations. The lower number of residuals still implies a certain uncertainty, which cannot be estimated at all due to lacking measurements. For a better analysis of the residuals of the remaining stations their distribution has been displayed in a histogram (Figure 6.15).

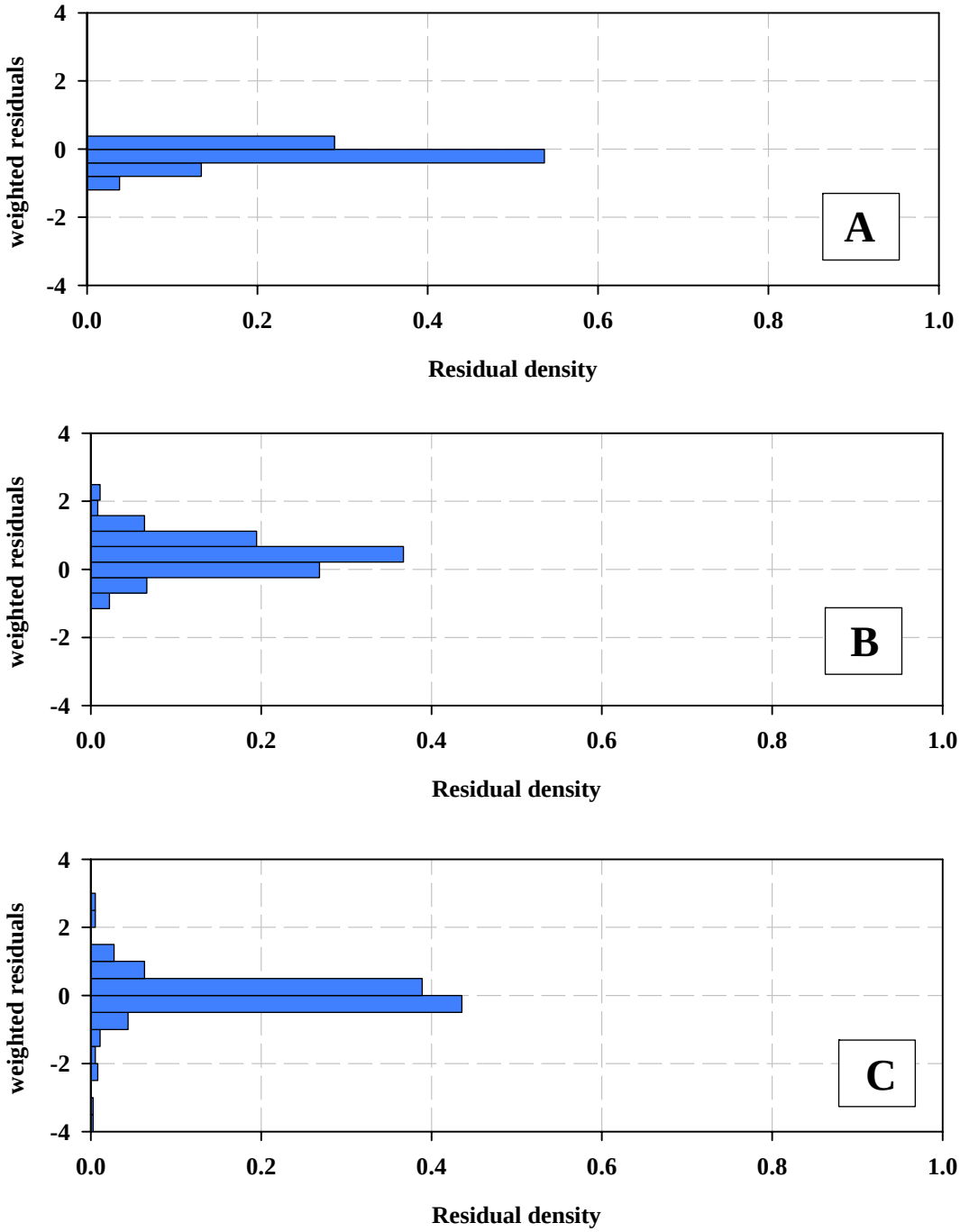

Figure 6. 15: Histograms of residual density of the Lake Lindu (A), Sopu (B) and Takkelemo (C) catchments for the calibration period (01.09.2002-31.08.2003).

With the mean value for the daily residual for the Lake Lindu sub-basin of R_x = -0.18, R_x = 0.39 for the Sopu subbasin and R_x = 0.03 for the Takkelemo subbasin all subbasins demonstrate a randomly distribution of residuals around a mean of zero. The comparison of the residual histograms (Figure 6.15) indicates qualitative differences. The residual distribution of the Danau Lindu subasin shows a far narrower margin around zero than the residual distribution of the Sopu and Takkelemo subbasin, which indicates a better model performance for the Danau Lindu subbasin. The wide margin of residual distribution with a low count for the extreme values for the Takkelemo subbasin reflects a small number of outliers within the simulated discharge.

Following the statistical and graphical evaluation of the achieved modelling results, a qualitative assessment of the water balance for the different subbasins was carried out. Table 6.11 shows the simulated yearly water balance *(01.09.2002-31.08.2003)* for the three subbasins and furthermore for the whole Gumbasa River catchment. For a better comparison of the subcatchments the several components of the water balance are displayed as a percentage of the respective total input (= areal precipitation). The comparison reflects the spatial variability of the water balance components due to their catchment characteristics. The differences of the total percentage of interception and evapotranspiration are mainly related to the variance of the LAI, stomata resistance and effective crop height according to elevation for the land use type forest and moreover to the decreasing potential evapotranspiration by increasing elevation. Although the main land use type of the Danau Lindu catchment is natural forest with a high percentage (56 %) of natural forest above 1200 m.a.s.l., less water is intercepted and evaporated (total = 62 %) in comparison with the whole Gumbasa catchment (total = 78 %), which is characterised by a relatively low percentage of natural forest above 1200 m.a.s.l. (Gumbasa = 32 %). Compared to the whole Gumbasa catchment more total discharge and more groundwater recharge is generated by the Danau Lindu catchment. This signifies the high impact of tropical mountain forests on the discharge generation.

Table 6. 11: Water balance of the calibration period (01.09.2002-31.08.2003) for all subbasins and the whole Gumbasa watershed.

water balance [%]	Danau Lindu	Sopu	Takkelemo	Gumbasa
Areal Precipitation	2075 mm	2080 mm	2119 mm	1994 mm
	100 %	100 %	100 %	100 %
Interception	19 %	24 %	23 %	22 %
Surface runoff	9 %	9 %	3 %	5 %
Infiltration	71 %	66 %	74 %	73 %
Evapotranspiration	43 %	48 %	45 %	56 %
Interflow	30 %	20 %	31 %	21 %
Baseflow	20 %	9 %	19 %	16 %
Total discharge	40 %	30 %	34 %	26 %
Storage change	18 %	8 %	17 %	13 %

6.5.3 Nopu headwater catchment

KLEINHANS [2003] has successfully undertaken a simulation of the Nopu catchment (2.3 km²) with WASIM-ETH for the period 01.11.2001-19.02.2003 with an achieved model efficiency of R^2=0.85. A daily temporal resolution and spatial grid of 30*m**30*m* was applied for the model construction. The catchment is equipped with three gauging stations, two climate stations and a total of six rain gauges. Within the model construction of the Gumbasa River catchment this well observed Nopu headwater catchment was defined as a subcatchment, but the available period where discharge data is available for both models *(01.09.2002-19.02.2003)* was not included into the calibration process of the Gumbasa River model. Therefore the comparison of observed versus simulated discharge allows to evaluate the performance of the constructed model without the calibration influence of this particular gauging site. Though in comparison to the Gumbasa catchment model the constructed model by KLEINHANS [2004] was equipped with a far smaller grid size and a denser net of meteorological stations, the impact of grid size and station density could be analysed. Figure 6.16 shows the observed versus the simulated discharge with the simulated baseflow for the Nopu headwater catchment for the period 01.09.2002-19.02.2003.

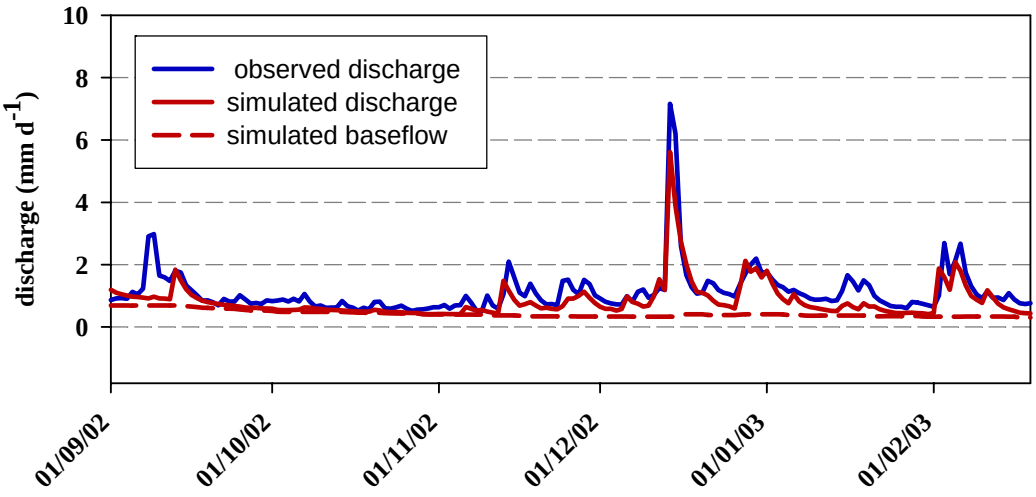

Figure 6. 16: Observed versus simulated discharge with simulated baseflow for the Nopu subbasin (daily resolution, 500*m**500*m* grid) for the period (01.09.2002-19.02.2003); model efficiency R^2=0.84.

The achieved model performance for the considered time period with a model efficiency of R^2=0.84 is surprisingly very good and can be compared to the model performance achieved by KLEINHANS [2004]. A grid size of 30*m**30*m* results for a 2.4 km² catchment in about 2667 grid cells, whereas a grid size of 500*m**500*m* results in a total of about 9.6 grid cells. The comparison of different grid sizes shows that apparently for the simulation of specific discharge of the total headwater catchment the loss of spatial pattern by a factor of 277 does not influence the achieved model efficiency. The Nopu catchment was taken as a leitcatena for the whole Gumbasa River catchment, which means that the actual soil physical properties are best represented at the Nopu catchment itself. Therefore with respect to the model efficiency of other sub-basins, for example the Takkelemo subbasin, good model efficiencies could be expected for the Nopu catchment. Surprisingly the calibration of the adjustable parameter k_{rec} for the PHAs with discharge data of other sub-basins lead to satisfactory results for the uncalibrated Nopu catchment. The results of the Nopu catchment demonstrate that the classification and parameterisation PHA's as soil units are valid for the entire catchment. Moreover the derived optimum parameter set, which is defined by the minimum objective function is also valid for ungauged sub-catchments.

6.5.4 Validation

Similar to the Takkelemo test catchment the same validation method was also applied for the Gumbasa River catchment. Again the validation was split into the pure validation period *(01.09.2003-31.08.2004)*, and the total period of simulation *(01.09.2002-31.08.2004)*. The Gumbasa River gauging site was excluded from the validation process, because due to technical problems no continuous hydrograph was available. Table 6.12-6.14 list the complete calibration and validation results for all considered statistical measures (coefficient of efficiency R^2, index of agreement *d*, ratio root mean square error, mean square error Δ *RMSE / MSE*) of the Danau Lindu, Sopu and Takkelemo gauging sites simulation results on a daily and weekly resolution. Compared to the calibration period, the daily and weekly coefficients of efficiency describe a moderate decline for all gauging sites for the split sample validation period. For the whole validation period R^2 reaches acceptable results. Simultaneously the degree of outliers increases on a daily resolution, which is indicated by the rise of the Δ *RMSE / MSE* ratio. Since it has been already discussed that for the adaptation of the factors that control the calculation of areal precipitation one year of calibration period is not adequate the instability of areal precipitation is reflected by the decline of model efficiency due to the existence of outliers. Here the weekly resolution does not seem to be an appropriate measure to analyse the overall model performance, the existence of outliers is obviously smoothed in some cases by a weekly mean value. The index of agreement *d* shows stable results for the considered validation periods, indicating an overall satisfying performance of the hydrological model.

Table 6. 12: List of the coefficient of efficiency R^2 for Danau Lindu, Sopu and Takkelemo sub-catchment on a daily and weekly resolution for the calibration, validation-split sample and validation-whole period.

R^2	Danau Lindu		Sopu		Takkelemo	
	daily	weekly	daily	weekly	daily	weekly
calibration period	0.83	0.86	0.79	0.77	0.58	0.77
validation period - split sample	0.61	0.62	0.58	0.44	0.41	0.50
validation period - whole	0.74	0.76	0.69	0.68	0.45	0.61

Table 6.12: List of the index of agreement d for Danau Lindu, Sopu and Takkelemo sub-catchment on a daily and weekly resolution for the calibration, validation-split sample and validation-whole period.

d	Danau Lindu		Sopu		Takkelemo	
	daily	weekly	daily	weekly	daily	weekly
calibration period	0.96	0.96	0.94	0.93	0.85	0.93
validation period - split sample	0.87	0.93	0.80	0.93	0.76	0.89
validation period - whole	0.93	0.94	0.87	0.91	0.82	0.89

Table 6. 13: List of ∆ RMSE / MSE for Danau Lindu, Sopu and Takkelemo sub-catchment on a daily and weekly resolution for the calibration, validation-split sample and validation-whole period.

△ RMSE / MSE	Danau Lindu		Sopu		Takkelemo	
	daily	weekly	daily	weekly	daily	weekly
calibration period	0.10	0.57	0.15	0.88	0.23	0.70
validation period - split sample	0.14	0.12	0.21	1.2	0.28	0.14
validation period - whole	0.13	0.8	0.17	0.91	0.25	0.93

6.5.5 Predictive uncertainty analysis

To run PEST [DOHERTY, 2003] in predictive analysis mode the value of the objective function below which the model can be considered to be calibrated has to be determined. This value is just slightly above the objective function value below which the model can be considered to be calibrated. For the predictive uncertainty analysis of the WASIM-ETH hydrological model for the Gumbasa River watershed a "dual model" consisting of the model run under both calibration and predictive conditions was set up. With the predictive uncertainty analysis the adjustable parameters were varied in such a way, that the variation of these parameters had no effect on model outcomes under calibration conditions. The same adjustable parameter set as for the calibration run with PEST was used (see Chapter 6.4.1). The period for the predictive uncertainty analysis was alike the whole validation period from 01.09.2002 until 31.08.2004. The initiation objective function of the critical point p1 ($\Phi_{min} + \delta$) was defined 10 % higher as the objective function of the calibration run p0 (Φ_{min}). Then the predictive uncertainty analysis determines iteratively the critical point where maximum model prediction is compatible with calibration imposed constraints on parameter values. The calculated value of p1 has a difference of 4.34 from the initial estimated p1 and an overall correlation coefficient of 0.955 was achieved for the model prediction that is associated with the determined critical point. Table 6.14 compares the residual analysis for the calibration run and the predictive uncertainty analysis with PEST for the Danau Lindu sub-catchments. The comparison demonstrates that with the parameter set of the determined critical point the calibration during the predictive sensitivity analysis stays stable within certain limits.

Table 6. 14: Statistical residual analysis for the calibration run and the predictive sensitivity analysis for the Danau Lindu sub-catchment.

Residual analysis	**Danau Lindu sub-catchment**	
	calibration run	predictive uncertainty analysis
Number of residuals	365	365
Mean value of residuals	-0.18	-0.47
Maximum residual	0.38	-0.06
Minimum residual	-1.12	-1.72
Variance of residuals	0.11	0.32
Standard error of residuals	0.33	0.56

Figure 6.17 shows the observed discharge versus the simulated discharge of the Danau Lindu sub-catchment for the model prediction of the critical point parameter set. The visual comparison of the observed and simulated discharge indicates a loss of model efficiency during the calibration period, but overall good model efficiency for the whole modelling period. The results of the predictive uncertainty analysis prove that the calibrated parameter set for the hydrological model WASIM-ETH of the Gumbasa River catchment describes a global optimum and can be applied for further model simulations of future scenarios.

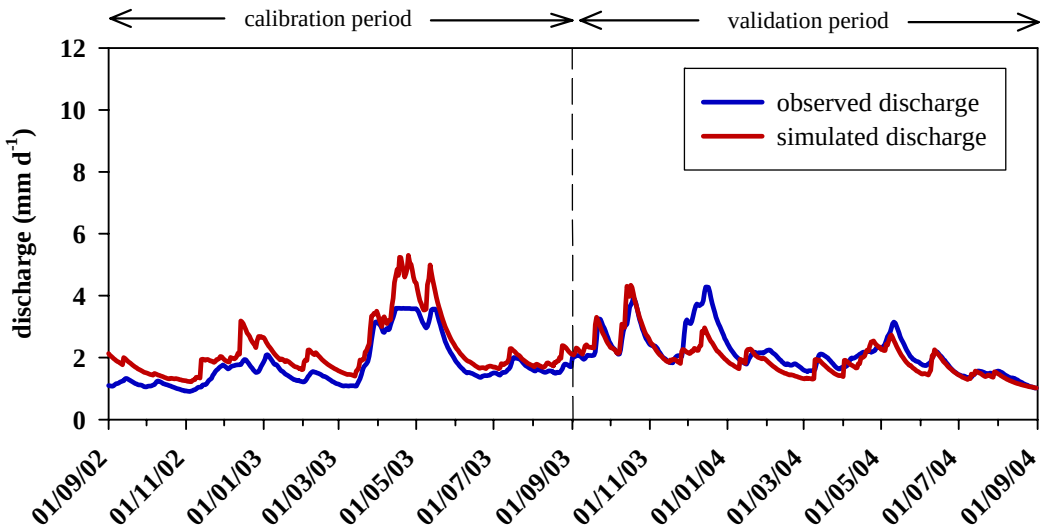

Figure 6. 17: Results of the predictive uncertainty analysis *(01.09.2002-31.08.2004)* of the Danau Lindu sub-catchment (daily resolution): comparison between observed and simulated (R^2=0.52) discharge.

6.6 DISCUSSION AND CONCLUSION

It has been demonstrated that the process-based, distributed hydrological model WASIM-ETH is an appropriate management model for prediction and scenario analysis for a mesoscale humid tropical catchment. Humid tropical catchments are usually characterised as data deficient regions and therefore require general simple models like e.g. lumped catchment models [BARNES & BONELL, 2005]. The ramifications of these areas were overcome by a detailed measurement campaign of the particular catchment area. The process-based, distributed hydrological models have considerable value and benefits in the assessment of forestry, agricultural and human impacts on the hydrological behaviour of the catchment [CHAPPEL et. al, 2005]. The application of the hydrological model WASIM-ETH on the Gumbasa River catchment in Central Sulawesi, Indonesia is the model's first simulation of the water balance of a mesoscale humid tropical catchment. The achieved model efficiencies can be evaluated with other WASIM-ETH model applications in various catchment studies of different climatic regions [SCHULLA, 1997; JASPER *et al.*, 2002; PIEPHO, 2003]. The modularly based character of WASIM-ETH allows a general adaptation of the hydrological model to different climatic regions and catchment data bases in space and time. The predictive uncertainty analysis, which was conducted to assess the overall parameter uncertainty, has proven the overall predictive ability of the calibrated hydrological model. In comparison with the commonly applied Monte-Carlo Analysis the predictive sensitivity analysis results in a capable number of simulation runs. If there are several adjustable parameters, the Monte-Carlo-Analysis, result in an unrealistic million of model runs, because the parameter sets are determined randomly and are not tied to a defined range around objective function, [DOHERTY, 2003].

If the overall model uncertainty is assessed with regard to the available spatial data set, the land use and the soil classification represent the major sources of uncertainty. With regard to land use classification derived from satellite images like Landsat ETM+, it should be further analysed if different land use classification methods result in different modelling results. Furthermore the dramatic land use changes within the catchment area are a source of error for the simulation of the water balance of the status quo. These dramatic land use changes within the Gumbasa River catchment during the calibration period reflect the aspect of the non-stationarity of tropical

catchments, which is defined by KLEMES [1993] as one major aspect of tropical hydrology. Whereas in reality the land use was changing constantly during the calibration period, for the model application the same static land use classification from a previous satellite scene was taken for the whole period. If the purpose of the model application is the evaluation of land use scenarios, this unfocussed representation of the actual land use during the calibration run might alter the overall predictive ability of the model. It is promising that today with fast developing of remote sensing data products and a data delivery which occurs closer to “real time” on a routine basis [HELD & RODRIGUEZ, 2005], future applications of hydrological model will be calibrated with the real time fluctuation of land use changes. Due to an inadequate soil map of the watershed area the soil classes were generated on the basis of similar topographic properties. For the simulation of the hydrological processes of the catchment area this soil classification concept proved to be sufficient for hydrological modelling purposes. For the regionalization of hydrological response units this concept of classification of similar soil process units was already conducted by GEROLD *et al.* [2003], and seems to be a promising soil regionalization concept for hydrological modelling purpose if no adequate soil map is available. The parameterisation of soil hydraulic properties by an already analysed catena within the catchment represents a further development of this concept.

A longer time series than the observed two year’s time series would lead to a more stable and reliable modelling results. This conclusion about the overall modelling performance underlines the statement by BEVEN & FEYEN [2002] to generally invest more in field measurement techniques and support long-term catchment measurement campaigns, instead just to focus on the development of computing and modelling. The results of the modelling performance demonstrated that the areal precipitation for which the model is very sensitive was not represented well for single storm events, which led to an overall decrease of the achieved model performance. The miscalculation of areal precipitation is a result of the climate station density within the catchment and on the other hand of inappropriate regionalization methods, which are provided by the hydrological model WASIM-ETH. The comparison of the application of WASIM-ETH on a smaller subcatchment (79 km²) with the total catchment (1275 km²) has emphasized the hypothesis that smaller watersheds require

more precise areal precipitation estimates. If the catchment would be equipped with a denser and spatially more distributed net of climate stations at different elevations the areal precipitation could be calculated by ordinary griging, which is a geo-statistic least-square-method of spatial prediction [WEBSTER & OLIVER, 1999]. This method is promising for the estimation of areal precipitation though it makes the best use of existing station data knowledge by taking into account that precipitation varies in space, but requires a certain number of observation stations. A study by JASPER *et al.* [2002] has demonstrated the potential usefulness of radar images for the calculation of areal precipitation as input data for the hydrological model WASIM-ETH. Further a study by ROLLENBECK *et al.* [2005] has shown that the application of radar technique for the generation of areal precipitation seems to be promising also for humid tropical mountain catchments. An alternative theoretical method to overcome the problem of small convective storm events, which are characteristic for the humid tropics, was undertaken by NOORDWIJK *et al.* [2003] within the Sumber Jaya catchment, Lampung, Indonesia. A rainfall generator was incorporated within a hydrological model that simulated small convective patchy storm events. NOORDWIJK *et al.* [2003] concluded that at a landscape level patchy rainfall leads to a more homogeneous riverflow, and therefore generated rainfall is a suitable artificial areal precipitation generator. The discussion on the quality of precipitation interpolation techniques shows that appropriate methods to be integrated within hydrological models especially for tropical catchments are still in progress. Nevertheless, without long-term data and dense station grids for humid tropical catchments no further improvements about the proper methodology will be made.

The soil module using the *Richards-Equation* shows the well known weakness of most of the hydrological models, especially the non-existent simulation of preferential flow, because the soil column is assumed to be a homogeneous matrix [NIEHOFF, 2001]. The results of various hydrological studies of tropical hill slopes [VERTESSY et. al, 2000; BONELL, 2005] have emphasized the particular role of pipes and makropores for hydrological processes. Therefore the solution conducted in the study by KLEINHANS [2004] was also applied for this model application. Here preferential flow was simulated by simply increasing the saturated soil hydraulic conductivity of the soil matrix. Increasing the saturated soil hydraulic conductivity leads to an artificial representation of hydrological flow paths and has to be evaluated

as a temporary solution. GRAYSON & BLÖSCHL [2000] argue that it is possible to reproduce the effects of lateral flow of makropores by using *Darcy's* equation and a very high value of hydraulic conductivity. While the simulation of lateral fluxes might be correct the distribution of flow velocity is not, because the hydraulic conductivity of the soil is characterised by anisotropy. Therefore the vertical fluxes are not properly presented. The Gumbasa River watershed is characterised by steep slopes, which means that for the simulation of the hydrological processes the lateral fluxes prevail and predominately lateral fluxes generate the total discharge.

Another uncertainty of the model application is the parameterisation of the vegetation's physical properties, which is mainly undertaken by a literature review. This leads to additional uncertainty in the calculation of evapotranspiration. Considering that up to 60% of the calculated total water balance of the Gumbasa River catchment is dominated by evaporation of rainfall intercepted by the vegetation canopy and transpiration of water taken up from the soil by the root system the required parameters should be determined with more precision. For example ROBERTS *et al.* [2005] found the leaf area index (LAI) for lowland tropical rainforests, to fall between LAI=3 and LAI=11. Further the evapotranspiration rate is calculated on a leaf scale and then is simply up-scaled by vegetation cover in m^2, which might lead to up scaling errors. These considerations demonstrate that there is still an urgent need for further plant physiological research and associated up-scaling methods for tropical vegetation types for further assessment of the performance of hydrological models. With regard to model uncertainty of the Gumbasa River model, it should be mentioned that the calculated evapotranspiration rates of WASIM-ETH are a coarse simulation of the evapotranspiration rate, but still within a realistic range, which could be shown by a comparison with other tropical catchment studies.

The comparison of the simulated water balance of the Nopu subcatchment (500*m** 500*m*), with the Nopu study conducted by KLEINHANS [2004] on a far finer grid element size (30*m**30*m*) demonstrates that for the considered period the loss of catchment pattern information by up-scaling to a bigger element size surprisingly does not influence the overall model performance for the simulation of the specific discharge. This result indicates that if the applied hydrological model, due to its representation of the key processes, may not require a detailed pattern of the catchment heterogeneity to improve the simulation of the hydrological catchment

response. These findings are contrary to the statement of GRAYSON & BLÖSCHL [2000], who see an overall dependence of the hydrological model on DTM resolution, though model parameter values are likely to change with the size of the element. Here it is more likely that the achieved efficiency is particular sensitive to the spatial pattern of soil physical properties. If the data to define the spatial variability of the model parameters for soil properties is not available, there is probably no advantage in using very small elements [GRAYSON & BLÖSCHEL, 2000]. Therefore it can be assumed that due to the number and spatial distribution of soil analysis, the spatial variability of the soil pattern can be represented by a 500*m**500*m* grid size element. A spatial grid size resolution of 30*m**30*m* will not give any further information about the soil pattern variability. With regard to the simulation of the discharge process, the spatial pattern of soil data seems to be dominant over the spatial pattern of land use, which is available with a finer resolution (Landsat ETM resolution = 30*m**30*m*).

SCENARIO APPLICATION

Prediction of climate is an essential aspect of planning of water resources in changing environmental conditions [FU *et al.*, 2004]. The implications of possible climate and land use conditions in the future on the water balance of a mesoscale tropical catchment (sample catchment Gumbasa River) were assessed by a scenario analysis, which simulates a sequence of possible future events.

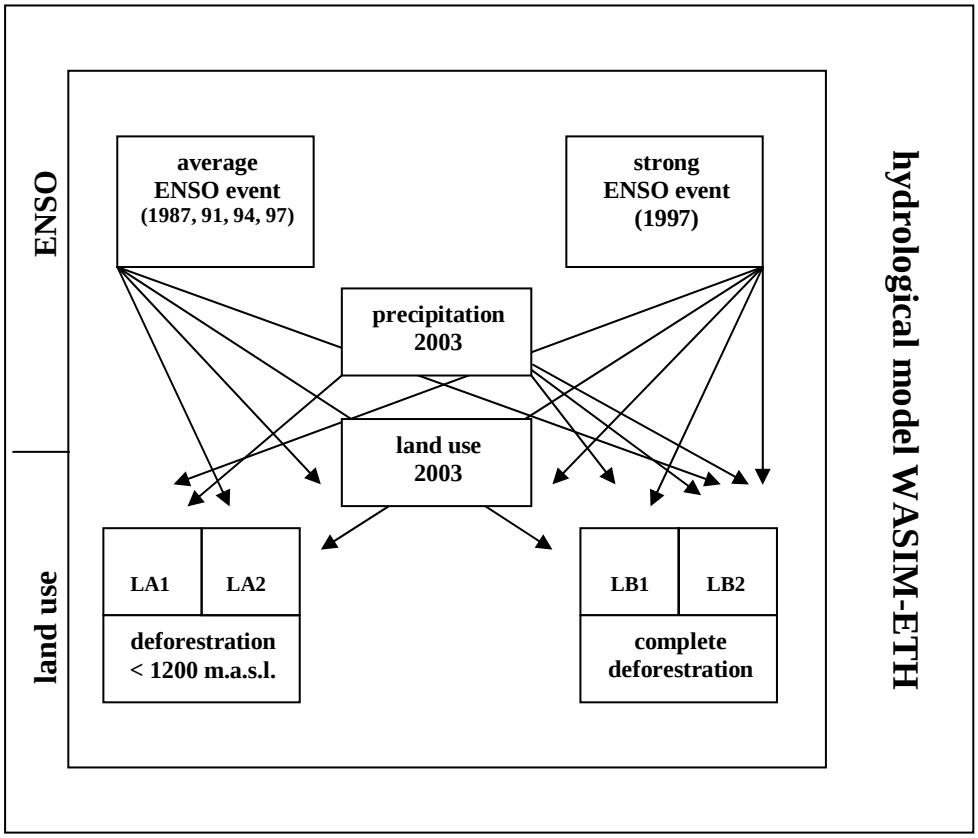

Figure 7. 1: Diagram of the applied ENSO caused rainfall anomalies and land use scenarios for the Gumbasa River catchment with the hydrological model WASIM-ETH.

Basis of the scenario simulation is the calibrated and validated hydrological model (WASIM-ETH) of the basin for the year 2003. The scenarios quantify effects on the water balance for the year 2003 if the climate or the land-use change. Figure 7.1 describes the sequence of the applied climate and land use scenarios. First of all the implications of ENSO caused rainfall anomalies on the water balance were simulated. The ENSO caused rainfall anomaly scenarios were generated by a statistical approach and describe an average ENSO event, and a strong ENSO event. Here the special focus of the scenario analysis was on the spatial and temporal discharge variability within the catchment. Furthermore two land use scenarios with one succession phase per land use scenario were applied for the modelling year 2003. Each succession phase describes the land use situation after five years. This scenario application investigates the impact of land use changes on the water balance.

7.1 ENSO SCENARIO GENERATION

A statistical scenario approach was applied to generate scenarios of spatially and temporally variable ENSO caused rainfall anomalies as input data for a hydrological scenario run of the Gumbasa River watershed. Five climate stations with a long term historical record (1981-1999) were located within the area around the climate stations, which were used for the calculation of areal precipitation. The interdisciplinary climate research group of the IMPENSO project calculated the monthly precipitation anomaly of ENSO years in percent related to the mean monthly precipitation of the observed years. Therefore two graded ENSO scenarios which reflect the mean anomaly of all observed ENSO events (1987, 1991, 1994, and 1997) and on the other hand the extreme ENSO event of 1997, were generated. Thereafter the climate stations used for the interpolation of areal precipitation were allocated to one of the long term stations according to their elevation and topographic position. The allocation is mainly basin related although each of the long-term climate stations is located within one of the main basins,. The study of ALDRIAN [2003] has shown that ENSO events have a significant influence on the climate of Central Sulawesi between the dry period from June till October. The ENSO scenario was applied for this time frame which is affected by ENSO related precipitation anomalies. For the generation of the two graded ENSO scenarios the modelling year 2003 was taken as a base year. According to the SOI-Index 2003 is not characterised as an “ENSO” year (Figure 7.2). The year 2003 serves as a reference year for

"normal" meteorological conditions and moreover as basis data for the generation of ENSO caused precipitation anomalies.

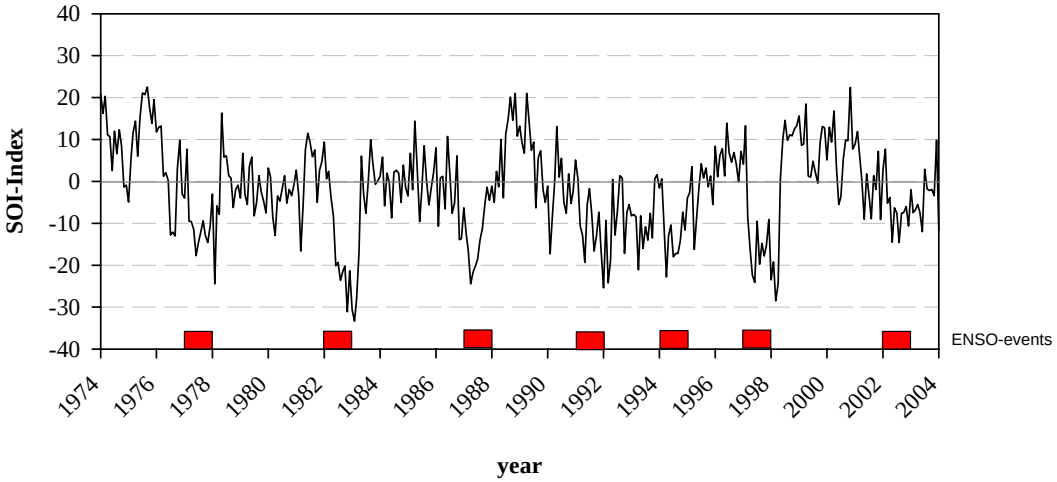

Figure 7. 2: SOI – Index 1974 – 2004, SOURCE: SOI Archive since 1864, Australian government, bureau of meteorology.

To generate an ENSO related precipitation anomaly scenario the monthly precipitation rate during June till October was altered for each station according to the ENSO related monthly decrease of precipitation and adjusted to one of the long term record climate stations. Similar to the normal modelling year 2003, the scenario areal precipitation was then calculated with the altered station data. Table 7.1 describes precipitation anomalies of each long term station in percent for an average ENSO year (ENSO Scenario A) and for the extreme event of 1997 (ENSO Scenario B). These values were used for the generation of an ENSO scenario areal precipitation. The monthly precipitation anomaly for an average ENSO event and the extreme event of 1997 reflect the overall spatial and temporal variability within the Palu River watershed. For the generation of the ENSO scenarios only the precipitation anomalies were taken into account. Feedback mechanisms of the precipitation anomalies with other climatic parameters were not considered.

Table 7. 1: Applied monthly ENSO caused rainfall anomalies for an average (av.) and a strong (97) ENSO scenario

station	June		July		August		September		October	
	av.	97.	av.	97	av.	97.	av.	97.	av.	97
Kalawara (68 m.a.s.l) (1°10'00S, 119°55'53E)	-21 %	+10 %	- 27%	+87%	-48%	-100 %	-80 %	- 88%	- 40 %	- 84
Pandaya (1050 m.a.s.l.) (1°04'07S, 120°04'44E)	-25 %	-56 %	-35 %	-13 %	-74 %	- 94 %	-90 %	-100 %	- 71 %	-50 %
Wuasa (1187 m.a.s.l.) (1°25'30S, 120°19'22E)	-41 %	-71 %	-29 %	-11 %	-25 %	+28 %	-24 %	+ 3%	-60 %	-65 %
Bora (125 m.a.s.l.) (1°01'39S, 119°55'53E)	-5 %	-13 %	-53 %	-81 %	-20 %	-100 %	-83 %	-100 %	20 %	-40 %
Kulawi (850 m.a.s.l.) (1°28'11S, 119°59°45E)	-0.4 %	-58 %	-44 %	- 40 %	-8 %	- 57 %	-62 %	- 61 %	-40 %	- 68 %

7.2 LAND USE SCENARIO GENERATION

The Archipelago of Indonesia has an annual forest cover change of -1.2 % (Brazil – 0.4 %), which indicates a dramatic deforestation rate [FAO, 2003]. The island Sulawesi itself still has a total forest cover of 48 % [HOLMES, 2000]. The natural resource tropical rainforest of Sulawesi is constantly threatened by the development of new agricultural land and illegal logging activities. With a population growth of 66 % over the past two decades around the area of the Gumbasa River watershed [MAERTENS *et al.*, 2004] massive land cover changes have changed the land use pattern of the watershed. In reality land use change of the watershed happens in patches and is relatively slow. To emphasize the impact of land use changes on the water budget, an elevation dependent total change scenario was chosen. The first land use scenario LA assumes that all the forest up to an elevation of 1200 m.a.s.l. is logged and for the first succession phase LA1 annual crops are planted. In a long term for the second succession phase LA2 the annual crops are exchanged by cacao plantations. Cacao is the main cash crop of Sulawesi. The island is producing 67 % of the Indonesian cacao production [ICCO, 2003] with increasing yearly expansion rates. Optimal growing conditions for cacao trees are characterised by a humid climate with a mean daily temperature of 25 °C. Moreover the night temperature should not fall beneath 18 °C [REHM, 1989]. Therefore it may be assumed that the local farmers try to build cacao plantation up to 1200 m.a.s.l. The second land use

scenario LB describes a worst case scenario with a total deforestation of all altitudinal intervals. On above 1200 m.a.s.l. natural shrub vegetation with cogongrass *(Imperata cylindrica)* and different fern species *(Aspidaceae)* would develop, because they cannot be used for plantations within the first succession phase LB1. Cogongrass characterises degraded site conditions [IMPERIAL AGRICULTURAL BUREAU, 1944], therefore for the second succession phase LB2 the vegetation would not change.

To set up the land use scenarios within WASIM-ETH the vegetation parameters were altered according to the land use scenario. Table 7.2 describes the applied vegetation parameters for each land use scenarios. The water budget was then calculated with the applied land use dynamic. For the shrub vegetation the same plant characteristics as for grassland were used.

Table 7. 2: Applied vegetation parameters for the succession land use scenarios.

land use class	α	R_C	LAI	v	z_0	z_w	p	ψ_g
annual crops	0.18	100	1.5	0.3	2.0	0.3	-1	3.55
cacao	0.15	270	5	0.6	5	1.0	-0.5	3.55
shrub vegetation	0.26	200	1	0.2	0.5	0.2	-1	3.55

Only the physical vegetation parameters were altered for the application of the land use scenarios. Alterations of the soil physical parameters due to the degradation of the soil were not considered. Also two way fluxes between the atmosphere and the land surface were not incorporated within the hydrological model. Deforestation leads to changes in the surface energy, inducing changes in the evapotranspiration and therefore resulting in changes of the local climate.

7.3 GENERAL RESULTS

Scenario simulations with WASIM-ETH were performed for the above described rainfall anomaly and land use change scenarios for the year 2003. The following table (7.3) describes the control run, which simulates the current climate and land use conditions of 2003 and the 14 ENSO and land use scenario combinations that were applied for the Gumbasa River catchment.

Table 7. 3: Applied climate and land use scenarios for the year 2003 (Gumbasa River catchment).

Scenario	**ENSO**	**land use**
E0L0	current climate conditions 2003	current land use 2003
E0LA1	current climate conditions 2003	< 1200 m.a.s.l. annual crop
E0LA2	current climate conditions 2003	< 1200 m.a.s.l. cacao plantation
E0LB1	current climate conditions 2003	< 1200 m.a.s.l. annual crop > 1200 m.a.s.l. shrub vegetation
E0LB2	current climate conditions 2003	< 1200 m.a.s.l. cacao plantation > 1200 m.a.s.l. shrub vegetation
EAL0	scenario A (average ENSO event)	current land use 2003
EALA1	scenario A (average ENSO event)	< 1200 m.a.s.l. annual crop
EALA2	scenario A (average ENSO event)	< 1200 m.a.s.l. cacao plantation
EALB1	scenario A (average ENSO event)	< 1200 m.a.s.l. annual crop > 1200 m.a.s.l. shrub vegetation
EALB2	scenario A (average ENSO event)	< 1200 m.a.s.l. cacao plantation > 1200 m.a.s.l. shrub vegetation
EBL0	scenario B (ENSO event 1997)	current land use 2003
EBLA1	scenario B (ENSO event 1997)	< 1200 m.a.s.l. annual crop
EBLA2	scenario B (ENSO event 1997)	< 1200 m.a.s.l. cacao plantation
EBLB1	scenario B (ENSO event 1997)	< 1200 m.a.s.l. annual crop > 1200 m.a.s.l. shrub vegetation
EBLB2	scenario B (ENSO event 1997)	< 1200 m.a.s.l. cacao plantation > 1200 m.a.s.l. shrub vegetation

In order to evaluate the spatial variability of the hydrological impact of the applied scenarios the analysis of the induced changes on water resources should incorporate different catchment types. Therefore the Gumbasa River catchment and its sub-catchments Danau Lindu and Takkelemo were selected as representative sample catchments. The whole Gumbasa River catchment and the selected sub-catchments Takkelemo and Danau Lindu represent three different catchment types: (A) Danau Lindu: a medium mesoscale catchment (525 km²) with a high storage capability, (B) Takkelemo: a fast responding small mesoscale catchment (79 km²) and (C) Gumbasa River: a mesoscale catchment (1275 km²), which integrates the spatial variability of all sub-catchments. The results of the scenario simulations were analysed according to the spatial variability of the different subcatchments, changes in the yearly water balance, and temporal variability.

7.4 WATER BALANCE

Table 7.4 compares the changes induced by climate and land use scenario of the following water balance components for all examined sample catchments: areal precipitation P, evapotranspiration ETR and total discharge Q. The current conditions of 2003 serve as a control run for the evaluation of the proportional changes.

During ENSO scenario A the total yearly areal precipitation of the Gumbasa River catchment is reduced by 25 %, whereas the total yearly evapotranspiration rate is only slightly minimised by 3 %. The main difference of the yearly water balance were observed for the total yearly discharge, which is reduced by 31 %. With a reduction of the total discharge by 25 %, the Danau Lindu sub-catchment is least affected by the precipitation anomaly, whereas the small Takkelemo catchment reaches similar reduction values like the Gumbasa River catchment. Even though the strong ENSO event of 97 is applied by ENSO scenario B, total yearly changes of the water balance in comparison with ENSO scenario A are minimal. For example the decrease of the yearly total discharge only is reduced by 0.7 % for the Gumbasa River catchment. The comparison of the yearly water balance of the three different catchment types shows that the ENSO caused precipitation anomaly leads to a slight variance of the yearly precipitation decline among the catchments of 2.9 % for ENSO scenario A and 3.7 % for ENSO scenario B. For both ENSO scenarios the Danau Lindu subcatchment indicates with 22.0 % (Scenario A) and 22.5 % (Scenario

B) the lowest yearly precipitation decline, whereas the Gumbasa River catchment has a yearly average precipitation decline of 24.9 % (Scenario A) and 26.2 % (Scenario B). The simulated yearly precipitation decline is not linear with the simulated yearly discharge decline, which indicates a far wider variance of the different catchment types with 8.4 % for ENSO scenario A and 9.1 % for ENSO scenario B. Again for both scenarios the Danau Lindu catchment has the lowest discharge decline with 23.6 % for both ENSO scenarios and the Gumbasa River catchment the highest discharge decline among the observed catchments with 32.0 % (ENSO scenario A) and 32.7 % (ENSO scenario B). The simulation for the Takkelemo catchment reaches almost similar precipitation and discharge decline values as for the Gumbasa River catchment. The simulated ENSO scenario results for yearly precipitation and discharge decline demonstrate the influence of the overall catchment characteristics on the potency of ENSO caused discharge anomalies. The weakest impact was observed for the Danau Lindu catchment.

The most significant changes of the yearly total water balance were observed for the applied land use scenarios. The reduction of the total evapotranspiration rate results in an overall increase of the total discharge. The highest yearly increase of the total discharge with 57 % occurs during the scenario run E0LB1 for the Gumbasa River catchment. For this scenario run the Danau Lindu catchment indicates a strong increase of total discharge with 37 %. Scenario variations of the total evapotranspiration show the highest increase (29 %) within the same scenario run for the Takkelemo catchment. In combination with the ENSO scenarios the reduction of the evapotranspiration rate for the land use scenarios leads to an overall increase of the total discharge. This counter-effect of the reduction of the total discharge during ENSO events is strongest for land use scenarios LA1 and LA2. During the succession phase 2 of the land use scenarios (LA2, LB2) the overall evapotranspiration increases, and total discharge decreases.

Table 7. 4: List of the water balances for the Gumbasa River catchment and two sub-catchments for the control run and all applied climate and land use scenarios; ΔP, ΔETR and ΔQ represent the changes of precipitation, evapotranspiration and total discharge in percent proportional to the total sum of the control run for each component of the water balance respectively.

Scenario	catchment	precipitation		evapotranspiration		total discharge	
		P [mm]	Δ P [%]	ETR [mm]	Δ ETR [%]	Q [mm]	Δ Q [%]
E0L0 (control run)	Gumbasa	2150	-	1543	-	590	-
	Danau L.	2192	-	1295	-	896	-
	Takkelemo	2259	-	1428	-	804	-
E0LA1	Gumbasa	2150	± 0.0	1265	- 20.0	838	+ 42.0
	Danau L.	2192	± 0.0	1112	- 14.1	1218	+ 35.9
	Takkelemo	2259	± 0.0	1124	- 21.3	1113	+ 38.4
E0LA2	Gumbasa	2150	± 0.0	1361	- 11.8	724	+ 22.7
	Danau L.	2192	± 0.0	1144	- 11.7	1097	+ 22.4
	Takkelemo	2259	± 0.0	1222	- 14.4	1000	+ 24.4
E0LB1	Gumbasa	2150	± 0.0	1176	- 23.8	926	+ 56.9
	Danau L.	2192	± 0.0	970	- 25.1	1231	+ 37.4
	Takkelemo	2259	± 0.0	1006	- 29.6	1224	+ 52.2
E0LB2	Gumbasa	2150	± 0.0	1293	- 16.2	812	+ 37.6
	Danau L.	2192	± 0.0	1045	- 19.3	1149	+ 28.2
	Takkelemo	2259	± 0.0	1131	- 20.8	1111	+ 38.2
EAL0	Gumbasa	1614	- 24.9	1496	- 3.0	401	- 32.0
	Danau L.	1710	- 22.0	1281	- 1.1	684	- 23.6
	Takkelemo	1724	- 23.7	1423	- 0.4	561	- 30.2
EALA1	Gumbasa	1614	- 24.9	1241	- 19.6	612	+ 3.7
	Danau L.	1710	- 22.0	1091	- 15.7	826	- 7.8
	Takkelemo	1724	- 23.7	1112	- 22.1	808	+ 0.5
EALA2	Gumbasa	1614	- 24.9	1358	- 12.0	521	- 11.7
	Danau L.	1710	- 22.0	1169	- 9.7	769	- 14.2
	Takkelemo	1724	- 23.7	1241	- 13.1	720	- 10.5
EALB1	Gumbasa	1614	- 24.9	1148	- 25.2	681	+ 15.4
	Danau L.	1710	- 22.0	945	- 27.0	946	+ 5.6
	Takkelemo	1724	- 23.7	989	- 30.8	910	+ 13.2
EALB2	Gumbasa	1614	- 24.9	1266	- 17.5	591	+ 0.2
	Danau L.	1710	- 22.0	1023	- 21.0	890	- 0.7
	Takkelemo	1724	- 23.7	1118	- 21.7	822	+ 2.2
EBL0	Gumbasa	1586	- 26.2	1487	- 3.1	397	- 32.7
	Danau L.	1699	- 22.5	1279	- 1.2	684	- 23.6
	Takkelemo	1709	- 24.4	1421	- 0.5	557	- 30.7
EBLA1	Gumbasa	1586	- 26.2	1234	- 19.6	606	+ 2.7
	Danau L.	1699	- 22.5	1088	- 16.0	827	- 7.7
	Takkelemo	1709	- 24.4	1110	- 22.3	804	± 0.0
EBLA2	Gumbasa	1586	- 26.2	1351	- 12.0	515	- 12.7
	Danau L.	1699	- 22.5	1167	- 9.9	769	- 14.2
	Takkelemo	1709	- 24.4	1239	- 13.2	715	- 11.1
EBLB1	Gumbasa	1586	- 26.2	1141	- 23.6	679	+ 15.1
	Danau L.	1699	- 22.5	942	- 27.3	946	+ 5.6
	Takkelemo	1709	- 24.4	987	- 30.9	907	+ 12.8
EBLB2	Gumbasa	1586	- 26.2	1258	- 18.0	587	- 0.5
	Danau L.	1699	- 22.5	1022	- 21.1	888	- 0.9
	Takkelemo	1709	- 24.4	1116	- 21.5	817	+ 1.6

7.5 SPATIAL AND TEMPORAL VARIABILITY

The comparison of the yearly water balance gives a general first overview about the impact of climatic and land use changes on the hydrological performance of the observed watershed [SCHULLA, 1997]. Especially the yearly scenario variations of evapotranspiration and discharge indicate the consequences of the applied scenarios on the hydrological cycle and moreover on connected physical earth processes, e.g. sediment transport. For a detailed analysis of the implications of the applied scenarios on water resources of the catchment, the spatial and temporal variability of the components of the water balance is essential. The discharge is one of the most important water balance components according to its significance for the water resource availability. Figure 7.3 describes the low pass flow duration curve of the whole Gumbasa River, the Takkelemo and the Danau Lindu sub-catchment for the control run with current conditions and the applied ENSO scenarios A and B. The low pass flow duration curve displays the yearly number of days (x-axis), which fall below a certain discharge (y-axis). The low pass flow duration curves for the ENSO scenarios indicate for all catchment types increasing discharge variability due to decreasing low water discharge. Generally a lower mean discharge is simulated for the ENSO scenarios of all catchment types, whereas the high water discharge is constant for all scenarios. The further analysis of the low pass flow duration curve emphasises the retention capability of the Danau Lindu catchment with relative low discharge variability, indicated by the relative flat gradient of the low pass flow duration curve. Since for the control run the gradient of the Danau Lindu catchment is characterised by reduced discharge variability due its retention capability, the discharge variability during ENSO events is significantly higher.

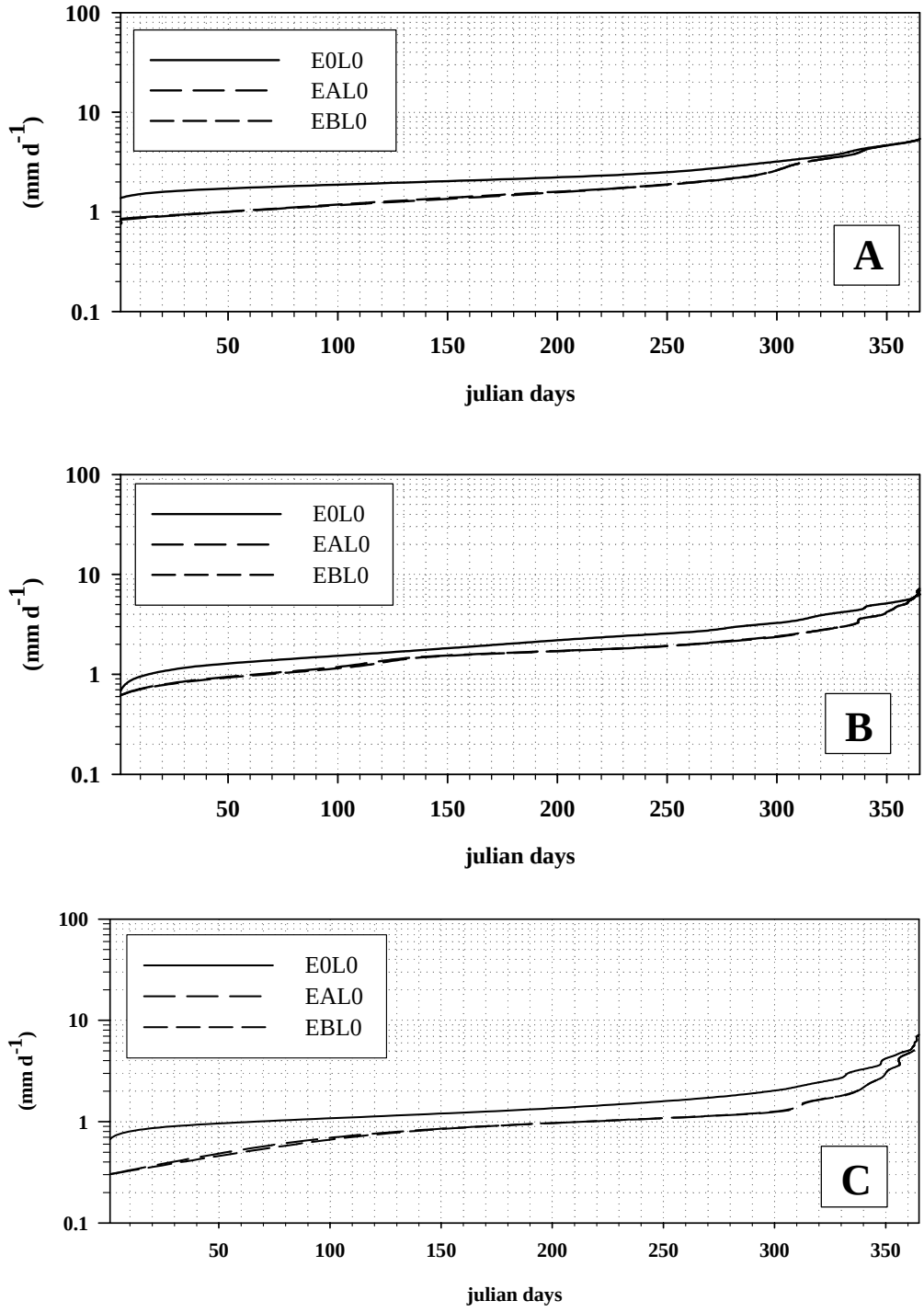

Figure 7. 3: Low pass flow duration curve fort the control run and ENSAO scenario A and B for the Danau Lindu (A), Takkelemo (B) and Gumbasa River (C) catchment.

The same characteristics can be observed for the Gumbasa River catchment, whereas the small Takkelemo catchment already has a relative small low water discharge, which is not further decreased by ENSO caused precipitation anomalies. This effect is mainly related to the overall higher discharge variability of a fast responding small catchment like the Takkelemo catchment, whereas the Gumbasa River and the Danau Lindu catchment have an overall higher low water discharge because they integrate precipitation over a far bigger catchment area. Therefore during ENSO events the discharge variability within the catchment clearly increases. In general the simulated differences of the low pass flow duration curve of the ENSO scenarios in comparison with the current climate conditions demonstrate that ENSO events have a significant impact on the hydrological process of the catchments within periods of low water and mean discharges. In order to demonstrate the influence of ENSO caused precipitation anomalies on the temporal discharge variability of the catchment samples the monthly regime was calculated for the current climate conditions of 2003 and precipitation anomaly scenarios A and B (Figure 7.4). Since the monthly regime values are calculated by varying mean yearly discharges for the current conditions and the applied scenarios they are not directly comparable. The relative monthly changes of the flow regimes only describe the overall yearly discharge trend. During the simulation of ENSO events a decline of the discharge regime occurs beginning of July for all sample catchments, stabilizes towards end of November, before the regime again slightly increases beginning of December. The yearly variation of the flow regime underlines the slight timely shift from the occurrence of the precipitation anomalies till the decrease of the discharge regime. Furthermore the implications on the discharge regime last till end of December.

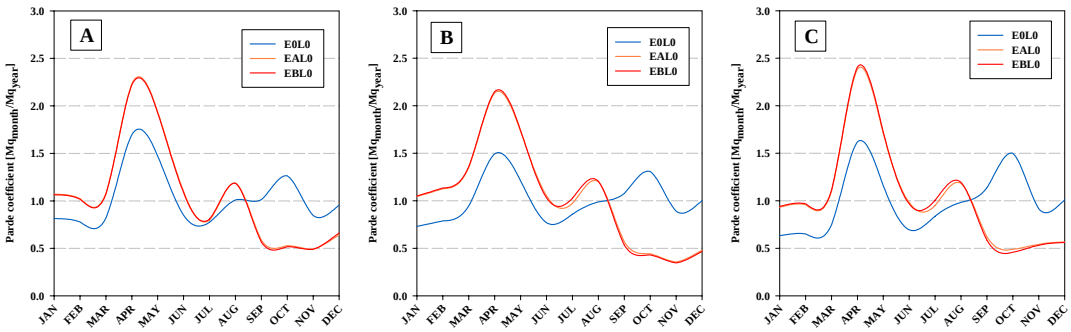

Figure 7. 4: Monthly regime for actual conditions and ENSO scenario A and B, Danau Lindu (A), Takkelemo (B) and Gumbasa (C) catchment.

Following this the impact of land use changes on the sample catchment during ENSO events was analysed. First the above described land use scenarios were applied to the sample catchments for the current climate conditions of 2003 to determine the overall implications of land use changes on the hydrological processes.

Figure 7.5 shows the variation of the low pass flow duration curve for the applied land use scenarios in comparison with the current land use conditions of 2003 for all sample catchments. The impact of the different land use scenarios on the low pass flow duration curve is recorded by an overall positive shift of the flow duration curve, indicating an overall increase of the mean discharge, low water and the high water discharge. The differences between the different land use scenarios are significantly smaller compared to the differences proportional to the current land use conditions. The various catchment types show different shift trends of the low pass flow duration curves. The Danau Lindu catchment responses to the applied land use scenarios with a more even distributed shift, whereas the Takkelemo catchment has a clear shift to the high water discharge and the Gumbasa River catchment to the low water discharge. For the assessment of the implication of land use changes on the hydrological processes during ENSO events the same analysis was conducted for the Gumbasa River catchment for current climate conditions and ENSO scenario A and B. The sequence of the low pass flow duration curve for different land use and ENSO scenarios is projected in Figure 7.6.

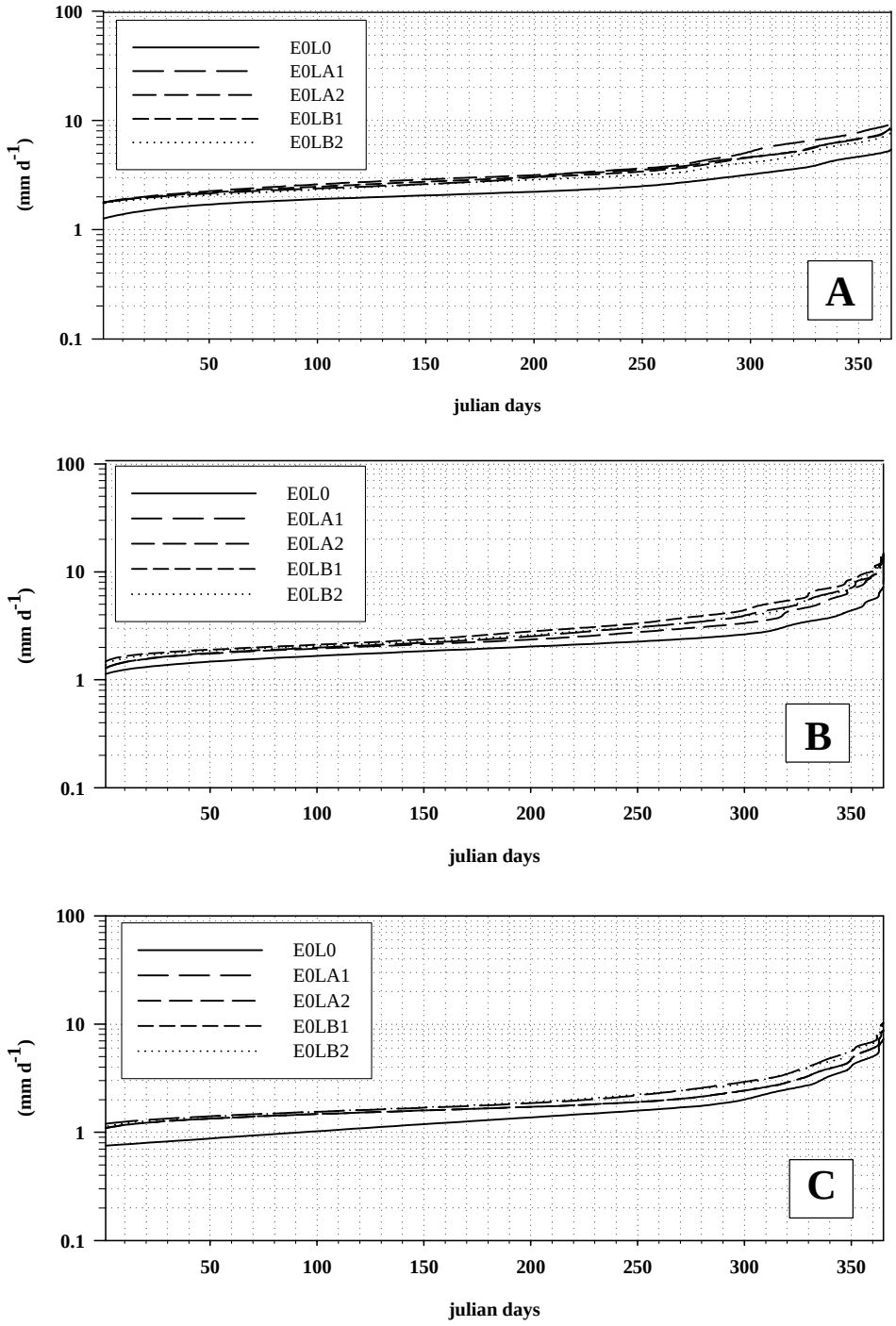

Figure 7. 5: Low pass flow duration curve for the current climate conditions 2003 and land use scenarios LA1, LA2, LB1 and LB2 for the Danau Lindu (A), Takkelemo (B) and Gumbasa River (C) catchment.

The applied land use changes lead during ENSO conditions (scenario A, B) to a significant higher yearly discharge variability, which is expressed by an increase of the extreme low water and high water discharge events. In order to evaluate the impact of land use changes on the temporal variability during ENSO events the monthly NQ, MQ and HQ was calculated for ENSO scenario A for the Gumbasa river catchment (Figure 7.6). The diagram of the monthly variation of the low discharge NQ demonstrates a moderate monthly rise if the land use alters from forest to plantations. The impact of the different land use scenarios increases the mean monthly discharges (MQ) and are significant for the high water monthly discharges (HQ). This implies that the applied land use scenarios have a more important influence on high water than on low water discharges. The worst case land use scenario LB, succession phase 1 indicates the highest impact on the high water discharge. In contrast the lowest impact of land use changes on the high water discharge. In contrast the lowest impact of land use changes on the high water discharge is caused by land use scenario LA, succession phase 2.

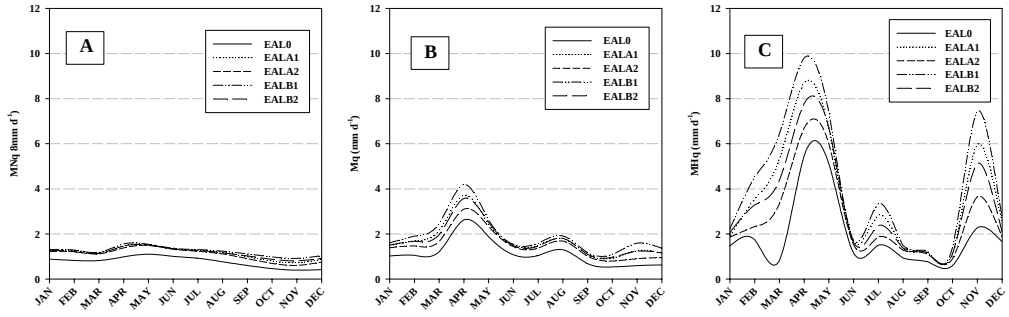

Figure 7. 6: Monthly NQ (A), MQ (B) and HQ (C) for ENSO scenario A and different land use scenarios, Gumbasa River catchment.

7.6 DISCUSSION

In the catchment study presented here the applied methodology has demonstrated its ability to investigate and quantify the impact of ENSO caused precipitation anomalies on the water balance of a mesoscale tropical catchment. The calculated decrease of the yearly total discharge by about 30 % corresponds with the findings of the prestudy for the Miu and Wuno River catchment, where by a cross-correlation analysis of the discharge time series of the Miu and Wuno River and the ENSO indices SST and SOI, the seasonal impact of ENSO related climate variability on the water resources of the Palu River watershed was confirmed. It should be noted that cross-correlation analysis of discharge time series are only adequate for regions, where long time series are available. The correlation results of the Miu and Wuno River should be interpreted with caution because only a time series of seven years (1996-2003) was available. The applied analysis gave a first impression on the impact of ENSO caused precipitation anomalies on the hydrology of the Palu River catchment. Additional impacts on the water balance like land use changes [COLLISCHONN, 2001] or population pressure are difficult to distinguish from the impact of climate variability during long-term hydrological records.

The first research hypothesis, assuming that ENSO caused precipitation anomalies lead to an overall increase of the discharge variability was approved by the ENSO scenario simulations of the hydrological model. Moreover the ENSO scenario discharge simulations showed that mainly the low water and mean discharges are affected by ENSO caused precipitation variability. In addition an analysis of the monthly discharge regime during ENSO events determined the yearly period when ENSO events affect the water resources of the catchment from August till end of December. Here a shift of one to two months until the impact of the precipitation anomaly on the hydrological system became obvious was observed.

The proximate hypothesis, that ENSO caused precipitation anomalies are characterised by a high spatial variability could not be demonstrated by the scenario simulation of the chosen sample Gumbasa River catchment. This effect can be explained by the generation of the precipitation anomaly influenced areal

precipitation of the chosen catchment site, which is mainly dependent on one reference station (Pandaya). This leads to a calculation of a more homogeneous catchment areal precipitation anomaly. In general the regionalisation of the ENSO caused precipitation anomalies for the Palu River catchment would show a higher spatial variability, because all long term climate stations (Table 7.1) would be incorporated for the areal precipitation calculation. Strong monthly precipitation anomaly variability can be observed among all long term climate stations that are located within or adjacent to the Palu River catchment. It is most likely that this recorded spatial precipitation anomaly variability caused the observed differences of the yearly discharge decline during the strong ENSO event of 1997 for the Miu and Wuno catchment. Despite these considerations, an influence of certain catchment characteristics can not be excluded. The impact of the catchment characteristics on the ENSO caused hydrological response magnitude were demonstrated by a discharge comparison of two subcatchments and the total Gumbasa River catchment. The relative damped lower discharge decrease during the simulated ENSO events of the Danau Lindu catchment is due to two reasons: (a) the retention capability of Lake Lindu and (b) the reduced evapotranspiration rate of high altitude rain forest, which leads to an overall higher discharge coefficient of the catchment. The Takkelemo headwater catchment showed the lowest increase of discharge variability during ENSO events, because during normal conditions it is already characterised by a marginal low water discharge, which is related to its small catchment size. The hydrological system of the total Gumbasa River catchment is more sensitive to ENSO caused precipitation anomalies. This finding is expressed by the highest calculated yearly discharge decline and the greatest simulated discharge variability. It can be concluded that the catchment characteristics have a certain influence on the impact magnitude of ENSO related rainfall anomalies on the water balance of a catchment, but the strong discharge anomaly varieties for the Miu and Wuno catchments are most likely related to the spatial variability of the ENSO caused rainfall anomalies.

The results of the applied land use scenarios confirmed the land use change hypotheses. Furthermore, the land use change scenario results agree with the findings of the tropical catchment study by KLEINHANS [2003], who applied the hydrological model WASIM-ETH on a small headwater catchment of the

Gumbasa River catchment. Both studies used the same hydrological model, therefore it was likely that similar land use scenario results would be also calculated on a bigger scale. Experimental paired catchment studies confirm the simulated increases of peak flows after forest removal [BONEL & BALEK, 1993; CHANDLER & WALTER, 1998], which is explained by the associated reduction in ET that causes the soil to be wetter and therefore more responsive to rainfall [BRUIJNZEEL, 2004]. Furthermore the scenario results show that after the complete conversion of all deforested area into cacao plantations still the high water discharge is characterised by enhanced peak flows, which indicates a continued alteration of the water balance for cacao plantations.

But special caution is needed when interpreting the model results for the dry season flow, which is mainly affected during ENSO events in the research area. Regarding the dry season flow and deforestation BRUIJNZEEL [2004] raised the discussion about the “low flow problem”. He emphasises the contradiction that although reduced evaporation associated with the removal of forest should have produced higher baseflow, numerous studies of smaller tropical catchments show a reduced low flow after forest removal, whereas some other studies report an increased baseflow. Whether the baseflow is raised or reduced after forest removal is strongly connected to the degree of surface disturbance. COSTA [2005] argues that as a result of the decreased hydraulic conductivity due to soil consolidation less water can infiltrate which results in an increased direct discharge and actually leads to a decrease of the low water discharge. It should be noted that because data on the soil physical alterations after forest removal was not available for the land use change scenario analysis, only the vegetation physical parameters were altered and the soil hydraulic properties were kept constant for the scenario analysis. Further work on the changes of soil physical properties after deforestation is required. Additionally tropical catchment studies should also monitor the groundwater level fluctuation and incorporate them into physically based modelling applications (e.g. WASIM-ETH coupled with Modflow).

There is a general need to investigate the geological controls of catchment hydrological behaviour when analysing the effects of land use change on the

discharge [BRUIJNZEEL, 2004]. Moreover alterations of the surface energy balance due to the changed vegetation physics are not considered by the applied methodology. If atmospheric feedbacks would be included within the scenario analysis changes in run-off tend to be buffered [COSTA, 2005]. This is also true for the applied ENSO scenarios, where ENSO caused precipitation anomalies would also alter the meteorological parameters like temperature, relative humidity and global radiation. Hence an increased potential evapotranspiration rate may be assumed during ENSO events, which again would alter the discharge rate. To achieve a complete analysis of the impact of ENSO caused precipitation anomalies on the hydrology of a catchment, a model which incorporates the atmospheric-vegetation feedback system on a catchment level would improve further analysis.

Therefore the final research hypothesis on the impact of land use change on the amplitude of hydrological response during ENSO events can not be sufficiently answered by the scenario application of the hydrological model, because the alterations of the soil physical properties and the surface energy balance as a side effect of the land use change were not incorporated within the scenario analysis. It can be clearly stated that deforestation leads to intensified yearly flash floods, causing considerably increased yearly discharge variability and reforestation by cacao plantations again mitigates this effect. But the “low flow problem” requires further research in tropical catchments compromising additional groundwater measurements, soil physical studies on soil degradation and coupled hydrological / meteorological modelling. Catchment projects like the GLOWA Volta project [VAN DE GIESSEN, 2002] that incorporate feedback mechanisms between climate, land use and hydrology are groundbreaking for further hydrological catchment studies.

Studies on the effects of deforestation in larger river basins (<100 km²) usually do result in similar relationships like in abundant small scale hydrological studies [COSTA *et al.*, 2003]. Due to the costs of large scale experiments and their enormous environmental impact it is not appropriate to apply the same method as for small scale catchment studies. To study the impact of forest conversion or

climate variability for large river basins COSTA [2005] advises the application of process-(physically) based hydrological models which incorporate also a climate system model. Further he states that the main difference between small and large scale-hydrological phenomena is the feedbacks through the atmosphere.

REGIONAL IMPACT

ON RICE PRODUCTION

Various studies have outlined the impact of ENSO events on national food production [TRAVASSO *et al.*, 2003; ZUBAIR, 2001; SELVARAJU, 2002] for ENSO influenced countries like Sri Lanka, India and Argentinia. All studies emphasize the importance to use ENSO predictions for agricultural planning. The following case study shows with a simple calculation of the potential irrigation area of the Gumbasa River Irrigation scheme how results of the scenario analysis of the hydrological model could be implemented for further agricultural evaluation and management. The hydrological model WASIM-ETH simulated the daily amount of discharge also for the outlet of the Gumbasa catchment, where irrigation water is extracted for the main irrigation scheme of the Palu valley. Technically a certain discharge of the Gumbasa River is required before the water level of the Gumbasa River is high enough to be extracted by the main irrigation channel. For the calculation of the available daily irrigation water this minimum discharge was abstracted from the total discharge. The value for the minimum discharge was defined a bit higher than the actual value, because not all discharge of the Gumbasa River would be technically extracted for irrigation purpose. Moreover also a maximum level of discharge was defined, because during high water the weir of the irrigation channel would be closed due to high sedimentation rates during flood events. The statistical agricultural report of the agricultural authorities of Palu sums the harvested area of wet rice for the Palu valley for the year 2002 to 14 627 ha. Within the same report the farm area for technical and semi-technical irrigation of the Palu valley amounts to a total of 6 500 ha. For a comparison for the possible irrigation area during ENSO events both values were taken as a reference and were defined as a minimum and maximum total irrigation area. To calculate the possible farm area of irrigated rice during normal and ENSO conditions the following

assumptions were made: The sensible phase during ENSO events for rice farming in Central Sulawesi is the period from August to November.

According to the INTERNATIONAL RICE INSTITUTE [2005] the growth of the rice plant is divided into 3 phases: the vegetative, the reproductive and the ripening phase. During the vegetative phase, which lasts approximately 45 days it was assumed that the paddy fields are ponded by irrigation water. Also during the reproductive phase (ca. 55 days) the rice crop required regular irrigation. As a rule of thumb 10 mm m^{-2} of water per day were defined as required irrigation water for a rice crop. This amount of daily water demand was converted into required irrigation water during the vegetative and reproductive phase of the rice crop. For each day of the simulation year 2003 the potential irrigation area was calculated on the basis of the daily available irrigation water. Figure 8.1 demonstrates the monthly mean potential irrigation area (ha) for the year 2003 and for the simulated ENSO scenarios A and B.

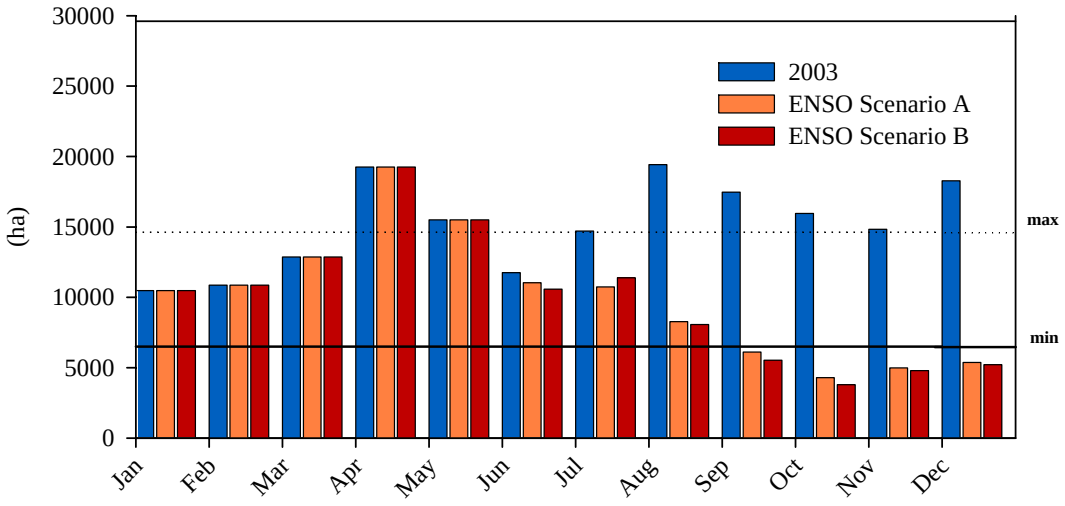

Figure 8. 1: Monthly potential irrigation area [ha] for the simulation year 2003 and the ENSO scenarios A and B on the basis of simulated maximum available irrigation water in comparison with the minimum and maximum total farm area of the Gumbasa Irrigation scheme

The solid black line marks the minimum (6 500 ha) and the dotted line the maximum rice irrigation area (14 627 ha) of The Gumbasa River Irrigation Scheme. The comparison of the simulation year 2003 and the applied ENSO scenarios illustrates that during the ENSO affected months from June till December the possible irrigation area is reduced considerably and even declines in September beneath the bench mark of the minimum total rice irrigation area. With respect to the time frame of the impact of ENSO events in Central Sulawesi, which is dated from June-November we assumed that irrigation water is required for the period 16.09.-24.12 (vegetative + reproductive phase) of the simulation year. Then the total losses of irrigation area in comparison with the minimum and maximum value of the total irrigation area of the Gumbasa River Irrigation scheme was calculated (Table 8.1). The calculated values demonstrate that for the considered simulation year 2003 for the minimum and as well for the maximum total irrigation area a sufficient amount of irrigation water is available.

Table 8. 1: Gains and losses of irrigation area in % for the simulation year 2003 and the ENSO scenarios A and B in comparison to the minimum and maximum total irrigation area of the Gumbasa River Irrigation Scheme.

gains and losses of irrigation area	min. (6500 ha)	max. (14 627 ha)
2003	+ 117 %	+ 15 %
ENSOA	- 23%	-66%
ENSOB	-31%	-69%

For the ENSO scenario A and B about 23 – 31 % less irrigation area with respect to the minimum total irrigation area was calculated. If the maximum irrigation area was taken as reference area the potential irrigation area was reduced by 66-69 %.

The local agricultural authorities of the Palu district reported that during the last ENSO event of 1997 only 40 % for the paddy fields could be irrigated [oral communication, PAK SALIMARIS, PUBLIC WORKS PALU, 2005]. This communicated value more or less corresponds with the calculated values of the losses of irrigation area during ENSO scenarios for the maximum total irrigation area. The remaining difference of irrigated area during ENSO events might be due to the insecurity of the total value of the irrigation area. The losses in rice yield during ENSO events can be further calculated. Using quantitative interviews Sub-project C

estimated a mean rice yield per harvest of 1500 kg / ha for the paddy fields of the Gumbasa River watershed. In January 2002 the nominal price of rice in Indonesia amounted to 1200 Rp kg^{-1} rice [TIMMER, 2004]. This value was taken as a reference rice price for the economical evaluation of the rice yield losses during ENSO events. For a better comparison of the economic losses the rice price in Indonesian Rupiah was transformed in US$. Therefore the economic losses of rice yield refer to the Indonesian rice price and the US$ exchange rate of January 2002.

Table 8. 2: Rice yield losses in total tonnes and $ (Indonesian Rice price and US $ exchange rate = Jan. 2002) for the simulation year 2003 and the ENSO scenarios A and B fort he minimum and maximum total irrigation area of the Gumbasa River Irrigation Scheme.

	min. (6500 ha)		max. (14 627 ha)	
rice yield losses	[t]	$	[t]	$
ENSO A	2 199	253 126	14 389	1 656 317
ENSO B	3 036	349 473	15 226	1 752 664

The estimated rice yield losses for ENSO scenario A and B (Table 8.2) are severe and emphasize the high impact of ENSO caused precipitation anomalies on the agricultural production and income in Central Sulawesi. The rough calculations of economic losses during ENSO events highlight the potential of distributed hydrological models such as WASM-ETH for water resource management of catchment areas. The daily available irrigation water could serve as input data for more sophisticated agricultural crop growth models such as ORYZA 2000 [INTERNATIONAL RICE INSTITUTE, 2005] or the widely used CROPWAT [FAO, 1989]. Crop growth models provide a more precise calculation of expected rice yield losses during ENSO events and therefore could serve as an important management tool for agricultural purpose.

CONCLUSIONS

AND PERSPECTIVES

Hydrological studies that investigate the impact ENSO caused precipitation anomalies on the water resources of a catchment mainly analyse cross-correlations of discharge time series and ENSO indices like SST or SOI [e.g. GUITERREZ & DRACUP, 2001; AMASEKERA *et al.*, 1996, COLLISCHONN *et al.*, 2001, ELTAHIR, 1996, SIMPSON *et al.* 1993; SHRESTHA & KOSTASCHUK, 2003]. The outline, methodology, results and implications of the presented case study on the impact of ENSO events on the water resource availability of a mesoscale tropical catchment in Central Sulawesi Indonesia represents a useful foundation for the implementation of an Integrated Water Resource Management (IWRM) in contrast to the numereous statistical hydrological ENSO impact studies. For the assessment of the implications of climate variability such as ENSO events on the water resources of a catchment, a physically based distributed hydrological model serves as an essential analytic tool for the quantification and visualisation of the expected changes of the water balance. Despite the remaining uncertainties of hydrological model application they provide an important flexibility to investigate problems at different scales and are important tools for assessing different types of water planning and management issues [ABBOTT & REFSGAARD, 1996]. In general the scenario simulations of the hydrological models show a great potential to outline critical water resource situations in space and time, which again results in an increased awareness of the concerned stakeholders and creates a basis for further water resource management decisions. The chosen catchment unit as a research area represents an ideal scale, because the global and local scale, which used in many other hydrological studies [e.g. GÜNTNER, 2002; DÖLL *et al.*, 2002; GODSEY *et al.*, 2004; FLEISCHBEIN *et al.*, 2005; KLEINHANS, 2004] is far from the regional reality [FALKENMARK & ROCKSTRÖM, 2004] where decisions on water resource management are developed and implemented.

Even though the socio-economic aspect with regard to climate hazards like ENSO caused drought is integrated within the comprehensive frame project IMPENSO the ecosystem link is still missing, for a complete description of the catchment dynamics and furthermore for the evaluation of its overall sustainability. With regard to the ecosystem functions within a catchment FALKENMARK & ROCKSTRÖM [2004] state that the links between society and the landscape are important for understanding the main phenomena behind the development of environmental problems and ecosystem degradation. The protection of ecosystem services has to be linked to the management of the catchment, compromising close linkages between land, water and ecosystems [FALKENMARK & FOLKE, 2002]. Hydrosolidarity is a process which incorporates preparedness for change and transinient situations, which may need modification of the management on various levels. The comprehensive project IMPENSO aims to provide the concerned stakeholders with important back ground information about the development of the guidelines for hydrosolidarity. Climate variability, land use change and socio- economic factors are the main driving forces that change the water balance of a catchment and hence alter its water resource availability [GLOBAL WATER PARTNERSHIP, 2000]. The distribution of these changes in space and time will determine the general strategy for the management of water resources. Within a catchment the land use changes and socio economic factors are highly correlated and have a strong impact on the water balance. The green/blue water concept partitions rainfall into blue and green water flow and has been introduced by the FAO in 1995. Blue water flow represents the visible liquid water flow moving above and below the ground as surface or sub-surface runoff, respectively and green water flow is defined as the invisible flow of vapour to the atmosphere [FAO, 1995b, 1997]. Especially in the humid tropics the green water flow represents a main component of the water balance (see Chapter 6.4.4). Therefore the present land use that mainly regulates the flow of vapour to the atmosphere plays an important role for the water balance of a catchment.

Land use decisions are also a decision about water resources, as it has been demonstrated by the conducted land use scenario of this study. With regard to the overall degradading consequences of discharge variability like low flow or flash floods it is crucial for the water resource management to predict potential consequences of land use change in space and time. The application of the

distributed hydrological model WASIM-ETH on the Gumbasa River Sample catchment and of other comparable hydrological impact studies in developing countries [KITE, 2001; CHALISE *et al.*, 2003] showed that the input data availability strongly determines the model efficiency and its predictability. If we want to face water resource shortages with Integrated Water Resource Management, there is an urgent need to implement a better meteorological and hydrological data monitoring system within the affected catchment areas. This issue is not only a challenge of time-limited research projects, but moreover has to be effectively integrated within the local infrastructure of the responsible administrative authorities. For international organisations like the Agricultural Organization of the United Nations (FAO), reliable hydrological base data is also crucial to assess the state of the world-wide water resources and furthermore to develop water resource programs [ELIASSON *et al.*, 2003].

Climate impact as well as water resources research studies require the coupling of hydrological and atmospheric models, because the coupling considers more appropriately the interaction of the atmospheric and land-surface component of the water cycle. In order to derive a consistent parameterisation and spatial discretisation of the coupling the hydrological model should be process-based and fully distributed [MÖLDERS, 2005]. Climate scenarios generated by the atmospheric model like e.g. ENSO prediction scenarios can be directly incorporated by the hydrological model to generate the impact of these climate scenarios on the water balance.
The next milestone of the research project IMPENSO implies the coupling of the local climate model MM5 (Pennsylvania State University/National Center for Atmospheric Research mesoscale model) operated by IMPENSO sub-project A with the hydrological model WASIM-ETH which is applied in this study for the Gumbasa River watershed. The models will be coupled by the one-way coupling method. This way of coupling intends to drive hydrological models by the output of atmospheric models. The climate model MM5 and the hydrological model WASIM-ETH are coupled in a cascade manner, first running the atmospheric model and then running the hydrological model. The disadvantage of this method is that due to the cascading nature of one-way coupling, no feedback effects of the hydrological model can influence the simulation of the atmospheric model [MÖLDERS, 2005]. If the

hydrological cycle would be simulated for large river basins (e.g. Amazonian basin) a one-way coupling system would lead to wrong estimations of the water fluxes from the land surface to the atmosphere, which might lead to wrong precipitation simulation. For the mesoscale Gumbasa River catchment this error is rather vanishing, and the one-way coupling sufficiently answers the research questions of the regional climate impact study IMPENSO. Two-way coupling systems like e.g. SEWAB [MENGELKAMP *et al*., 1999] or even more sophisticated hydro-meteorological models are the hydro-meteorological modelling solutions for the future. However, it is still difficult to keep the model manageable data vice and to identify and incorporate the right feedback mechanisms on the adequate scale. MÖDERS [2005] states that one big challenge of hydro-meteorology is not to couple what can be coupled all into one integrated model, but rather to couple only what makes sense to answer a question that could not be addressed without coupling.

REFERENCES

Abbott,M.B. & Refsgaard,J.P. (1996): Terminology, modelling protocol and classification of hydrological model codes. In: Abbott, M. B. and Refsgaard, J. P. (Eds.): Distributed hydrological modelling. Kluwer Academic Publishers, Dordrecht, Boston, London, 17-37.

Achten,A. (1991): Wasserwirtschaft. In: Wetzell, O. (Eds.): Wendehorst Bautechnische Zahlentafeln. Teubner, Stuttgart, 761-869.

Adi,S. (2003): Proposed soil and water conservation strategies for lake Rawa Dano, West Java, Indonesia. In: Blöschl, G., Franks, S., Kumagai, M., Musiake, K., and Rosbjerg, D. (Eds.): Water Resources Sytems-Hydrological Risk, Management and Development. IAHS, Wallingford, 248-258.

Aldrian,E. (2003): Simulations of Indonesian Rainfall with a Hierachy of Climate Models. Dissertation, Universität Hamburg, 23-45.

Aldrian, E. & Susantu, R. (2003): Identification of three dominant rainfall regions within Indonesia and their relationship to sea surface temperature. International Journal of Climatology, 23, 1435-1452.

Amarasekera, K. N., Lee, R. F., Williams, E. R., & Eltahir, E. (1996): ENSO and the natural variability in the flow of tropical rivers. Journal of Hydrology, 200, 24-39.

Andersen, J., Refsgaard, J. C., & Jensen, K. H. (2001): Distributed hydrological modelling of the Senegal River Basin-model construction and validation. Journal of Hydrology, 247, 200-214.

Anderson, M. L., Kavvas, M. L., & Mierzwa, M. D. (2001): Probalistic/ensemble forecasting: a case study using hydrologic response distributions with El Niño Southern Oscillation (ENSO). Journal of Hydrology, 249, 134-147.

Andreassian, V., Perrin, C., Michel, C., Usart-Sanchez, I., & Lavabre, J. (2001): Impact of imperfect rainfall knowledge on the efficiency and the parameters of watershed models. Journal of Hydrology, 250, 206-223.

Asdak, C., Jarvis, P. G., van Gardingen, P., & Fraser, A. (1998): Rainfall interception loss in unlogged and logged forest areas of Central Kalimantan, Indonesia. Journal of Hydrology, 206, 237-244.

Barnes,C. & Bonell,M. (2005): How to chose an appropiate catchment model. In: Bonell, M. and Bruijnzeel, L. A. (Eds.): Forests, Water and People in the Humid Tropics. University Press, Camebridge, 717-741.

Berlage,H.P. (1949): Rainfall in Indonesia. Mean rainfall figures for 4339 rainfall stations in Indonesia, 1879 - 1941. Department van Verkeer, Energie en Mijnwezen, Meteorologische en Geophysische Dienst, Koninklijk Magnetisch en Meteorologisch Observatorium.,

Beven,K. (2001): Rainfall - Runoff modelling. JOHN WILEY & SONS, Chichester, New York, Weinheim, 53-84.

Beven, K. & Feyen, J. (2002): The future of distributed modelling. Hydrological Processes, 16, 169-172.

Blöschl,G. (1996): Scale and scaling in hydrology. Dissertation, TU Wien, 1-22.

Bohman,K. (2004): Functional and morphological diversity of trees in different land use types along a rainforest margin, in Sulawesi, Indonesia. Dissertation, Universität Göttingen, 55-63.

Bohne, K., Horn, R., & Baumgartl, T. (1993): Bereitstellung von van - Genuchten Parametern zur Charakterisierung der hydraulischen Bodeneigenschaften. Zeitschrift für Pflanzenernährung und Bodenkunde, 156, 229-233.

Bonell,M. & Balek,J. (1993): Physical processes. In: Bonell, M., Hufschmidt, M., and Gladwell, J. (Eds.): Hydrology and water management in the humid tropics. Camabridge University Press, Camebridge, 176-177.

Bonell,M. (2005): Runoff generation in tropical forests. In: Bonell, M. and Bruijnzeel, L. A. (Eds.): Forests, Water and People in the Humid Tropics. University Press, Camebridge, 314-406.

Böhner, J. (1996): Sakuläre Klimaschwankungen und rezente Klimatrends Zentral- und Hochasiens. Göttinger Geographische Abhandlungen, 101, Verlag Erich Goltze GmbH & Co. KG, Verlag Erich Goltze GmbH & Co. KG, 100-102.

Bronstert,A. & Niehoff,D. (2003): Prozessbezogene Regionalisierung der Hochwasserentstehung. In: Hennrich, K., Rode, M., and Bronstert, A. (Eds.):

6. Workshop zur großskaligen Modellierung in der Hydrologie. kassel university press GmbH, Kassel, 57-68.

Bruijnzeel,L.A. (1996): Hydrology of moist tropical forests and effects of conversion: a state of knowledge review. UNESCO International Hydrological Programme, 20-20.

Bruijnzeel,L.A. (2000): Tropical forests and water yield. IUFRC Task Force on forests and water, Laxenburg, Austria.

Bruijnzeel, L. A. (2004): Hydrological functions of tropical forests: not seeing the soil for the trees? Agriculture, Ecosystems & Environment, 104, 185-228.

Brutsaert,W. (1982): Evaporation into the atmosphere: theory, history and applications. Reidel, Dordrecht,

Chalise, S. R., Kansakar, S. R., Rees, G., Croker, K., & Zaidman, M. (2003): Management of water resources and low flow estimation for the Himalayan basins of Nepal. Journal of Hydrology, 282, 25-35.

Chandler, D. G. & Walter, M. F. (1998): Runoff responses among common land uses in the uplands of Matalom, Leyte; Phillipines. Transactions of the ASAE, 41, 1635-1641.

Chang,J.H. (1993): Hydrology in the humid tropical asia. In: Bonell, M., Hufschmidt, M., and Gladwell, J. (Eds.): Hydrology and water management in the humid tropics. Camebridge University Press, Camebridge, 55-66.

Chappell,N.A., Bidin,K., Sherlock,M.D., & Lancaster,J.W. (2005): Parsimonious spatial representation of tropical soils within dynamic rainfall-runoff models. In: Bonell, M. and Bruijnzeel, L. A. (Eds.): Forests, Water and People in the Humid Tropics. University Press, Camebridge, 756-769.

Cluis,D. (1998): Analysis of long runoff series of selected rivers of the Asia-Pacific region in relation with climate change and El Nino effects. Global Runoff Center, Koblenz, 13-20.

Collischonn, W., Tucci, C. E. M., & Clarke, R. T. (2001): Further evidence of changes in the hydrological regime of the River Paraguay: part of a wider phenomenon of climate change? Journal of Hydrology, 245, 218-238.

Coppin,P.A. (1977): The albedo of natural surfaces. Flinders Institute For Atmospheric ans Marine Science, Bedfork Park, South Australia., 22-22.

Costa, M. H., Botta, A., & Cardille, J. A. (2003): Effects of large-scale changes in land cover on the discharge of the Tocantins River, Southeastern Amazonia. Journal of Hydrology, 283, 206-217.

Costa,M.H. (2005): Large-scale hydrological impacts of tropical forest conversion. In: Bonell, M. and Bruijnzeel, L. A. (Eds.): Forests, water and people in the humid tropics. University Press, Camebridge, 590-598.

Cunderlik, J. M. & Burn, D. H. (2002): Analysis of the linkage between rain and flood regime and its application to regional flood frequency estimation. Journal of Hydrology, 261, 115-131.

Dijk, A. & Bruijnzeel, L. A. (2001): Modelling rainfall interception by vegetation of variable density using an adapted analytical model. Part 2. Model validation for a tropical upland mixed cropping system. Journal of Hydrology, 247, 239-262.

Doherty,J. (2002): PEST.

Doherty,J. (2003): PEST Model-Independent Parameter Estimation. 1-9.

Döll, P., Kaspar, F., & Lehner, B. (2003): A global hydrological model for deriving water availability indicators: model tuning and validation. Journal of Hydrology, 270, 105-134.

Dracup, J. & Kahya, E. (1994): The relationship bewtween U.S. streamflow and La Nina events. Water Resources Research, 30, 2133-2141.

Dyck,S. & Peschke,G. (1989): Grundlagen der Hydrologie. VEB Verlag für Bauwesen, Berlin, 58-80.

Eliasson, A., Faures, J. M., Frenken, K., & Hoogeveen, J. (2003): Sixth water information summit: Breaking the barriers. WAter Web Consortium and IRC international water and sanitation Centre, Delft,

Elsenbeer, H. (2001): Pedotransfer functions in hydrology. Journal of Hydrology, 251, 121-122.

Elsenbeer, H. (2001): Hydrologic flowpaths in tropical rainforest soilscapes - a review. Hydrological Processes, 15, 1751-1759.

Eltahir, E. (1996): El Niño and the natural variability in the flow of the Nile River. Water Resources Research, 32, 131-137.

Erasmi, S., Twele, A., Ardiansyah, M., Malik, A., & Kappas, M. (2004): Mapping deforestration and land cover conversion at the rainforest margin in Central Sulawesi, Indonesia. ,

Falk,U. (2004): Turbulent fluxes of CO2, H2O and enery in the atmospheric boundary layer above tropical vegetation investigated by Eddy-Covariance measurements. Dissertation, Universität Göttingen, 91-92.

Falkenmark,M. (1989): Comparative hydrology - a new concept. In: Falkenmark, M. and Chapman, T. (Eds.): Comparative hydrology. UNESCO, Paris, 19-

Falkenmark,M. & Rockström,J. (2004): Balancing water for humans and nature. Earthscan, London, 181-199.

FAO (1989): Manual for CROPWAT. Rome,

FAO (1995): Land and water integration and river basin management. Food and Agricultural Organization, Rome,

FAO (1997): Irrigation in Africa- A basin approach. Food and Agricultural Organization, Rome,

Fleischbein, K., Wilcke, W., Goller, R., Boy, R., Valarezo, C., Zech, W., & Knoblich, K. (2005): Rainfall interception in a lower montane forest in Ecuador: effects of canopy properties. Hydrological Processes, 19, 1355-1371.

Fleming,P.M. (1993): The impact of land use change on water resources in the tropics: An Australian view of the Scientific Issues. In: Bonell, M., Hufschmidt, M., and Gladwell, J. (Eds.): Hydrology and water management in the humid tropics. University Press, Camebridge, 405-414.

Fu,C., Yasunari,T., & Lütkemeier,S. (2004): The Asian Monsoon. In: Kabat, P., Claussen, M., and Dirmeyer, P. (Eds.): Vegetation, Water, Humans and the Climate. Springer-Verlag, Berlin, 115-127.

Gardiol, J. M., Serio, L. A., & Maggiora, A. I. (2003): Modelling evapotranspiration of corn (zea mays under different plant densities). Journal of Hydrology, 271, 188-196.

Garrelts,A. (2000): Geomorphological study of the Sopu valley, Central Sulawesi, Indonesia. Dissertation, Universiteit Wageningen,

Gerold, G., Sutmöller, J., Krüger, J.-P., Herbst, M., Busch, G., Peschke, G., Zimmermann, S., Etzenberg, C., & Töpfer, J. (2003): Reliefgestützte und wissensbasierte Regionalisierung in der Hydrologie. EcoRegio, Band 6, Shaker Verlag, Shaker Verlag, 19-32.

Global Water Partnership (2000): Integrated Water Resources Management. Stockholm, 51-67.

Godsey, S., Elsenbeer, H., & Stallard, R. (2004): Overland flow generation in two lithologically distinct rainforest catchments. Journal of Hydrology, 295, 276-290.

Grayson,R. & Blöschl,G. (2000): Spatial modelling of catchment dynamics. In: Grayson, R. and Blöschl, G. (Eds.): Spatial Patterns in Catchment Hydrology. Camebridge University Press, Camebridge, 51-81.

Green, W. H. & Ampt, G. A. (1911): Studies on soil physics: The flow of air and water through soils. Journal of agricultural science, 4, 1-24.

Guitierrez, F. & Dracup, J. (2001): An analysis of the feasibility of long-range streamflow forecasting for Colombia using El Nino-Southern Oscillation indicators. Journal of Hydrology, 246, 181-196.

Gurtz, J., Zappa, M., Jasper, K., Lang, H., Verbunt, M., Badoux, A., & Vitvar, T. (2003): A comparative study in modelling runoff and its components in two mountainous catchments. Hydrological Processes, 17, 297-311.

Güntner,A. (2002): Large-Scale hydrological modelling in the Semi-Arid North-East of Brasil. Dissertation, Universität Potsdam.

Hamilton,W. (1979): Tectonocs of the indonesian region. U.S. Gov. Print Off., Washington D.C., 275-280.

Held,A.A. & Rodriguez,E. (2005): Remote sensing tools in tropical forest hydrology: new sensors. In: Forests, Water and People in the Humid Tropics. University Press, Camebridge, 671-674.

Herschy,R.W. (1978): Hydrometry: principles and practices. Wiley & Sons, Chichester, 127-130.

Herschy,R.W. (1995): Streamflow measurement. Spon, London,

Herschy,R.W. (1999): Flow Measurement. In: Herschy, R. W. (Eds.): Hydrometry, Principles and Practices. John Wiley & Sons, Chichester, 9-84.

Herschy,R.W. (1999): Uncertainties in hydrometric measurements. In: Herschy, R. W. (Eds.): Hydrometry, Principles and Practrices. John Wiley & Sons, Chichester, 355-368.

Hodnett, M. G. & Tomasella, J. (2002): Marked differences between van Genuchten soil water-retention parameters for temperate and tropical soils: a new water retention pedo-transfer functions developed for tropical soils. Geoderma, 108, 155-180.

Holmes,D. (2000): Deforestation in Indonesia - A review of situation in 1999. World Bank, Jakarta.

Hölscher, D., Köhler, L., Dijk, A., & Bruijnzeel, L. A. (2004): The importance of epiphytes to total rainfall interception by a tropical montane rain forest in Costa Rica. Journal of Hydrology, 292, 308-332.

IAHS (2003): Prediction in ungauged basins. International Hydrology today, 26-28.

ICCO (2005): International cacoa organization. http://www.icco.org/.

Imperial agricultural bureau. (1944): Imperata cylindrica: taxonomy, distribution, economic significance and control. Imperial forest bureau, Oxford,

International Rice Research Institute (2005): Rice knowledge bank. http://www.irri.org/.

IPPC (2005): Climate change 2001. http://www.ipcc.ch/.

Jackson, R. B., Canadell, J., Ehleringer, J. R., Mooney, H. A., Sala, O. E., & Schulze, E. D. (1996): A global analysis of root distributions for terrestrial biomes. Oecologia, 108, 389-411.

Jasper, K., Gurtz, J., & Lang, H. (2002): Advances flood forecasting in Alpine watersheds by coupling meteorological observations and forecasts with a distributed hydrological model. Journal of Hydrology, 267, 40-52.

Keil, A., Gunawan, D., Gravenhorst, G., Leemhuis, C., Gerold, G., Birner, R., & Zeller, M. (2005): IMPENSO: The impact of ENSO (El Nino Southern Oscillation) on sustainable water management and the decission making community at a rainforest margin in Indonesia. German Aerospace Center, Bonn, 150-155.

Keller,R. (1962): Gewässer und Wasserhaushalt des Festlandes. B. G. Teubner Verlagsgesellschaft, Leipzig, 266-288.

Kessler,P.J.A., Boos,M.M., & Sierra Daza,S.E.C. (2002): Checklist of woody plants in Sulawesi. 1-160.

Kite, G. (2001): Modelling the Mekong: hydrological simulation for environmental impact studies. Journal of Hydrology, 253, 1-13.

Kleinhans,A. (2004): Einfluss der Waldkonversion auf den Wasserhaushalt eines tropischen Regenwaldeinzugsgebietes in Zentral Sulawesi (Indonesien). Dissertation, Universität Göttingen,

Klemes,V. (1993): The problems of the humid tropics-oppurtunities of reassessment of hydrological methodology. In: Bonell, M., Hufschmidt, M., and Gladwell, J. (Eds.): Hydrology and water management in the humid tropics. Camebridge University Press, Camebridge, 45-51.

Kortekaas,M. (2000): Napu under Reconstruction, Geomorphological study of the Napu basin, Central Sulawesi, Indonesia. Dissertation, Universiteit Wageningen,

Körner,C. (1994): Leaf diffusive conductances in the major vegetation types of the globe. In: Schulze, E. D. and Caldwell, M. M. (Eds.): Ecophysiology of Photosynthesis. Springer, Berlin, 463-490.

Landon,J.R. (1984): Tropical soil manual. Booker Agriculture International, New York, 289-291.

Latif,M. & Endlicher,W. (2001): El Niño /Southern-Oscillation-Phenemenon. In: Lozan, J., Graßl, H., and Hupfer, H. (Eds.): Climate of the 21st CENTURY: Changes and Risks. Wissenschaftliche Auswertungen, Hamburg, 45-60.

Legates, D. R. & McCabe, G. J. (1999): Evaluating the use of "goodness-of-fit" measures in hydrologic and hydroclimatic model validation. Water Resources Research, 35, 233-241.

Mackensen,J., Ampt,J., Garrelts,A., Kortekaas,M., & Veldkamp,A. (1999): Report on reconnaissance soil survey in the Napu and Sopu-valley, Central Sulawesi, Indonesia.

Maertens,M., Zeller,M., & Birner,R. (2004): Does technical progress in agriculture have aforest saving or a forest clearing affect? Theory and evidence from Central Sulawesi. In: Gerold, G., Fremerey, M., and Guhardja, E. (Eds.): Land use, nature conservation and the stabilty of rainforest margins in Southeast Asia. Springer, Berlin, Heidelberh, 180-194.

Manley,R.E. & Askew,A.J. (1993): Operational hydrology problems in the humid tropics. In: Bonell, M., Hufschmidt, M., and Gladwell, J. (Eds.): Hydrology and water management in the humid tropics. Camebridge University Press, Camebridge, 34-44.

Matthews, E. (1999): Global vegetation guide (1972-1983). http://www.daac.ornl.gov.

Mengelkamp, H. T., Warrach, K., & Raschke, E. (1999): SEWAB-a parameterization of the surface enery and water balance for atmospheric and hydrologic models. Advances in Water Resources, 23(2), 165-175.

Menzel,L. (1999): Flächenhafte Modellierung der Evapotranspiration mit TRAIN. 28-29.

Mo, X., Liu, S., Lin, Z., & Zhao, W. (2004): Simulating temporal and spatial variation of evapotranspiration over the Lushi basin. Journal of Hydrology, 285, 125-142.

Monteith,J.L. & Unsworth,M. (1990): Principles of Environmental Physics. Arnold, London, 184-198.

Motzer, T. (2003): Bestandesklima, Energiehaushalt und Evapotranspiration eines neotropischen Bergregenwaldes. Mannheimer Geographische Arbeiten, 56, Geographisches Institut, Universität Mannheim, Geographisches Institut, Universität Mannheim, 7-10.

Mölders,N. (2005): Feedbacks at the hydrometeorological interface. In: Bronstert, A., Carrera, J., Kabat, P., and Lütkemeier, S. (Eds.): Coupled models for the hydrological cycle. Springer, Heidelberg, 192-201.

Nash, J. E. & Sutcliffe, J. V. (1970): River flow forecasting through conceptunal models. Journal of Hydrology, 10, 282-290.

Niehoff,D. (2001): Modellierung des Einflusses der Landnutzung auf die Hochwasserentstehung in der mesoskala. Dissertation, Universität Potsdam,

NOAA (2005): NOAA El Niño Page. http://www.elnino.noaa.gov/.

Noordwijk, M., Brouwer, G., Zandt, P., Meijboom, F., & Burgers, S. (1993): Root patterns in space and time: procedures and programs for quantification. 268, DLO-Instituut voor Bodemvruchtbaarheid, DLO-Instituut voor Bodemvruchtbaarheid, 19-20.

Noordwijk,M., Farida,A., Suyamto,D., Lusiana,B., & Khasana,N. (2003): Spatial variability of rainfall governs river flow and reduces eefects of land use change at landscape level: GenRiver and SpatRain simulations. International Center for Research in Agroforestry, Southeast Asian Regional Research, Bogor, Indonesia.,

Oyebande,L. & Balek,J. (1987): Humid warm sloping land. In: Falkenmark, M. and Chapman, T. (Eds.): Comparative hydrology. UNESCO, Paris, 224-274.

Pak Salimaris (2005): Irrigation area during ENSO events.

Parde,M. (1933): Fleuves et Rivieres. Armand Colin, Paris,

Peranginangin, N., Sakthivadivel, R., Scott, N. R., Kendy, E., & Steenhuis, T. S. (2004): Water accounting for conjunctive groundwater/surface water management: case of the Singkarak-Ombilin River basin, Indonesia. Journal of Hydrology, 292, 1-22.

Philander,S.G. (2004): Our affair with El Niño. Princeton University Press, Princeton.

Philip,J.R. (1969): The theory of infiltration. In: Chow, V. T. (Eds.): Advances in Hydroscience. Academic Press, New York, 216-296.

Piepho,B. (2003): Untersuchungen zum hydrologischen Reaktionsverhalten eines kleinen Einzugsgebietes unter Verwendung des Wasserhaushaltsmodells WaSiM-ETH. Dissertation, TU Braunschweig,

Purwanto,E. (1999): Erosion, sediment delivery and soil conservation in an upland agricultural catchment in West Java, Indonesia. Dissertation, Vrije Universiteit, Amsterdam, 218-218.

Refsgaard,A. & Storm,B. (1996): Distributed physically-based modelling of the entire land phase of the hydrological cycle. In: Abbott, M. B. and Refsgaard, J. C. (Eds.): Distributed hydrological modelling. Kluwer Academic Publisher, Dordrecht, 55-69.

Refsgaard, J. C. (1997): Parameterisation, calibration and validation of distributed hydrological models. Journal of Hydrology, 198, 69-97.

Rehm,S. (1989): Spezieller Pflanzenbau in den Tropen und Subtropen. Ulmer, Stuttgart, 437-446.

Richards,L.A. (1931): Cappilary conduction of liquids through porous media. Dissertation, Cornell University NY,

Rijsdijk,A. & Bruijnzeel,L.A. (1990): Erosion sediment yield and land use patterns in the upper Konto watershed, East Java, Indonesia. Malang, Indonesia., 58-59.

Roberts,J.M., Gash,J.H.C., Tani,M., & Bruijnzeel,L.A. (2005): Controls on evaporation in lowland tropical rainforest. In: Bonell, M. and Bruijnzeel, L. A. (Eds.): Forests, Water and People in the Humid Tropics. University Press, Camebridge, 287-313.

Rollenbeck, R. (2002): Wasser-und Energiehaushalt eines neotropischen Tieflandregenwaldes. Mannheimer Geographische Arbeiten, 55, Universität Mannheim, Universität Mannheim.

Rollenbeck, R., Fabian, P., & Bendix, J. (2005): Precipitation dynamics and chemical properties in tropical mountain forests of Ecuador. The El Nino Phenemen and its global impact, EGU, Guayaquil, Ecuador., 108-109.

Schellekens,J. (2000): Hydrological processes in a humid tropical rainforest: a combined experimental and modelling approach. Dissertation, Vrije Universiteit Amsterdam, 7-9.

Schulla, J. (1997): Hydrologische Modellierung von Flussgebieten zur Abschätzung der Folgen von Klimaänderungen. Züricher Geographische Schriften, Verlag Geographisches Institut ETH Zürich, Verlag Geographisches Institut ETH Zürich.

Schulla,J. & Jasper,K. (1999): Model Description WASIM-ETH.

Schulla,J. & Jasper,K. (1999): WASIM-ETH.

sci Lands (2003): Erstellung eines Digitalen Geländemodells (DGM) und einer bodenkundlich orientierten Landschaftsgliederung für das Gebiet des Lore Lindu Nationalparks (Sulawesi, Indonesien).

Scurlock, J. M. O., Assner, G. P., & Gower, S. T. (2001): Global Leaf Area Index from Field Measurements, 1932-2000. http://www.daac.ornl.gov.

Selvaraju, R. (2002): Impact of El Niño-Southern Oscillation on indian food production. International Journal of Climatology, 23, 187-206.

Sevruk,B. & Klemm,S. (1989): World Meteorological Organization, World Meteorological Organization.

Shrestha, A. & Kostaschuk, R. (2005): El Nino/Southern Oscillation (ENSO)-related variablity in mean-monthly streamflow in Nepal. Journal of Hydrology, 308, 33-49.

Simpson, H. J., Cane, M. A., Herczeg, A. L., & Zebiak, S. E. (1993): Annual River Discharge in Southeastern Australia Related to El Niño Southern-Oscillation Forecasts of Sea Surface Temperartures. Water Resources Research, 29, 3671-3680.

Sinukaban, N. & Pawitan, H. (1998): Impact of soil and water conversation practices on streamflows in Citere catchment, West Java, Indonesia. Adv.GeoEcol., 31, 1275-1280.

Sobieraj, J. A., Elsenbeer, H., & Vertessy, R. A. (2001): Pedotransferfunctions for estimating saturated hydraulic conductivity: implications for modeling storm flow generation. Journal of Hydrology, 251, 202-220.

Stephan,K. & Diekkrüger,B. (2003): Analyse der Unsicherheiten bei der rasterbasierten hydrologischen Modellierung als Folge der Aggregierung der Eingangsdaten. In: Hennrich, K., Rode, M., and Bronstert, A. (Eds.): 6. Workshop zur großskaligen Modellierung in der Hydrologie. university press, Kassel, 131-142.

Tereshchenko, I., Filonov, A., Gallegos, A., Monzon, C., & Rodriguez, R. (2002): El Niño 1997-98 and the hydrometeorological variabiliy of Chapala, a shallow tropical lake in Mexico. Journal of Hydrology, 264, 133-146.

Timmer,C. (2004): Food security in Indonesia. Center for Global Development,

Timmermann, A., Bacher, A., Esch, M., Latif, M., & Roeckner, E. (1999): ENSO response to greenhouse warming. Nature, 398, 694-697.

Travasso, M., Margin, G., & Rodriguez, G. (2003): Relations between sea-surface temperature and crop yields in Argentinia. International Journal of Climatology, 23, 1655-1662.

UNESCO (2003): Water for people Water for life. UNESCO, Perth.

Van de Giessen,N., Kunstmann,H., Jung,G., Liebe,J., Andreini,M., & Vlek,P. (2002): The GLOWA Volta project: Integrated assessment of feedback mechanisms between climate, landuse and hydrology. In: Beniston, M. (Eds.): Climatic Change: Implications for the hydrological cycle and for Water management. Kluwer Academic Publishers, Dordrecht, 151-170.

Van Genuchten, M. TH. (1980): A closed form equation for predicting the hydraulic condictivity of unsaturated soils. Soil Science Society, 44, 892-898.

Verbunt, M., Gurtz, J., Jasper, K., Lang, H., Warmerdam, P., & Zappa, M. (2003): The hydrological role of snow and glaciers in alpine river basins and the distributed modelling. Journal of Hydrology, 282, 36-55.

Vertessy,R.A., Elsenbeer,H., Bessard,Y., & Lack,A. (2000): Storm generation at la Cuenca. In: Grayson, R. and Blöschl, G. (Eds.): Spatial pattern in catchment hydrology. Camebridge University Press, Camebridge, 247-271.

Voituriez,B. & Jaques,G. (2000): El Niño - Fact and fiction. UNESCO, Paris, 65-96.

Wang,Q.J., McConachy,F.L.N., & Chiew,F.H.S. (2001): Maps of evapotranspiration. 1-4.

Webster,R. & Oliver,M.A. (1999): Geostatistics for environmental scientists. JOHN WILEY & SONS, Chichester, 149-166.

Whitten,T. & Henderson,G.S.M.M. (2002): The ecology of Sulawesi. Periplus, Singapore, 1-33.

Willmott, C. J. (1981): On the validation of models. Physical Geography, 2, 184-194.

Wösten, J. H. M., Schuren, C. H. J. E., Bouma, J., & Stein, A. (1990): Use of practical aspects of soil behaviour to evaluate different methods to generate soil hydraulic functions. Hydrological Processes, 4, 110-118.

Wösten, J. H. M., Pachepsky, Y. A., & Rawls, W. J. (2001): Pedotransfer functions: bridging the gap between available basic soil data and missing soil hydraulic characteristics. Journal of Hydrology, 251, 123-150.

Zubair, L. (2001): El Niño-Southern Oscillation influences on rice production in Sri Lanka. International Journal of Climatology, 22, 249-260.

Appendix A. 1: Takkelemo gauging station equipped with a float operated shaft encoder with integral data logger.

Appendix A. 2: Sopu gauging site equipped with a radar level sensor with a multi-channel datalogger.

Appendix A. 3: Lake Lindu gauging station equipped with a float operated shaft encoder with integral data logger.

Appendix A. 4: Tongoa climate station equipped with a precipitation pulse transmitter and a two channel datalogger for air temperature and humidity.

Appendix A. 5: Tropical montane rainforest, Gumbasa River watershed.

Appendix A. 6: Deforestation, Lore Lindu National Park.

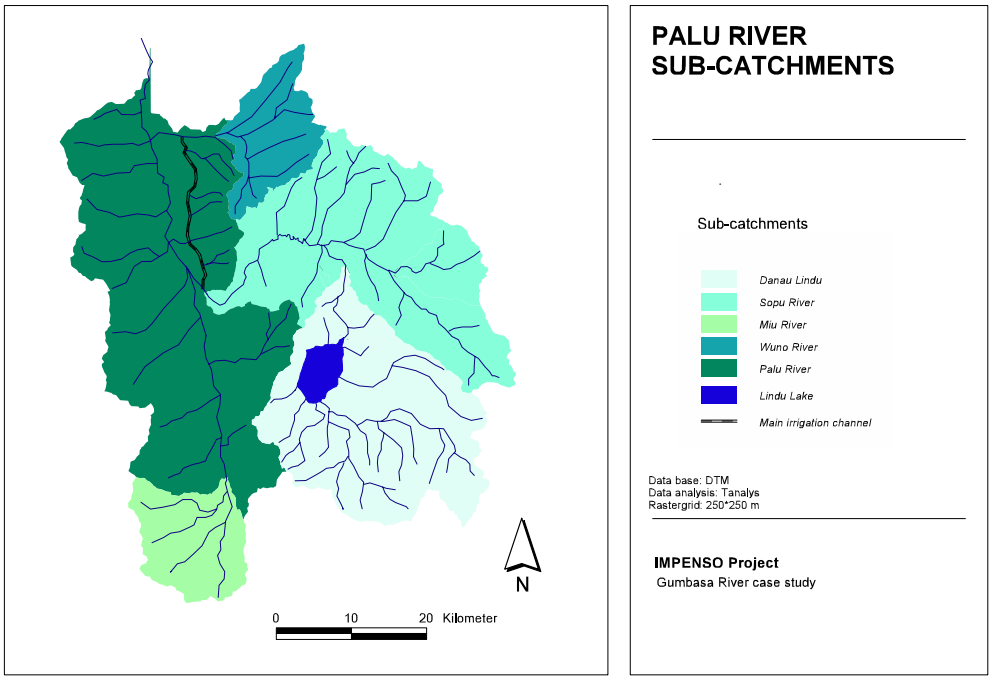

Appendix B. 1: Palu River sub-catchment. See also Chapter 2.5.

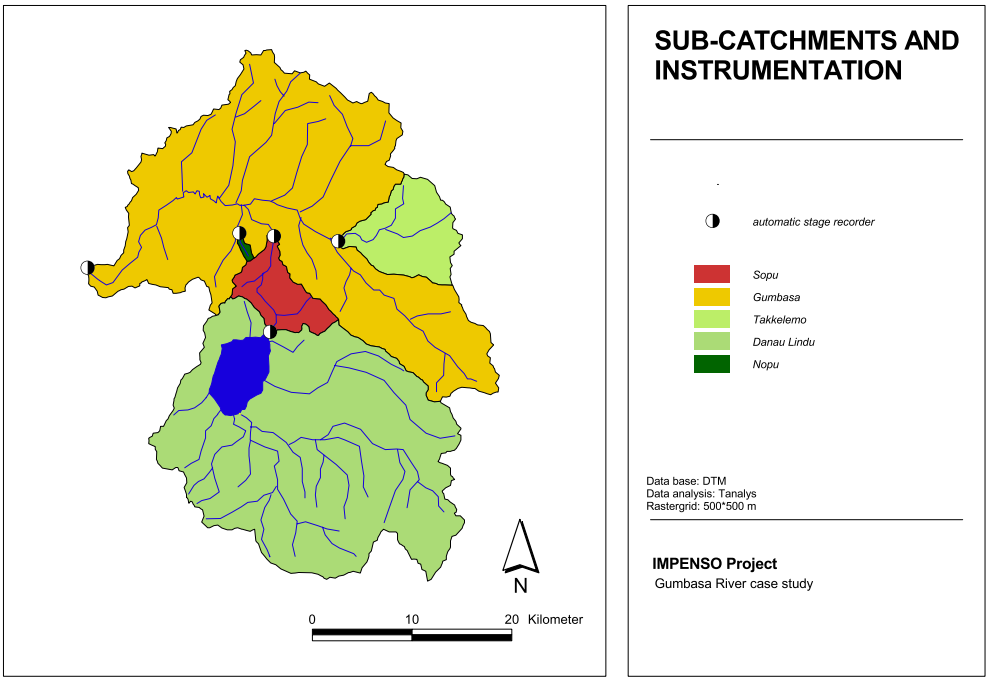

Appendix B. 2: Gumbasa River sub-catchments for WASIM-ETH modelling application. See also Chapter 6.5.1.

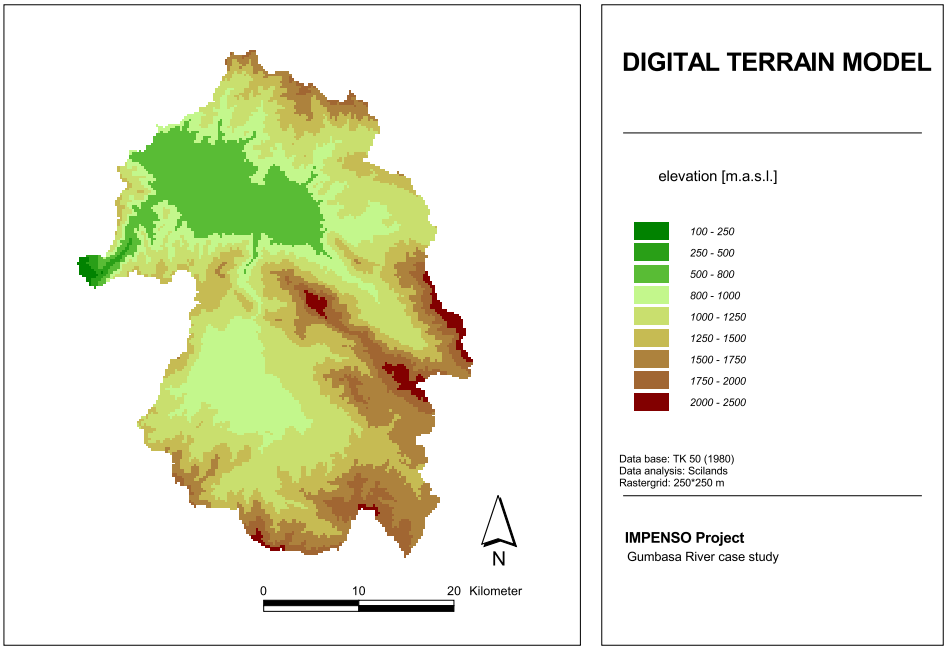

Appendix B. 3: Digital Terrain model, Gumbasa River watershed. See also chapter 6.1.1.

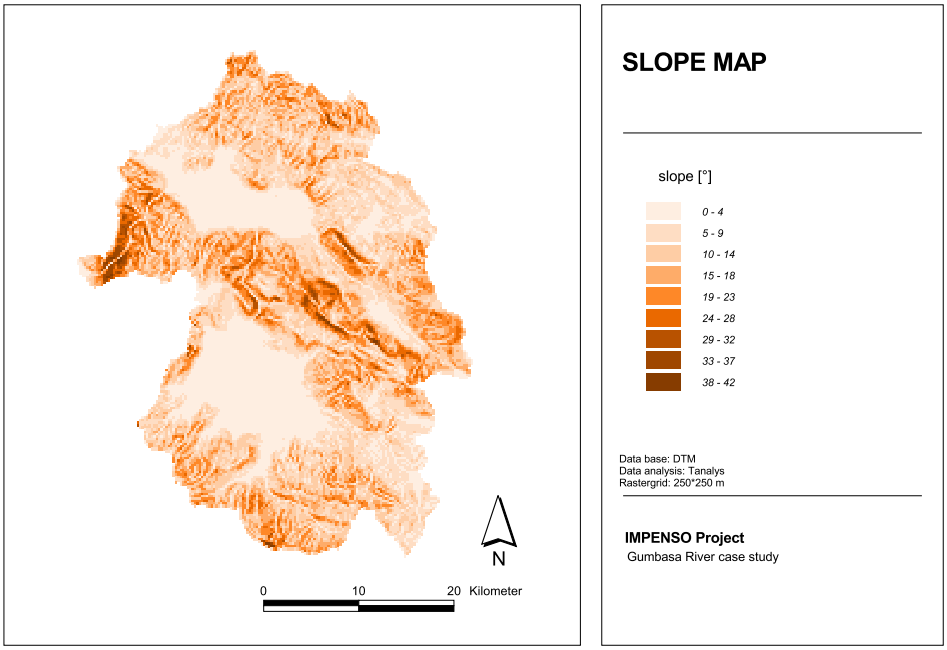

Appendix B. 4: Slope map, Gumbasa River watershed. See also Chapter 6.3.1.

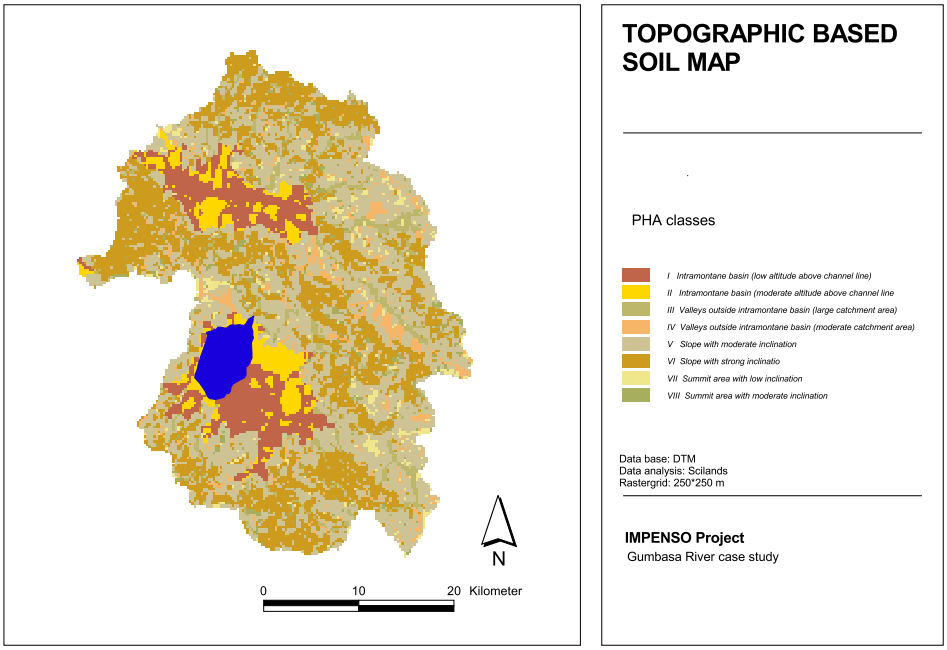

Appendix B. 5: Topographic based soil map, Gumbasa River watershed. See also Chapter 6.1.2.

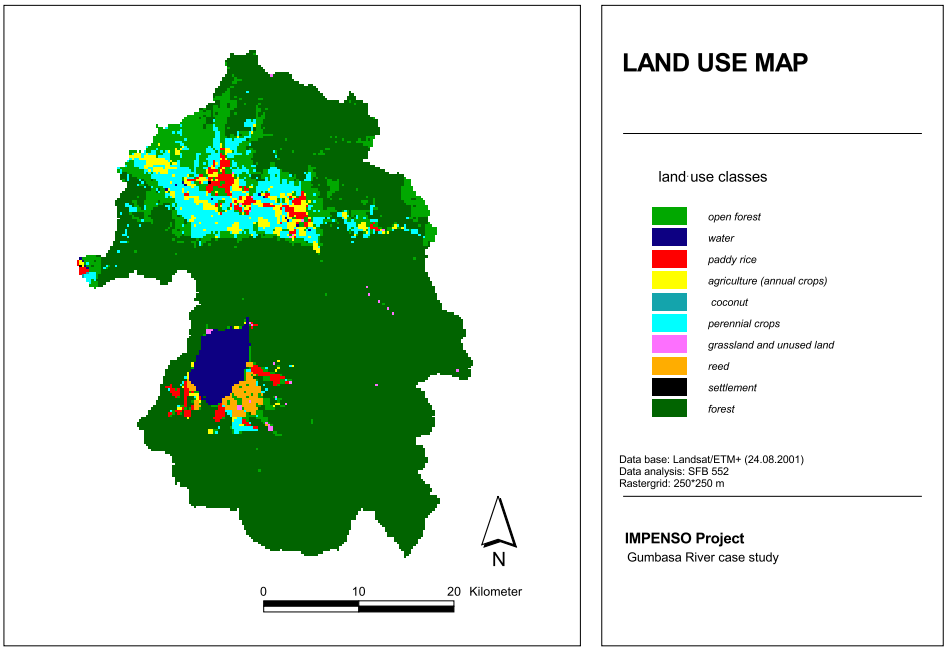

Appendix B. 6: Land-use Gumbasa River watershed. See also Chapter 6.1.3.

CURRICULUM VITAE

Name:	Constanze Leemhuis
Geburtsdatum:	22. April 1974
Geburtsort:	Düsseldorf
Staatsangehörigkeit:	Deutsch

Seit 09/2001	Wissenschaftliche Mitarbeiterin in der Abteilung Landschaftsökologie am Geographischen Institut der Georg-August-Universität Göttingen. Promotionsthema: The Impact of El Niño Southern Oscillation Events on Water Resource Availability in Central Sulawesi, Indonesia.
04/2000-04/2001	Wissenschaftliche Mitarbeiterin im SHYLOC (System for hydrology using land observation for model calibration) Projekt, Joint Research Centre, Ispra, Italien.
04/1999–03/2000	Diplomarbeit: Assessing available and new technologies for wetland restoration and management.
1993–1999	Diplomstudium der Landeskultur und Umweltschutz an der Agrar- und Umweltwissenschaftlichen Fakultät, Universität Rostock.
1984–1993	Abitur, Humboldtgymnasium Solingen.